Foreword

Welcome to the latest edition of our AtkinsRéalis Technical Journal. In this issue we are proud to feature papers from our Emerging Professionals and focus on Social Value and Impactful Engineering, showcasing where we have produced solutions that make a real difference to society and the environment.

This edition features some of the work we have been doing in civil, structural and geotechnical engineering, transport planning, asset management and fire engineering. It highlights our strong focus on the environment through efforts to reduce carbon in new infrastructure and to address climate resilience and air pollution in existing infrastructure. It also highlights how our work has been extending the safe life of existing assets and improving the safety of new designs.

To help safeguard the environment, we have carried out a study into reducing concrete strength to use cement efficiently and reduce embodied carbon, showing that industry over-specifies concrete strength in many situations and that many designs would still be adequate with a 20% lower concrete strength than originally specified. We have developed a Trunk Road Adaptation Plan for Transport Scotland, using innovative data-driven methods to assess climate risks, propose adaptation actions and help to deliver a resilient transport system for future generations. And we have assisted councils in implementing UK Government-mandated clean air zones to improve air quality through supporting technology integration to monitor vehicle registrations, developing business cases and stakeholder engagement.

CHRIS HENDY

Editor-in-Chief AtkinsRéalis
Technical Journal
AtkinsRéalis Fellow, Professional
Head of Bridge Engineering
and Transportation
Technical Director

To extend the safe life of existing assets, we have integrated non-destructive testing (NDT) data for bridge structures into a digital twin framework, standardizing data import workflows and supporting better data analysis and decision-making in maintenance and inspection practices. We have proposed methods for estimating parts failure rate for critical rail components under sparse data conditions using Frequentist and Bayesian methods, aiding RAMS engineers in reliability assessments and decision-making for rail systems. And we have automated Polished Stone Value (PSV) calculations for skid resistance on the M25 Pavement Renewal Scheme, enhancing efficiency and accuracy and reducing calculation review time by over 60%.

To help improve the safety of design methods, we have reviewed the Deep Soil Mixing (DSM) ground improvement technique, particularly for peaty soils, and highlighted the risks and proposed mitigation measures. To improve fire safety in design, we have analysed ways to control interpretation errors from non-homogeneous smoke conditions, which is crucial for designing fire smoke extraction systems and emergency egress paths.

The above examples provide only a small insight into the wealth of innovation that AtkinsRéalis creates day to day and we hope you find this collection of papers as enjoyable, inspiring and informative as we do. Thank you for joining us in celebrating the remarkable contributions of our Emerging Professionals.

Avant-propos

CHRIS HENDY

Rédacteur en chef de la Revue
technique d'AtkinsRéalis
Fellow d'AtkinsRéalis,
chef professionnel,
Ingénierie des ponts et
directeur technique, Transports

Bienvenue dans la toute dernière édition de la Revue technique d'AtkinsRéalis. Dans ce numéro, nous présentons avec fierté des articles de nos professionnelles émergentes et professionnels émergents. Nous mettons l'accent sur la valeur sociale et l'impact de l'ingénierie, en présentant les solutions que nous avons produites et qui changent réellement la donne pour la société et l'environnement.

Cette édition présente une partie du travail que nous avons accompli dans les domaines de l'ingénierie civile, structurale, et géotechnique, de la planification des transports, de la gestion des actifs, et de l'ingénierie des incendies. Elle souligne notre approche fortement orientée sur l'environnement grâce aux efforts de réduction du carbone dans les nouvelles infrastructures, et de lutte contre les changements climatiques et contre la pollution atmosphérique dans les infrastructures existantes. Elle met également en avant la façon dont notre travail a permis de prolonger la durée de vie sécuritaire des actifs existants et d'améliorer la sécurité des nouvelles conceptions.

Pour aider à protéger l'environnement, nous avons réalisé une étude sur la réduction de la résistance du béton afin d'utiliser le ciment efficacement et réduire le carbone intrinsèque, démontrant ainsi que l'industrie impose des spécifications trop strictes pour la résistance du béton dans de nombreuses situations et que de nombreuses conceptions seraient tout de même adéquates avec une résistance du béton de 20 % inférieure à celle initialement spécifiée. Nous avons élaboré un plan d'adaptation des réseaux routiers et autoroutiers pour Transport Scotland, à l'aide de méthodes innovantes fondées sur des données pour évaluer les risques climatiques, proposer des mesures d'adaptation, et aider à fournir un système de transport résilient pour les générations futures. De plus, nous avons aidé les conseils à mettre en œuvre des zones d'air pur mandatées par le gouvernement du Royaume-Uni afin d'améliorer la qualité de l'air, en appuyant l'intégration technologique pour surveiller l'immatriculation des véhicules, développer des études de cas et l'engagement des parties prenantes.

Pour prolonger la durée de vie sécuritaire des actifs existants, nous avons intégré les données d'essais non destructifs (END) pour les structures de ponts dans un cadre de jumeau numérique, normalisant les flux d'importation des données et appuyant de meilleures analyses des données et prises de décisions dans les pratiques d'entretien et d'inspection. Nous avons proposé des méthodes pour estimer le taux de défaillance des pièces pour les composantes ferroviaires critiques dans des conditions où les données sont rares en utilisant les méthodes fréquentistes et bayésiennes. Cela permet d'aider les ingénieurs en Fiabilité, disponibilité, maintenabilité, sécurité (FDMS) à évaluer la fiabilité et à prendre des décisions pour les systèmes ferroviaires. Nous avons également automatisé les calculs du coefficient de polissage accéléré du granulat (CPA) pour la résistance au dérapage dans le plan de renouvellement des chaussées de la M25, ce qui améliore l'efficacité et la précision, et réduit le temps d'examen des calculs de plus de 60 %.

Pour aider à améliorer la sécurité des méthodes de conception, nous avons examiné la technique d'amélioration du sol qu'est le malaxage des sols, en particulier pour les sols tourbeux, et nous avons souligné les risques et proposé des mesures d'atténuation. Pour améliorer la sécurité incendie dans le domaine de la conception, nous avons analysé des façons de contrôler les erreurs d'interprétation des conditions de fumée non homogènes, ce qui est essentiel pour concevoir des systèmes d'extraction de fumée d'incendie et des voies d'évacuation d'urgence.

Les exemples ci-dessus ne donnent qu'une petite idée de la richesse de l'innovation que crée quotidiennement AtkinsRéalis et nous espérons que vous trouverez cette série d'articles aussi agréable, inspirante et informative que nous. Merci de vous joindre à nous pour célébrer les contributions remarquables de nos professionnelles émergentes et professionnels émergents.

Editor-in-chief

Chris Hendy

FREng MA (Cantab)
CEng FICE Eur Ing

Technical Director; Fellow;
Professional Head of Bridge
Engineering

UK & Ireland – Transportation

Epsom, UK

Production Team

Dorothy Gartner

MLIS

Sr Librarian

Office of the COO,
Global Operations

Montreal, Canada

Samantha Morley

CAPM

Project Controls Analyst I

US – Operational Services

Omaha, NE, USA

Cheryl Law

MEng CEng MICE

Associate Director

UK & Ireland – Infrastructure

Epsom, UK

2025 Editorial Board Members

Contents

[EP] Emerging Professional

🌱 Paper covers the social value/
impactful engineering topic

01: Transport Scotland's First Trunk Road Adaptation Plan: Laying the Foundations for a Climate Resilient Network

Significance Statement

Scotland's changing climate is causing more extreme weather, threatening a large transport network with disruptions and damage, making adaptation measures essential. The Trunk Road Adaptation Plan delivered for Transport Scotland by AtkinsRéalis demonstrates innovative ways to assess and plan for climate change risks. Climate and road data were combined to create detailed climate risk maps. The adaptation plan outlines forty-five ways to adapt the trunk road network and make it more resilient to climate change. This study sets a benchmark for climate risk assessment and adaptation planning for transport providers and operators across the transport sector.

Énoncé d'importance

Les changements climatiques en Écosse causent davantage de phénomènes météorologiques extrêmes, menaçant un vaste réseau de transport du fait des perturbations et des dommages qui en découlent. Il est donc essentiel de prendre des mesures d'adaptation. Le plan d'adaptation des réseaux routiers et autoroutiers présenté par AtkinsRéalis à Transport Scotland démontre des solutions innovantes pour évaluer et planifier les risques liés aux changements climatiques. Les données climatiques et routières ont été combinées pour créer des cartes détaillées des risques climatiques. Le plan d'adaptation décrit 45 façons d'adapter les réseaux routiers et autoroutiers et de les rendre plus résilients aux changements climatiques. Cette étude établit un point de référence pour l'évaluation des risques climatiques et la planification de l'adaptation pour les fournisseurs et exploitants du secteur des transports.
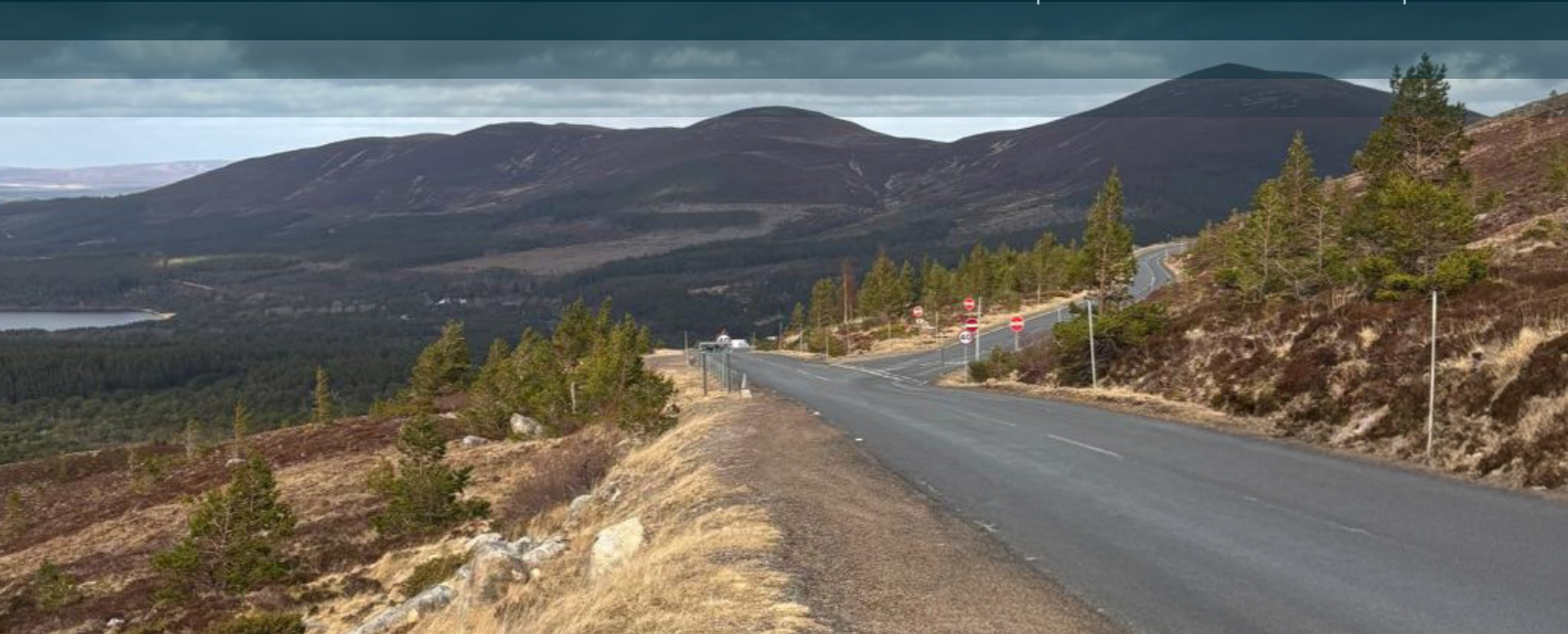
Cara-Marie O'Keeffe
Senior Climate Adaptation
Consultant
Infrastructure – UK & Ireland,
Sustainable Futures
London, UK

Lucas Everitt
Senior Climate Adaptation
Consultant
Infrastructure – UK & Ireland,
Sustainable Futures
London, UK

Michelle Spillar
Associate Consultant
Infrastructure – UK & Ireland,
Sustainable Futures
Exeter, UK

Abstract

The Trunk Road Adaptation Plan was developed for Transport Scotland by AtkinsRéalis to support their vision of a well-adapted transport system. The study used an innovative data-driven approach to quantifying risk. UKCP18 climate projections and Transport Scotland asset data were combined to map current and future risks to a 2km hex grid across the Trunk Road Network. The results highlighted hotspots of increased climate risk for nine climate hazards. A structured participative approach was then used to develop a comprehensive adaptation plan based on the risk assessment. The adaptation plan outlined forty-five themed adaptation actions together with strategic guidance for implementing an adaptation monitoring framework, providing a robust framework to enhance climate resilience. This study provides an exemplar of climate risk assessment and adaptation planning for transport networks. It delivers a key step towards Transport Scotland's goal of a safe, reliable, and resilient transport system for current and future generations.

KEYWORDS

1.   Introduction

Scotland's trunk road and motorway network provides "lifeline" infrastructure, connecting major urban centres, airports, seaports, and towns, and plays an instrumental role in facilitating the movement of goods and services that fuel the nation's economy. The trunk road network provides strategic and local connectivity between towns, cities, and rural areas facilitating the movement of people, services, and goods. Transport Scotland's trunk road network asset base is valued at £27.6 billion (Transport Scotland 2023), with 3.1 million motor vehicles licensed for use across Scotland (Transport Scotland 2023a). Unique challenges are faced by trunk road network users, especially those residing or travelling to and from rural and remote areas of Scotland where alternative routes may not exist in the event of road closures (Ferguson *et al.* 2023).

Climate records indicate that Scotland is becoming warmer and drier in summer and milder and wetter in winter. Climate projections indicate that these trends will continue, with extreme weather events becoming increasingly frequent (Sniffer 2021). These changes have the potential to cause significant disruption to the Scottish Trunk Road Network (TRN). The TRN is highly vulnerable to climate-related hazards and is already experiencing the impacts of climate change, with more frequent instances of weather-related disruption and increasing levels of damage to TRN infrastructure. It is imperative to understand where and how badly the network is affected by climate change (the exposures and vulnerabilities within the network, respectively) to support the development and implementation of adaptation and resilience measures that safeguard assets, the road network, and the system of services it provides.

AtkinsRéalis were contracted by Transport Scotland to facilitate the development of a Trunk Road Adaptation Plan (TRAP), informed by the most recent climate projection (UKCP18) information. The TRAP was identified as a key requirement by the UK's Climate Change Committee to ensure resilience of the Scottish TRN (Climate Change Committee 2023).

The overall aim of this project was to develop the TRAP and enable a well-adapted TRN that is safe for all users, reliable for everyday journeys, and resilient to weather-related disruption. The purpose of the TRAP is to provide a robust evidence base, being the first assessment by Transport Scotland to use the latest climate change projections (UKCP18) with the aim to:

- Identify and evaluate current and future climate risks and opportunities to the TRN to inform strategic decisions and increase future weather resilience; and,
- Inform Transport Scotland's Roads Risk Register and corporate risk register and support the development of an adaptation plan, founded on the climate vulnerability and risk assessment using the latest UK Climate Change Projections (UKCP18).

The TRAP was a significant requirement towards delivery of adaptation under Transport Scotland's Approach to Climate Change Adaptation and Resilience (ACCAR), which aims to provide an approach to adaptation to address the key climate risks affecting Scotland's transport system. The TRAP aligns with the ACCAR Vision for "a transport system which is well adapted and prepared for current and future impacts of climate change, safe for all users, reliable for everyday journeys, and resilient to weather related disruption." This TRAP provides a framework for adapting the TRN to climate change across three themes defined in Transport Scotland's ACCAR Vision for a safe, reliable, and resilient transport system.

2.   Methodology

The TRAP approach is rooted in UK Climate Impacts Programme methods and structured around the standard climate risk management project cycle (Figure 2.1) with clear and early definition of the adaptation problem followed by a series of screening, risk assessment, and adaptation planning steps to inform the TRAP. Our risk assessment approach aligns with guidance outlined in ISO 14092:2021 "Adaptation to climate change – Adaptation to Climate Change," evaluating climate risk as an intersection of hazard, exposure, and vulnerability (International Organization for Standardization, 2021).

FIGURE 2.1

Adaptation to Climate
Change Guidance.
Simplified from ISO14092
(International Organization
for Standardization, 2021)
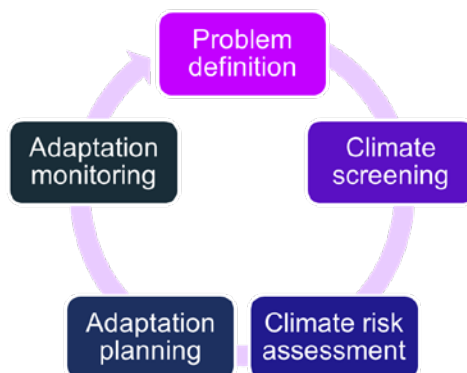
The methodology is described for the three key stages of the TRAP; the baseline screening (section 2.1), the future climate risk assessment (section 2.2), and adaptation recommendations (section 2.3).

Definitions of exposure and vulnerability (International Organization for Standardization, 2021)

- **Exposure:** presence of people, livelihoods, species or ecosystems, environmental functions, services and resources, infrastructure, or economic, social or cultural assets in places and settings that could be affected.
- **Vulnerability:** propensity or predisposition to be adversely affected.

2.1   BASELINE SCREENING

To perform a baseline climate screen of the Scottish TRN, risk was scored for both exposure of the TRN to climate-related hazards and vulnerability of the TRN to develop a high-level risk score:

- Exposure to the identified climate threats has been scored from an analysis of historical climate data sets and third-party GIS hazard layers; and,
- Asset vulnerability has been scored based on characteristic data sourced from Transport Scotland's asset management system.

The evaluation of screened risk across the network is scored based on the combination of exposure and vulnerability, in accordance with Table 2.1.

TABLE 2.1

Climate Risk Screen Scoring Table and classification

Risk Scoring Table

		Exposure				
		Low - 1	2	3	4	Extreme - 5
Vulnerability	Extreme - 5	5	10	15	20	25
	4	4	8	12	16	20
	3	3	6	9	12	15
	2	1	4	6	8	10
	Low - 1	1	2	3	4	5

Risk Score	Risk Classification
0-5	Low
5-10	Moderate
10-15	High
15-20	Very High
20-25	Extreme

The analysis has been conducted utilising Geographical Information System (GIS) software (QGIS) and assesses the TRN using a 2km boundary-length hex-grid approach (Figure 2.2). This reduces any skewed results based on road length and allows for more consistent results across neighbouring sections along the network, allowing a comparison of risk across consistent spatial units. The hex grid also allows for risk to be viewed for areas surrounding the road network which may have impacts on the network, for example, impacts of landslides in proximity to the road network.

FIGURE 2.2

Trunk Road Network 2km side hex grid layout
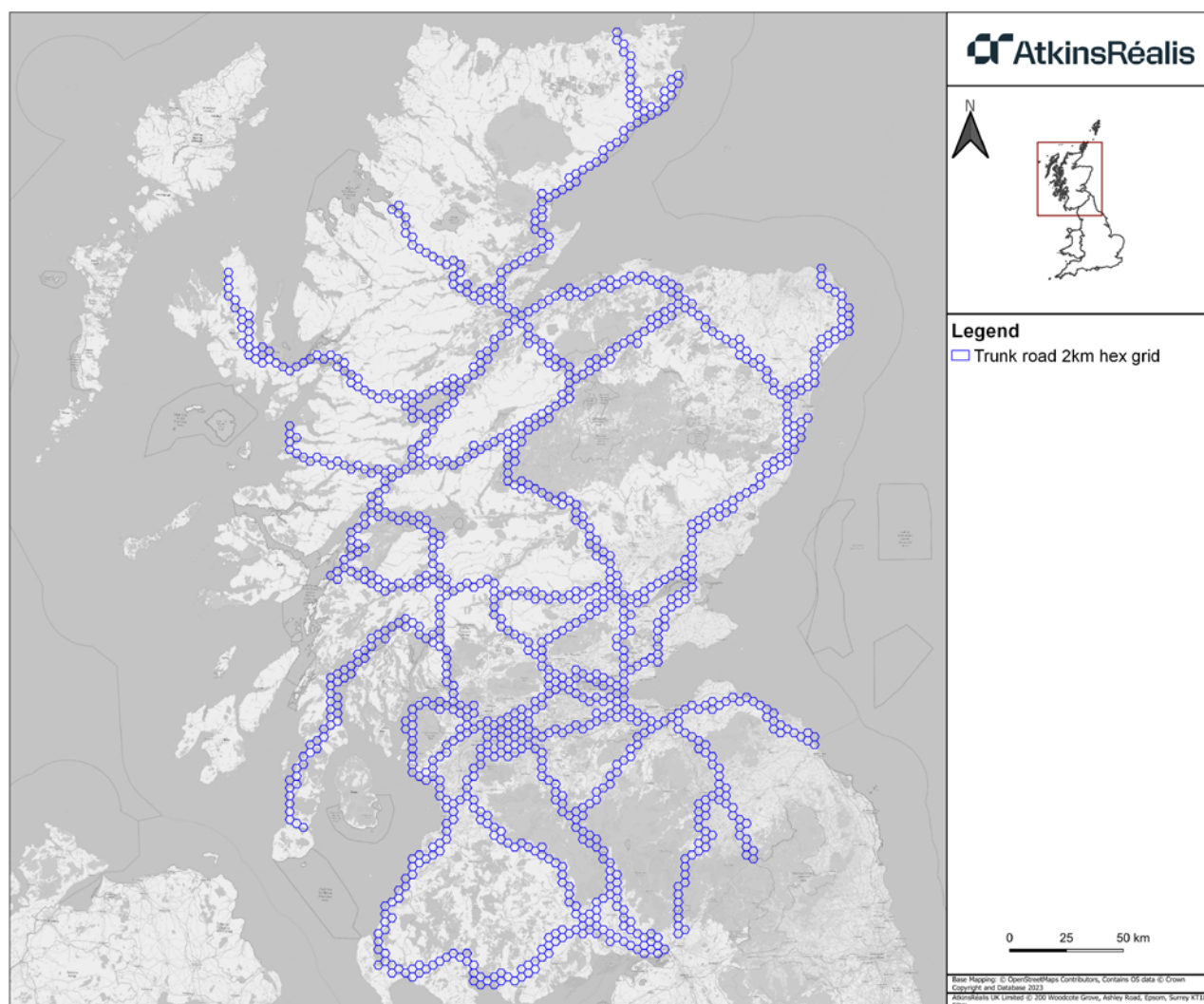
Each hex grid has been assigned an exposure score for each climate-related hazard and an asset vulnerability score to calculate overall baseline risk by climate hazard.

Variables used to inform climate hazard exposure and asset vulnerability

Data type	Variable	Description of data used to inform risk scoring	Source
Climate hazard and exposure	River flooding	Road length within a 1-in-200-year floodplain	SEPA 2023
	Pluvial flooding	Road length within a 1-in-200-year floodplain	
	Coastal flooding	Road length within a 1-in-200-year floodplain and an eroded area, influence or vicinity to coastal processes	SEPA 2023, Dynamic Coast 2023
	River scour	Bridge count (with a 10 m buffer) within a medium or high risk which are within velocity zones >1 m/s	SEPA 2023
	Landslides	Road length, bridge and culvert count, within "Significant" rated area, coincident with a count of rainfall days >25 mm	Met Office 2021, British Geological Survey 2023
	Extreme heat	Number of days with temperature above 25°C	Met Office 2021
	Cold spells	Number of days with temperature below 0°C, coincident with more than 1.2 mm rainfall between 1981 and 2000	
	High winds	99.9 percentile hourly mean wind speed (mph)	
Asset vulnerability	Surface Course Construction Date	Date of road surface construction (Age)	Transport Scotland (2023b)
	Bridge Condition Indicator (BCI)	The weighted average for a structure taking into account the condition of all structural elements	
	Structure Condition Score Average (SCS_{AV})	The weighted average of all Element Condition Index (ECI) scores for the structure	

GIS processes were used to assign hex grid exposure scoring, using an intersection analysis between the hex grid and gridded outputs from HadUK-grid data for landslide, heatwave, cold spells, and high winds. Where multiple HadUK-grid data were intersecting with a hex grid, an average of the HadUK-grid data was calculated and assigned to the hex grid. Likewise, an intersection analysis was completed on flooding extents to understand levels of fluvial, pluvial and coastal flooding exposure for each hex grid along the Trunk Road Network.

A high-level assessment of asset vulnerability has also been considered in this screen based on the average age or condition score of the collective assets within each hex grid. An intersection analysis was completed in GIS to assign each hex grid an average age or condition score of collective assets within each hex grid.

Separately, we created a community vulnerability scoring system, taking into account the Scottish Index of Multiple Deprivation and Scotland's wildness and remoteness, which outlines remoteness from public roads, rail and ferry networks (Scottish Government 2020, Scottish Government 2024). This provided a spatial understanding of where communities would be most vulnerable to climate change hazards, where road closures would have the greatest impact and a lower capacity to adapt (Ferguson *et al.* 2023).

2.2 FUTURE CLIMATE RISK ASSESSMENT

The future climate change risk assessment was initially informed by the transport risks identified in the Climate Change Committee's Independent Assessment of UK Climate Risk (CCRA3) (UK Climate Risk 2021). This was developed further through the use of climate model (UKCP18) datasets, focused on medium (RCP6.0) and high (RCP8.5) Representative Concentration Pathways for the 2050s and 2080s (Met Office 2022).

Explainer Box: RCPs

Representative Concentration Pathways (RCPs) describe 21st century pathways of greenhouse gas emissions and are used within UK and international climate change assessments (Met Office 2018). The RCPs represent the range of future potential scenarios of greenhouse gas emissions and are used to model and understand a broad range of potential climate outcomes in future (Climate Change Committee 2021).

Two RCPs are explored in this study as the UK Climate Change Committee recommends that the UK should adapt for at least 2°C warming above pre-industrial levels and prepare for the possibility of 4°C warming above pre-industrial levels by 2100 (Met Office 2018):

- **RCP6.0** – a **medium-high** greenhouse gas emissions scenario considered an "intermediate" scenario. Global surface temperature is projected to be **2.8°C higher in 2081-2100** compared to the pre-industrial period (1850-1900).
- **RCP8.5** – a **high** greenhouse gas emissions scenario considered a "worst case" scenario where greenhouse gas emissions continue to increase unmitigated. Global surface temperature is projected to be **4.3°C higher in 2081-2100** compared to the pre-industrial period (1850-1900).

It should be noted that all climate model projections have inherent uncertainty. RCPs are defined as pathways therefore are not definitive, with alternative future scenarios potentially occurring in reality.

There are key differences between the baseline screening assessment and future risk assessment in the calculation of risk. The baseline screening climate assessment highlighted key "climate risk" areas for the baseline period. The baseline screening assessment approach took into account hazard/exposure and asset vulnerability, unlike future risk which considers risk in terms of likelihood and impact. Different scoring systems are therefore used between the screening assessment and the future climate risk assessment.

Assessments were completed for nine key hazards: surface water flooding, river flooding, coastal flooding, river scour, landslides, extreme heat, cold spells, high winds, and cascading risks. To perform an assessment of material risks to the Scottish TRN, a number of discrete investigations were undertaken, both qualitative and quantitative, to assign each risk with a **likelihood** and **impact** score in alignment with Transport Scotland's corporate risk management processes:

- **Likelihood:** The likelihood of a risk event occurring has been scored based on analysis of event probability and annual probabilities of relevant climate drivers using the Met Office's UKCP18 climate datasets (Figure 2.3)., alongside any assumptions required to link climate hazards to impacts on the TRN. The likelihood scoring has been informed by Transport Scotland categories used in the Roads Risk Register, as well as aligned with SEPA flood map return periods for High, Medium, and Low likelihood events.
- **Direct impacts:** Direct impacts have been scored qualitatively based on combined evidence from historical Transport Scotland disruption data, stakeholder engagement, GIS exposure assessment, and other quantitative methods where sufficient data were available. Evidence used for scoring the impact of each risk is discussed in their respective sections.
- **Indirect impacts:** Indirect impacts have been considered qualitatively and supported by quantitative data from literature review where available, such as the monetary impact of climate-events on the UK or Scottish economy.

FIGURE 2.3

UKCP18 threshold analysis
to inform landslide
likelihood scoring
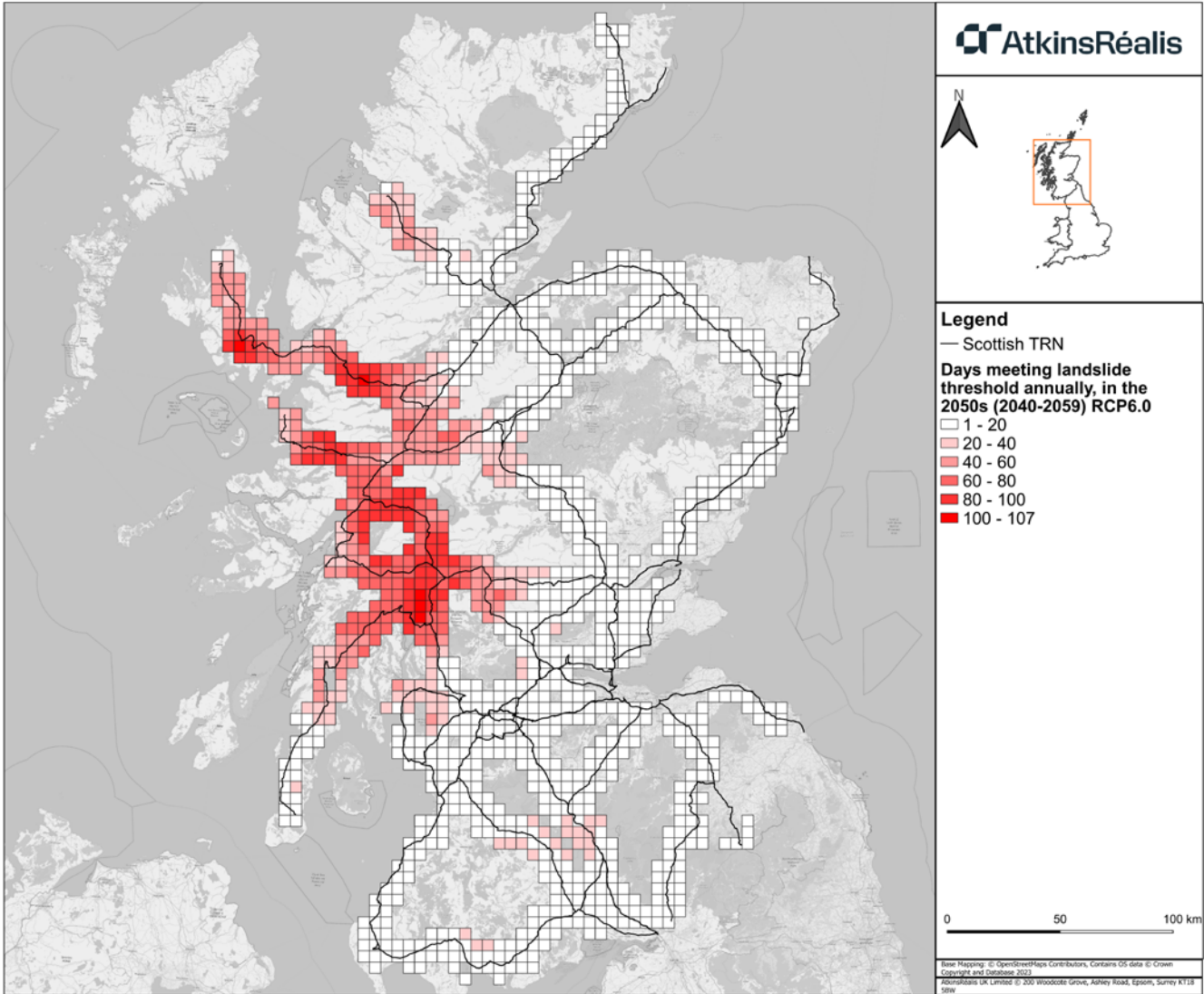
Potential impacts which were considered as part of the study included impacts on Transport Scotland's assets, services, and communities from climate change hazards included the following:

- **Remediation/response:** Financial and human resource requirements for repairs and maintenance associated with climate hazards.
- **Deterioration:** Financial impacts on the repair and maintenance of roads due to climate change hazards such as extreme heat or flooding damaging road surfaces.
- **Transport users:** Disruptions to journeys due to climate change hazards such as landslides and flooding closing roads resulting in diversions or delays on the network. Impacts on vulnerable communities, for example, those that live in remote areas.
- **Disruption:** Wider impact on the Scottish economy due to transport network disruptions.

Direct impacts were quantified for future flood risk using an innovative method of calculating damage to road surfaces based on SEPA defined flood depths and a depth-damage curve function. A depth damage curve was used to understand the cost of different flood depths for a trunk road assuming £4.3 million per km of highway inundated (Hess *et al.* 2021). This figure is based on European Trunk Roads and a higher average figure may be appropriate for Scotland of ca. £6.65 million per km of highway. These costings were combined with flood depths from SEPA flood risk maps for fluvial, surface, and coastal flooding. To understand future impacts from flooding, future scenarios of the cost of a flood event for a +2°C and +4°C by 2050 and 2080 were calculated based on uplifts in Expected Annual Damage from the UK CCRA3, which were applied to the cost of a current event for each scenario to derive final event costings (Sayers *et al.* 2020).

FIGURE 2.4

Trunk road landslide
repairs on the A83 in the
Scottish Highlands

2.3 ADAPTATION PLAN DEVELOPMENT

The method for developing Transport Scotland's first TRAP followed a structured, participatory approach built on the comprehensive risk assessment outputs. The process engaged stakeholders through workshops, targeted interviews, and expert elicitation to gather both local knowledge and quantitative inputs. The adaptation plan aimed to identify existing and potential future actions, align them with a clear vision for resilience, and establish a monitoring framework that tracks climate impacts and adaptation progress.

Risk Assessment Outputs: the development of the adaptation plan was built on the comprehensive risk assessment that identified the vulnerabilities and potential impacts of climate change on various assets and geographic areas.

24

Stakeholder Engagement and Participation: A core element of the methodology was stakeholder engagement, which was crucial for ensuring that the adaptation plan was grounded in local knowledge and aligned with the needs and priorities of the organisation and the communities it served. The following participatory approaches were employed:

- **Workshops:** Multi-stakeholder workshops were conducted to discuss risk assessment results and identify potential adaptation measures. These workshops were structured to ensure diverse representation, including engineering and emergency response managers, Transport Scotland's Vulnerable Operating Locations Group (VLOG), regional contractors, and climate hazard experts. Interactive exercises facilitated the exchange of knowledge and the prioritisation of adaptation actions based on shared understanding.
- **Targeted Interviews:** In-depth interviews were carried out with key stakeholders, including Transport Scotland resilience decision makers, Transport Scotland's VLOG, SEPA's flood forecasting team, and ScotRail's Climate Resilience Lead. These interviews provided qualitative insights into local perceptions of climate risks, existing coping strategies, and adaptation needs.
- **Expert Elicitation:** A panel of climate experts, engineers, and sector specialists was convened by AtkinsRéalis to provide technical inputs on the feasibility and effectiveness of potential adaptation actions. This expert elicitation process helped refine adaptation measures, ensuring they were both scientifically sound and contextually appropriate.

Visioning for Resilience: A clear vision for resilience was developed in collaboration with stakeholders. This vision set the long-term goals for adapting to climate change, focusing on the safety of all users, reliability of service, and resilient infrastructure. Stakeholders collectively defined these key adaptation objectives and ensured alignment with Transport Scotland's ACCAR Vision:

*"A transport system which is well adapted and prepared for current and future impacts of climate change, **safe** for all users, **reliable** for everyday journeys, and **resilient** to weather related disruption."*

Alongside the three key adaptation objectives, three "enabler" themes were identified to promote organisational governance, collaboration, and knowledge development.

Identification of Adaptation Actions: Based on the risk assessment outputs and stakeholder inputs, a comprehensive list of existing and potential future adaptation actions was developed. These actions were categorized into short-term, medium-term, and long-term measures, and were evaluated based on:

- **Effectiveness:** The potential of each action to reduce or mitigate identified climate risks.
- **Feasibility:** Consideration of financial, technical, and social feasibility, including the capacity of local institutions to implement actions.
- **Co-benefits:** The broader benefits of actions, such as opportunities for reducing emissions, environmental sustainability, and no-regret ("low-hanging fruit") options.

Monitoring and evaluation framework: An essential component of the adaptation plan was the recommendation of a robust monitoring and evaluation framework to track both climate impacts and adaptation progress over time. The framework was designed to:

- **Track Climate Impacts:** Key indicators related to climate change impacts (e.g., changes in temperature, frequency of extreme events) were identified and established to monitor ongoing trends.
- **Measure Adaptation Progress:** Indicators were developed to assess the implementation and effectiveness of adaptation actions. These included both process indicators (e.g., completion of planned actions) and outcome indicators (e.g., reduction in vulnerability or improvement in resilience).
- **Regular Feedback Loops:** Periodic assessments were planned to review the effectiveness of adaptation measures and adjust the plan as necessary based on new information or changing circumstances. Stakeholders were involved in regular reviews to ensure the plan remained dynamic and relevant.

Final Trunk Road Adaptation Plan: The final adaptation plan was developed by synthesizing the results from stakeholder engagement, risk assessments, expert inputs, and the visioning exercise. The plan provides a comprehensive roadmap for implementing adaptation actions, setting clear timelines, responsibilities, and resource requirements. Adaptation actions were grouped under the three key objective themes with additional cross-cutting, partnership, and governance actions grouped into the three enabler themes.

3.   Results

3.1   BASELINE SCREENING

The primary findings of the present-day baseline climate screening were completed based on the length of road or number of structures within an identified risk area and a percentage of the network affected. This was assessed using past disruption events, the spatial analysis and stakeholder engagement outputs. Surface water flooding, landslides, and river flooding were amongst the highest scoring risks, with assets on the TRN likely to be exposed to these climate-related hazards.

From the risk screening outputs, areas exposed to several climate hazards were assessed to identify potential vulnerable locations across the network. Risk scores for eight climate hazards, considering hazard, exposure, and asset vulnerability, assessed across 2km side "hexes," present the areas of the network subjected to the most risks in the Figure 3.1. The consolidated risk scoring is based on total score calculated as the total of individual risk scores for all eight climate hazards. Areas of high risk across on the TRN all climate hazards include the A74(M) to the south of Scotland and TRN in proximity to Glasgow (M8, M74).

FIGURE 3.1

Trunk road network 2km

side hex grid layout
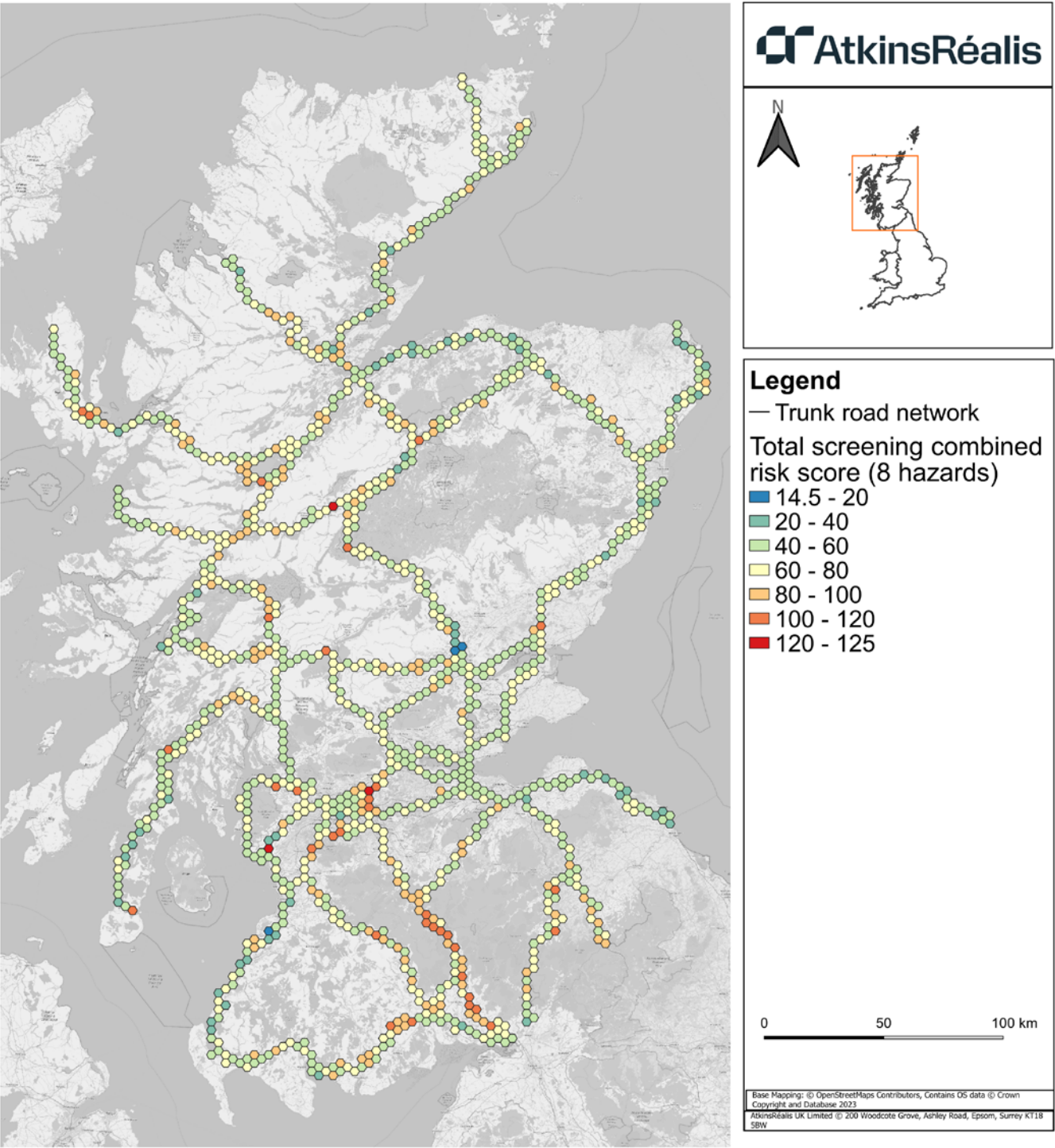
3.2 FUTURE CLIMATE CHANGE RISK ASSESSMENT

A summary of key risks is presented in Table 3.1 for the 2050s based on a medium-to-high emissions scenario (RCP6.0). The key risks highlighted include the risk of increased surface water flooding, river flooding, river scour, and landslides due to climate change damaging assets, causing network disruption, and resulting in safety risks.

TABLE 3.1

Future risk score card. Arrows indicate magnitude of change from current to future scenario (↑ = increase in risk, ↑↑ = substantial increase in risk, ↓ = decrease in risk, ↓↓ = substantial decrease in risk)

HIGH RISK	SURFACE FLOODING ↑ Increase in surface water flooding in Scotland due to heavy rainfall		RIVER FLOODING ↑ Increase in river flooding in Scotland due to heavy rainfall
	LANDSLIDES ↑ Increase in landslide events in Scotland due to continuous increased heavy rainfall		RIVER SCOUR ↑ Increase in river scour conditions in Scotland due to climate change
MEDIUM RISK	COASTAL FLOODING ↑↑ Increase in coastal flooding and erosion in Scotland due to sea level rise	HEAVY SNOW FALL AND ICE ↓ Decrease in heavy snow fall and ice events in Scotland due to climate change	CASCADING FAILURES ↑ Increase in cascading failures in Scotland triggering impacts across the Trunk Road Network
LOW RISK	HIGH WINDS ↑ Increase in extreme wind conditions in Scotland due to climate change		
VERY LOW	EXTREME HEAT ↑ Increase in extreme heat (>30°C) in Scotland due to climate change		

29

The risk scoring is outlined in further detail for the 2050s in the score card (Table 3.2), based on a medium to high emissions scenario for the 2050s and 2070s for high winds (RCP6.0 for landslides, extreme heat and cold spells, +2°C by 2100 for flooding hazards). The wind assessment is scaled down from a RCP8.5 emissions scenario in the 2070s to a medium emissions scenario in the 2050s to be in line with other hazards. The key risks highlighted include the risk of increased surface water flooding, river flooding, river scour, and landslides due to climate change damaging assets, causing network disruption, and resulting in safety risks.

TABLE 3.2

Future risk score card with likelihood and impact scoring

Risk description	Likelihood	Impact	Risk in 2050s
An increase in surface water flooding in Scotland due to heavy rainfall causing damage to assets, network disruptions, and safety risks.	Very High (5)	High (25)	125 ↑
An increase in river flooding in Scotland due to heavy rainfall causing damage to assets, network disruptions, and safety risks.	Very High (5)	High (25)	125 ↑
An increase in river scour conditions in Scotland due to climate change causing damage to assets, network disruptions and, safety risks.	High (4)	High (25)	100 ↑
An increase in landslide events in Scotland due to increased likelihood of intense rainfall events with antecedent rainfall causing damage to assets, network disruptions and, safety risks.	High (4)	High (25)	100 ↑
An increase in coastal flooding and erosion in Scotland due to sea level rise and storm events causing damage to assets, network disruptions, and safety risks.	Very High (5)	Medium (10)	50 ↑↑
An increase in cascading failures due to climate change in Scotland triggering impacts across the TRN including damage to assets, network disruptions, and safety risks.	Low (2)	High (25)	50 ↑
A decrease in heavy snowfall and ice events in Scotland due to climate change, though an increase in event magnitude causing damage to assets, network disruptions, and safety risks.	High (4)	Medium (10)	40 ↓
An increase in extreme wind conditions in Scotland due to climate change causing damage to assets, network disruptions, and safety risks.	Medium (3)	Medium (10)	30 ↑
An increase in extreme heat days (>30°C) in Scotland due to climate change causing damage to assets, network disruptions, and safety risks.	Rare (1)	Low (5)	5 ↑

3.3   TRUNK ROAD ADAPTATION PLAN (TRAP)

The development of the TRAP for Transport Scotland has resulted in a comprehensive Climate Adaptation Plan designed to enhance the resilience of Scotland's transport network. The TRAP outlines 45 recommended adaptation actions, systematically mapped against identified co-benefits to ensure alignment with broader environmental and sustainability goals (Table 3.3). Additionally, the plan provides strategic guidance for implementing an adaptation monitoring framework and an adaptation pathways approach, supporting Transport Scotland in addressing climate risks effectively.

TABLE 3.3

The Trunk Road Adaptation Plan – A Framework for Adaptation

ACCAR Vision		
*"A transport system which is well adapted and prepared for current and future impacts of climate change, **safe** for all users, **reliable** for everyday journeys, and **resilient** to weather related disruption."*		
TRAP Action Themes		
Safe	**Reliable**	**Resilient**
Enhancing safety measures in response to changing climate conditions.	Ensuring reliability for uninterrupted transportation, or reduced impacts of delay when they occur.	Improving resilience against extreme weather events such as floods, storms, and heatwaves.
TRAP Enabler Themes		
Engagement and Partnership	**Research and Understanding**	**Monitoring and Evaluation**
Collaboration within and external to Transport Scotland, including operating companies to effectively tackle the diverse challenges of climate change and identify opportunities to share resources.	Fill identified knowledge gaps in understanding the impacts of climate risk and foster innovation for the development of technologies and materials that future-proof road infrastructure.	Establishing a comprehensive monitoring framework, evaluating climate impacts and adaptation actions to demonstrate progress toward a well-adapted and prepared trunk road system.
Cross-cutting benefits		
Net-Zero Target	Environmental Benefit	Easy Win
Help deliver our net-zero target	Promote greener, cleaner choices	Low-cost, "no regret" actions

Through the TRAP, the following key outcomes have been achieved:

- **Development of 24 Adaptation Recommendations:** These recommendations span three critical action themes—safe, resilient, and reliable—ensuring that key climate risks are mitigated while advancing a transport system that is secure, dependable, and robust in the face of climate change.

- **Formulation of 21 Additional Enabling Recommendations:** Focused on three enabling themes—engagement and partnership, research and understanding, and monitoring and evaluation—these recommendations support governance, enhance knowledge, and promote long-term ownership within Transport Scotland and its key partners.

- **Integration with Strategic Priorities:** All adaptation actions have been mapped against considerations of Net Zero targets, environmental outcomes, and no-regret options, ensuring that climate adaptation efforts align with sustainability goals and deliver positive, long-lasting benefits.

- **Development of an Adaptation Monitoring Framework:** A structured framework has been proposed to track and assess the effectiveness of adaptation actions over time, facilitating ongoing improvements and informed decision-making.

- **Provision of Tools for Adaptive Pathways Development:** Guidance and tools have been provided to support the implementation of adaptive pathways, particularly for key vulnerable locations, enabling a flexible and phased approach to climate resilience.

Overall, the TRAP delivers a targeted, evidence-based approach to climate adaptation, equipping Transport Scotland with the necessary mechanisms to build a transport network that is not only safe, reliable, and resilient but also adaptable to future climate challenges.

4.   Discussion

The development of Transport Scotland's TRAP represents a comprehensive, data-driven, and participatory approach to enhancing climate resilience for critical transport infrastructure across Scotland. This discussion examines the key elements of the plan's development, including the integration of climate risk assessments, innovative risk quantification methods, and extensive stakeholder engagement throughout the process. The plan aligns with national directives such as the Scottish National Adaptation Plan, Transport Scotland's ACCAR, and recent directives from the UK Department for Transport.

Future Climate Risk Assessment Using UKCP18 Projections: Building on the baseline screening, the TRAP included a future-focused climate risk assessment using **UKCP18** climate projections. These projections, derived from the UK Climate Projections 2018 framework, provide a detailed assessment of hazard across a range of climate scenarios and timeframes, offering insights into potential future changes in temperature, rainfall, and extreme events across Scotland.

GIS outputs from the UKCP18 projections were mapped across the transport network, allowing for the visualization of potential risks and vulnerabilities under different climate scenarios (e.g., high emissions vs. low emissions pathways). This forward-looking analysis enabled Transport Scotland to assess both the likelihood and severity of future climate impacts on critical infrastructure, ensuring that adaptation actions were appropriately targeted at the most vulnerable assets and areas.

Novel Approaches for Quantifying Risk: A key innovation in the development of the TRAP was the application of novel methods for quantifying risk. This included the mapping of transport infrastructure assets across a **2km hex grid pattern** to assess climate **hazard, exposure,** and **vulnerability.** This approach allowed for more granular spatial analysis of climate risks, enabling a more precise understanding of how individual assets were exposed to specific climate hazards within a defined geographic area.

Transport Scotland's **Asset Condition datasets** were leveraged to assess the vulnerability of key transport infrastructure assets (e.g., roads, bridges, and culverts) based on their current condition and exposure to identified climate hazards. By integrating condition data with climate projections, a more nuanced understanding of asset vulnerability was developed. For instance, roads in poor condition were identified as more vulnerable to extreme weather events, such as flooding or heat stress.

Participatory Engagement and Development of Adaptation Actions: The TRAP was developed through a **structured, participatory engagement process** designed to integrate local knowledge and ensure the relevance and feasibility of proposed adaptation actions. Stakeholder engagement was an integral component throughout the entire process, ensuring that decision-makers, transport operators, and other key stakeholders were actively involved in verifying and validating the findings of the data analysis.

A series of **workshops,** interviews, and expert elicitation sessions were held with a diverse group of stakeholders. These engagement activities facilitated the identification of **45 recommended adaptation actions,** which were tailored to address the specific vulnerabilities of transport infrastructure as identified in the risk assessments. These actions ranged from short-term measures, such as improving drainage systems, to longer-term strategies, including the redesign and relocation of infrastructure to more resilient locations.

A significant component of the engagement process was the inclusion of **local knowledge** to cross-check the data-driven findings. This local expertise helped to identify perspectives that may not have been captured in the national datasets and ensured that the recommended adaptation actions were both practical and relevant to the local context.

Alignment with National Directives and Expectations: The development of the TRAP was closely aligned with national directives and expectations, ensuring that the plan contributed to broader efforts to increase resilience across Scotland. The plan directly supports the **Scottish National Adaptation Plan,** which outlines Scotland's approach to adapting to climate change. It also aligns with **Transport Scotland's ACCAR,** which emphasizes the importance of building resilience in Scotland's transport infrastructure.

In addition, the TRAP takes into account recent **directives from the Department for Transport,** which highlight the importance of integrating climate resilience into transport planning and infrastructure management. By meeting these national and international climate adaptation frameworks, the plan contributes to a coherent and coordinated approach to climate resilience in transport infrastructure.

Conclusion

The development of Transport Scotland's TRAP represents a cutting-edge, data-driven approach to addressing the climate risks faced by critical transport infrastructure. By combining historical climate data, future projections, innovative risk quantification methods, and extensive stakeholder engagement, the plan provides a robust framework for enhancing climate resilience across Scotland's trunk road network. The integration of local knowledge with scientific data, as well as the recommendation to apply adaptive pathways approaches for long-term resilience, ensures that the plan is both comprehensive and adaptable to future climate uncertainties. The TRAP not only meets national directives but also sets a precedent for future climate adaptation planning in transport infrastructure.

Acknowledgements

References

AtkinsRéalis (2023) Present-day climate screen, Transport Scotland Trunk Road Adaptation Plan.

AtkinsRéalis (2023) Climate change risk assessment, Transport Scotland Trunk Road Adaptation Plan.

AtkinsRéalis (2023) Climate adaptation plan, Transport Scotland Trunk Road Adaptation Plan.

British Geological Survey (2023) BGS Geosure Datasets. Available at: BGS Geosure Datasets [Accessed 5 February 2025].

Climate Change Committee (2022) CCC Insights Briefing 6 Undertaking a climate change risk assessment. Available at: CCC-Insights-Briefing-6-Undertaking-a-climate-change-risk-assessment.pdf [Accessed 5 February 2025].

Climate Change Committee (2023) Adapting to climate change – Progress in Scotland. Available at: Adapting to climate change - Progress in Scotland [Accessed 24 January 2025].

Dynamic Coast (2023) Data Index and Downloads. Available at: Dynamic Coast - Downloads [Accessed 5 February 2025].

Ferguson, N., Boura, G., Gray, A., Patelli, E. and Tubaldi, E. (2023) Vulnerability of the Scottish Road Network to Flooding. Available at: Vulnerability of the Scottish Road Network to Flooding [Accessed 5 February 2025].

van Ginkel, K. C. H., Dottori, F., Alfieri, L., Feyen, L., and Koks, E. E. (2021) Flood risk assessment of the European road network, Nat. Hazards Earth Syst. Sci., 21, 1011–1027, https://doi.org/10.5194/nhess-21-1011-2021

International Organization for Standardization (2021) ISO 14091:2021 Adaptation to climate change – Guidelines on vulnerability, impacts and risk assessment. Available at: ISO 14091:2021 - Adaptation to climate change — Guidelines on vulnerability, impacts and risk assessment [Accessed 24 January 2025].

Met Office (2018) UKCP18 Guidance: Representative Concentration Pathways. Available at: ukcp18-guidance---representative-concentration-pathways.pdf [Accessed 5 February 2025].

Met Office (2021) HadUK-Grid dataset. Available at: HadUK-Grid - Met Office [Accessed 5 February 2025].

Met Office (2022) UKCP18 Probabilistic Projections. Available at: Probabilistic Projections - Met Office [Accessed 5 February 2025].

Sayers, P.B, Horritt, M.S, Carr, S, Kay, A, Mauz, J, Lamb, R and Penning-Rowsell, E. (2020). Third UK Climate Change Risk Assessment (CCRA3) Future flood risk. Available at: Projections of Future Flood Risk - UK Climate Risk [Accessed 5 February 2025].

Scottish Government (2020) Scottish Index of Multiple Deprivation 2020. Available at: Scottish Index of Multiple Deprivation 2020 - gov.scot [Accessed 5 February 2025].

Scottish Government (2024) Scotland's wildness – remoteness. Available at: Scotland's wildness - remoteness - data.gov.uk [Accessed 5 February 2025].

Sniffer (2021) Evidence for the third UK Climate Change Risk Assessment (CCRA3) Summary for Scotland. Available at: CCRA-Evidence-Report-Scotland-Summary-Final-1.pdf [Accessed 24 January 2025].

SEPA (2023) SEPA Data publication. Available at: Environmental data | Scottish Environment Protection Agency (SEPA) [Accessed 6 February 2025].

Transport Scotland (2023) 2022-23 financial performance. Available at: 2022-23 financial performance | Transport Scotland [Accessed 5 February 2025].

Transport Scotland (2023a) Summary transport statistics 2023. Available at: Summary transport statistics | Transport Scotland [Accessed 5 February 2025].

Transport Scotland (2023b) Transport Scotland Asset Management Performance System (AMPS) data.

UK Climate Risk (2021) Transport Sector Briefing. Available at: Transport Sector Briefing - UK Climate Risk [Accessed 31 January 2025].

02: Automation of Polished Stone Value (PSV) Calculation: A Tool for Enhanced Efficiency

Significance Statement

Polished Stone Value (PSV) is a specification test that measures how smooth the stone in a road surface becomes after traffic wear, which affects skid resistance and road safety. This paper introduces an automated tool to simplify PSV specification calculations, traditionally done manually using Excel. Built with Python and integrated with GitHub and Streamlit, the tool reduces calculation time from minutes to seconds for the M25 network managed by Connect Plus Services, which requires PSV calculations for 150-200 road sections annually. It streamlines the process, minimizes errors, and eases the review, blending data science with civil engineering to improve efficiency and reduce workload.

Énoncé d'importance

Le coefficient de polissage accéléré du granulat (CPA) est un essai de caractérisation qui établit dans quelle mesure la pierre de la surface d'une route devient lisse après l'usure causée par la circulation, un facteur qui influe sur la résistance au dérapage et la sécurité routière. Cet article présente un outil automatisé qui simplifie les calculs de caractérisation du CPA, habituellement effectués manuellement dans Excel. Développé avec Python et intégré avec GitHub et Streamlit, l'outil fait passer le temps de calcul de quelques minutes à quelques secondes seulement pour le réseau de la M25 géré par Connect Plus Services, qui exige ces calculs pour 150 à 200 tronçons de route par année. Il simplifie le processus, réduit au minimum les erreurs et facilite l'examen, en combinant la science des données à l'ingénierie civile pour améliorer l'efficacité et réduire la charge de travail.

Shashank Vijayakumar Bolbandi
Assistant Engineer
Office of the COO – GTC
- Strategic Highways
Bangalore, India

Aistis Tamosiunas
Technology and Continuous
Improvement Manager
Transportation UK
- Highways Asset Services
Nova London, UK

Anthony Parry
Associate Director
Transportation UK
- Asset Management
Birmingham, UK

Abstract

Polished Stone Value (PSV) is a specification test (BS EN 1097-8, BSI 2020) for the coarse aggregates used in road surfaces and measures the resistance to polishing, contributing to road safety. In the UK, PSV requirements are based on each road section's specified skid resistance, geometry, and traffic level (DMRB CD 224 2020) (DMRB CD 236 2022). Traditionally, this process is conducted manually using Excel spreadsheets, which is time-consuming and prone to errors.

This paper presents a Python-based tool designed to automate PSV calculations, following the Plan-Do-Check-Act (PDCA) framework and Lean principles to enhance efficiency. The tool integrates with Streamlit for an interactive user interface and GitHub for version control and hosting. In the M25 Pavement Renewal Scheme, for which the AtkinsRéalis GTC India team provides support to Connect Plus Services in Pavement maintenance and improvement design of one of the UK's busiest road networks, the tool has reduced the time spent on checking and reviewing calculations by over 60 percent.

By automating PSV calculations, this tool streamlines the process, improves accuracy, and minimizes errors. It demonstrates the effective integration of data science with civil engineering, making it a valuable resource for engineers, planners, and data scientists working on infrastructure projects.

1. Introduction

1.1 IMPORTANCE OF SKID RESISTANCE AND PSV IN ROAD SAFETY

Skid resistance measures the frictional properties between a vehicle's tyre and a road surface. Adequate skid resistance enhances braking performance, reducing accident risks. In the UK, PSV is used to specify the skid resistance of road surface course materials. Ensuring appropriate PSV levels minimizes safety risks and helps maintain road performance.

One such project where PSV plays a crucial role is the M25 Pavement Renewal Scheme, focused on maintaining and improving the M25 motorway network—one of the UK's busiest roads. However, the traditional method of PSV calculation is done manually, consuming time and effort and necessitating a more efficient approach.

1.2 OVERVIEW OF THE M25 NETWORK AND MAINTENANCE CHALLENGES

The M25 motorway network, managed by Connect Plus Services (CPS)—a joint venture between AtkinsRéalis, Balfour Beatty, and Egis—spans 250 miles and includes (Connect Plus Services Documentation):

- 5 tunnels.
- 2,500 structures, including bridges, culverts, and overhead gantries.
- 140,000 other highway assets.
- 73 million journeys annually.

To effectively manage this vast infrastructure, the network is divided into approximately 1,420 Highways Agency Pavement Management System (HAPMS) link sections, of which 1,357 sections have an asphalt surface course. HAPMS serves as the national pavement management system for England's motorways and trunk roads, ensuring systematic maintenance and performance monitoring. (*National Highways. National Motorway Maintenance Manual – Part 2.*)

Each year, approximately 150-200 critical link sections of the M25 are chosen for renewal works, requiring PSV calculations. Given the scale of work involved, an efficient PSV calculation process is essential to maintain road safety and to design the Pavement renewal works.

1.3   AUTOMATING PSV CALCULATIONS USING PYTHON

Traditionally, PSV calculations have been performed manually using Excel spreadsheets, which took 10-15 minutes per section. The process is time consuming, repetitive, and prone to human errors.

To address these challenges, this paper presents a Python-powered tool designed to automate PSV calculations. The tool follows the Plan-Do-Check-Act (PDCA) framework and integrates Lean principles to enhance efficiency. Key features include:

- Calculation time reduced to mere seconds.
- Minimized risk of human errors in calculation, ensuring more accurate results in accordance with the Design Manual for Roads and Bridges (DMRB CD 224 and CD 236).
- User-friendly design, allowing easy data entry.
- Significant time savings, improving overall project efficiency.

1.4   ALIGNING WITH ATKINSRÉALIS' DIGITAL VISION

This tool aligns with AtkinsRéalis' vision of advancing digital transformation in infrastructure projects. By integrating programming with civil engineering, it offers an innovative solution that enhances efficiency and accuracy in highway maintenance.

Whether you are an engineer, data scientist, or a professional interested in how digital tools can improve road safety, this paper provides valuable insights into technical innovation and real-world application.

2.   Problem Statement and Objectives

2.1   PROBLEM STATEMENT

The traditional method of calculating PSV for pavement surface course aggregates is time-consuming, repetitive, and prone to human error, as it relies on manual calculations in Excel spreadsheets. Given the scale of resurfacing projects like the M25 Pavement Renewal Scheme, there is a strong need for an automated solution that streamlines the calculation process, reduces human errors, and improves efficiency while ensuring compliance with DMRB CD 224 and DMRB CD 236.

2.2   OBJECTIVES

The following objectives were considered in solving the problem:

a. **Automated PSV Calculation:** To develop a tool to replace manual Excel-based calculations, reducing processing time, minimizing errors, and improving efficiency.

b. **Support Decision-Making:** Provide reliable, instant results that help engineers, planners, and policymakers make informed decisions during the design stage.

c. **Integrate Modern Technology:** Use modern technological advances in creating and making the tool user-friendly.

d. **Reduce Manual Workload:** Minimize repetitive manual work, allowing engineers to focus on higher-value tasks.

3. Methodology

3.1 MANUAL PROCESS ANALYSIS

The traditional PSV calculation method relies on manual data entry and spreadsheet-based computations. The process involves the following steps:

Step 1: Extracting the traffic data into the spreadsheet

Traffic data are sourced from <u>WebTRIS</u>, an online portal providing real-time traffic information from road network sensors (National Highways, 2025, *WebTRIS traffic data*). Key data parameters include:

- **Average Annual Daily Traffic (AADT):** The daily traffic volume averaged over a year.
- **Percentage of Heavy Goods Vehicles (%HGV):** The proportion of HGVs in the total traffic.
- **Year of Analysis:** The year when the traffic data was collected to account for the design period.
- **Number of Lanes:** Lane distribution is considered for traffic calculations, using Impulse Roadshow Video for reference.

Step 2: Calculation of design traffic

- **Design Period Calculation:** Considers long-term traffic projections over a **20-year period**, calculated as:

    Design Period = 20 + (Current year – Year of Data Collected)

- **Traffic Flow Calculations:** The total AADT of the HGVs is calculated (Commercial vehicle flow), a default value of 11% is applied for conservative estimates if the %HGVs are less than 11% for CPS M25 Highway renewal design.
- The total Projected AADT for the HGVs (i.e the design traffic) is calculated using the formula (DMRB CD 224 2020):

$$F_i = F \times \left((1 + R)^i \right)$$

    where F is the Commercial vehicle flow, $R = 1.54$, and i is the design period (CD 224 Ref 2.N).

Step 3: Calculation of percentage of HGVs in the heaviest loaded lane

- The total projected volume of HGVs for the design period is distributed among the lanes based on traffic loading patterns.
- The heaviest loaded lane is assigned a higher proportion of HGV traffic, ensuring realistic traffic flow representation.
- For single-lane roads, all traffic is assigned to a single lane.
- For multi-lane roads, proportional distribution is determined using advanced formulas to account for lane usage.
- These calculations align with the methodologies outlined in DMRB CD 224, Section 2.21 to ensure accurate traffic distribution (DMRB CD 224 2020).

Step 4: Extract site category and investigatory levels

- **Site Category:** Assigned based on the geometric condition of the section (CD 236 Table 3.3a)
- **Investigatory Level (IL):** Defines the minimum acceptable skid resistance, correlating with collision risk. More challenging geometries and higher accident rates require higher IL values.
- These values are provided by the pavement asset team to the pavement design team in an excel spreadsheet.

Step 5: Determining the PSV value

- The projected traffic data for each lane of the section is compared against the site category and its respective IL values to find the PSV value from DMRB CD 236 Table 3.3b (DMRB CD 236 2022).
- Refer to Figure 1 for a visual representation of Table 3.3b.

FIGURE 1

Image of Table 3.3b,

DMRB CD 236

Table 3.3b PSV for coarse aggregate in thin surface course systems complying with clause 942 of the Specification (MCHW1)

Site category	Site description	Default	IL	PSV required for given IL, traffic level and type of site									
				Traffic (cv/lane/day) at design life									
				1-250	251-500	501-750	751-1000	1001-2000	2001-3000	3001-4000	4001-5000	5001-6000	Over 6000
A	Motorway		0.30	50	50	50	50	50	50	50	53	63	63
		*	0.35	50	50	50	50	50	53	53	53	63	63
B	Non-event carriageway with one-way traffic		0.30	50	50	50	50	50	50	50	53	63	63
		*	0.35	50	50	50	50	50	53	53	53	63	63
			0.40	50	50	50	50	53	58	58	58	63	68+
C	Non-event carriageway with two-way traffic		0.35	50	50	50	50	50	53	53	58	63	63
		*	0.40	50	53	53	58	58	63	63	63	68+	68+
			0.45	53	53	58	58	63	63	63	63	68+	68+
Q	Approaches to and across minor and major junctions, approaches to roundabouts and traffic signals	*	0.45	60	65	65	68+	68+	68+	68+	68+	68+	HFS
			0.50	65	65	65	68+	68+	68+	HFS	HFS	HFS	HFS
			0.55	68+	68+	HFS	HFS	HFS	HFS	HFS	HFS	HFS	HFS
K	Approaches to pedestrian crossings and other high risk situations	*	0.50	65	65	65	68+	68+	68+	HFS	HFS	HFS	HFS
			0.55	68+	68+	HFS	HFS	HFS	HFS	HFS	HFS	HFS	HFS
R	Roundabout	*	0.45	50	55	60	60	65	65	68+	68+	68+	68+
			0.50	68+	68+	68+	68+	68+	68+	68+	68+	68+	68+
G1	Gradients 5-10% longer than 50 m		0.45	55	60	60	65	65	68+	68+	68+	68+	68+
		*	0.50	60	68+	68+	HFS	HFS	HFS	HFS	HFS	HFS	HFS
G2	Gradient >10% longer than 50 m		0.45	55	60	60	65	65	68+	68+	68+	68+	68+
		*	0.50	60	68+	68+	HFS	HFS	HFS	HFS	HFS	HFS	HFS
			0.55	68+	HFS	HFS	HFS	HFS	HFS	HFS	HFS	HFS	HFS

Table 3.3b PSV for coarse aggregate in thin surface course systems complying with clause 942 of the Specification (MCHW1) (continued)

Site category	Site description	Default	IL	PSV required for given IL, traffic level and type of site									
				Traffic (cv/lane/day) at design life									
				1-250	251-500	501-750	751-1000	1001-2000	2001-3000	3001-4000	4001-5000	5001-6000	Over 6000
S1	Bends radius <500 m – carriageway with one-way traffic	*	0.45	50	55	60	60	65	65	68+	68+	HFS	HFS
			0.50	68+	68+	68+	HFS	HFS	HFS	HFS	HFS	HFS	HFS
S2	Bends radius <500 m – carriageway with two-way traffic		0.45	50	55	60	60	65	65	68+	68+	HFS	HFS
		*	0.50	68+	68+	68+	HFS	HFS	HFS	HFS	HFS	HFS	HFS
			0.55	HFS	HFS	HFS	HFS	HFS	HFS	HFS	HFS	HFS	HFS

Step 6: Data entry and self-check

- The collected values (Step 1) are manually entered into an Excel spreadsheet, where calculations (Steps 2, 3, 4) are performed and verified.
- Refer to Figure 2 for an example of the blank excel spreadsheet layout.

FIGURE 2

Manual calculation
blank sheet layout

3.2   AUTOMATED PROCESS

The Python-based automation tool streamlines PSV calculations, reducing processing time to seconds while improving accuracy. The methodology integrates data science and civil engineering for an efficient solution.

Step 1: Data collection

- Traffic data are collected from the WebTRIS website (same as Step 1 in the manual process).
- Site category and IL values are retrieved from pavement asset datasets.

Step 2: Enter the data

- Open the PSV calculation tool: https://psvcalculator.streamlit.app/
- Input the collected data into the tool's sidebar.
- Refer to Figure 3 for the visual representation of tool layout.

Step 3: Upload the PSV table

- Upload DMRB CD 236 Table 3.3b in Excel format.
- Refer to Figure 4 for a visual representation of Table 3.3b, DMRB CD 236 in Excel.

FIGURE 3

Visual representation of
tool layout with output data
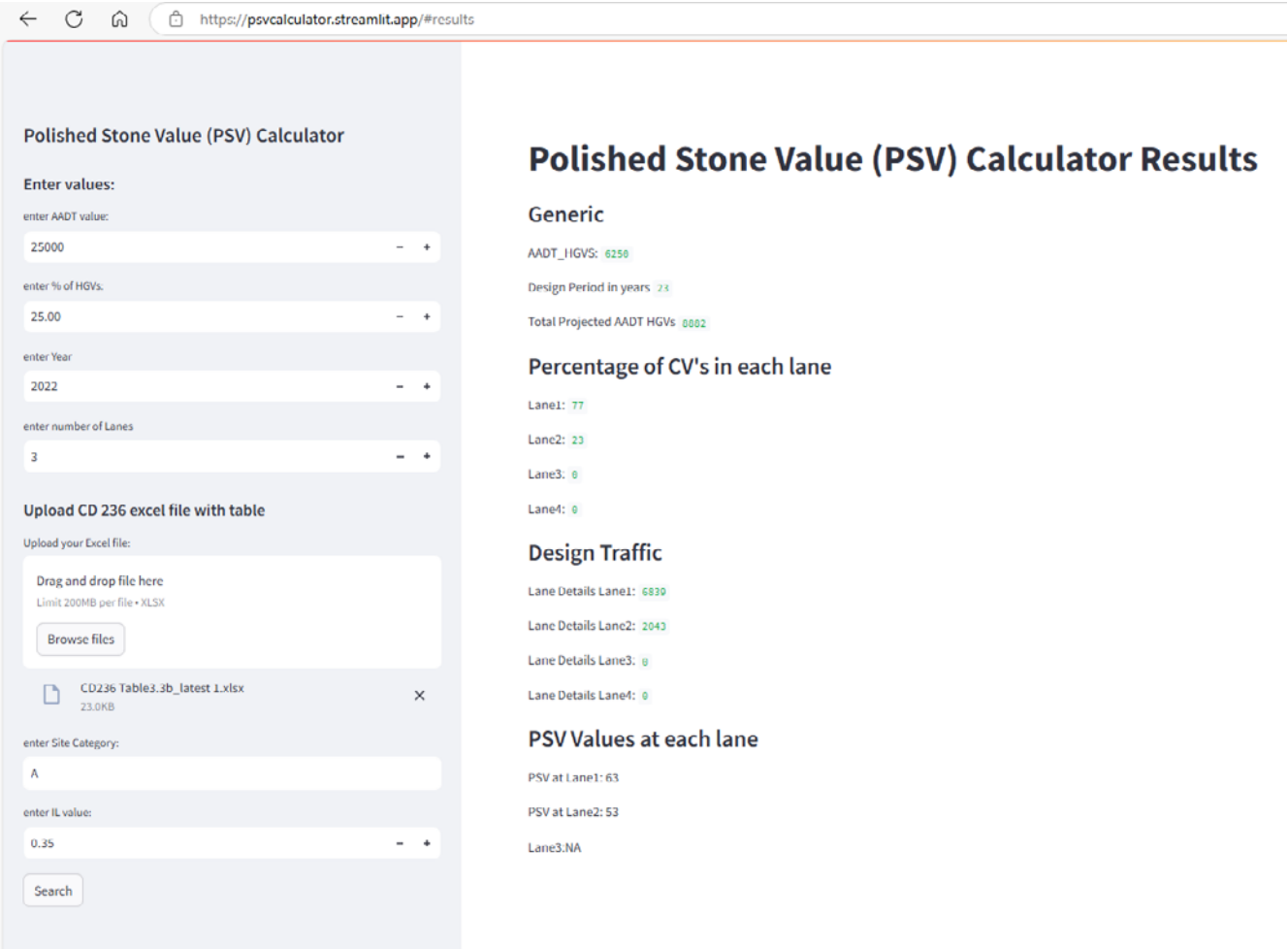
Step 4: Running the calculation

- Review the entered data to ensure accuracy.
- Click the "Search" button. The tool automatically processes the PSV calculation and displays the result instantly.
- Refer to Figure 3 for the visual representation of tool layout with output data.

FIGURE 4

Visual representation
of DMRB CD 236 Table
3.3b in Excel format

SiteCategory	SiteDescription	IL	1-250	251-500	501-750	751-1000	1001-2000	2001-3000	3001-4000	4001-5000	5001-6000	6000-50000
A	Motorway	0.3	50	50	50	50	50	50	50	53	63	63
A	Motorway	0.35	50	50	50	50	50	53	53	53	63	63
B	Non-event carriageway with one-way traffic	0.3	50	50	50	50	50	50	50	53	63	63
B	Non-event carriageway with one-way traffic	0.35	50	50	50	50	50	53	53	53	63	63
B	Non-event carriageway with one-way traffic	0.4	50	50	50	50	53	58	58	58	63	68+
C	Non-event carriageway with Two-way traffic	0.35	50	50	50	50	50	53	53	58	63	63
C	Non-event carriageway with Two-way traffic	0.4	50	53	53	58	58	63	63	63	68+	68+
C	Non-event carriageway with Two-way traffic	0.45	53	53	58	58	63	63	63	63	68+	68+
Q	Approaches to and across minor and major junctions, approaches to roundabouts and traffic signals	0.45	60	65	65	68+	68+	68+	68+	68+	68+	HFS
Q	Approaches to and across minor and major junctions, approaches to roundabouts and traffic signals	0.5	65	65	65	68+	68+	68+	HFS	HFS	HFS	HFS

Step 5: Saving the data

- Once the calculation is complete, the output can be saved as a screenshot on your drive using the following naming format:

Section Number + Date + PSV Value

4.   Problem Identification and Tool Development Process

4.1   ORIGIN OF THE IDEA

The PSV calculation problem involved inefficiencies in processing site data, leading to excessive manual input and delays in generating values. The issue was identified during a workshop with the Client CPS. During the workshop with CPS and subsequent desk analysis, it was recognized that the problem at hand bore similarities to previously encountered challenges. To address this, the principles from the *Theory of Inventive Problem Solving (TRIZ)*, developed by Genrich Altshuller, were applied. TRIZ posits that many problems have already been solved in some form; thus, by examining existing solutions across various fields, we can adapt and implement them effectively in our context. Leveraging experience in data science and reflecting on solutions identified a parallel approach that could be adapted to address the civil engineering PSV problem we face currently.

4.2   APPLYING LEAN METHODOLOGY

Lean methodology is a systematic approach to continuous process improvement through the elimination of waste. Lean methodology was developed by Kiichiro Toyoda, the founder of Toyota, after World War II. It was originally used in manufacturing, but is now used in many fields, including healthcare and software development (Simplilearn 2024).

To tackle the PSV problem, the team adopted Lean methodology, focusing on waste elimination and process improvement. The PDCA framework, a cornerstone of Lean, was selected for its iterative approach to process enhancement. The PDCA cycle supported problem resolution by enabling structured planning, execution, and continual refinement (see Figure 5).

4.2.1   PDCA Methodology to Solve the PSV Problem

The following Lean tools were instrumental in identifying issues and creating actionable plans:

- **Project Charter:** Used in the "Plan" phase to define the problem, objectives, and business case, ensuring alignment among team members.
- **Stakeholder Analysis:** Helped understand stakeholder needs, ensuring solutions were tailored to meet their requirements.
- **Process Mapping:** Enabled identification of key steps, waste analysis, baseline establishment, and opportunity identification, forming the foundation for realistic objectives.

By leveraging these tools, the team developed a project plan, selected appropriate technology, and implemented an improved process aligned with the identified needs.

FIGURE 5

PDCA framework outline for PSV calculation problem
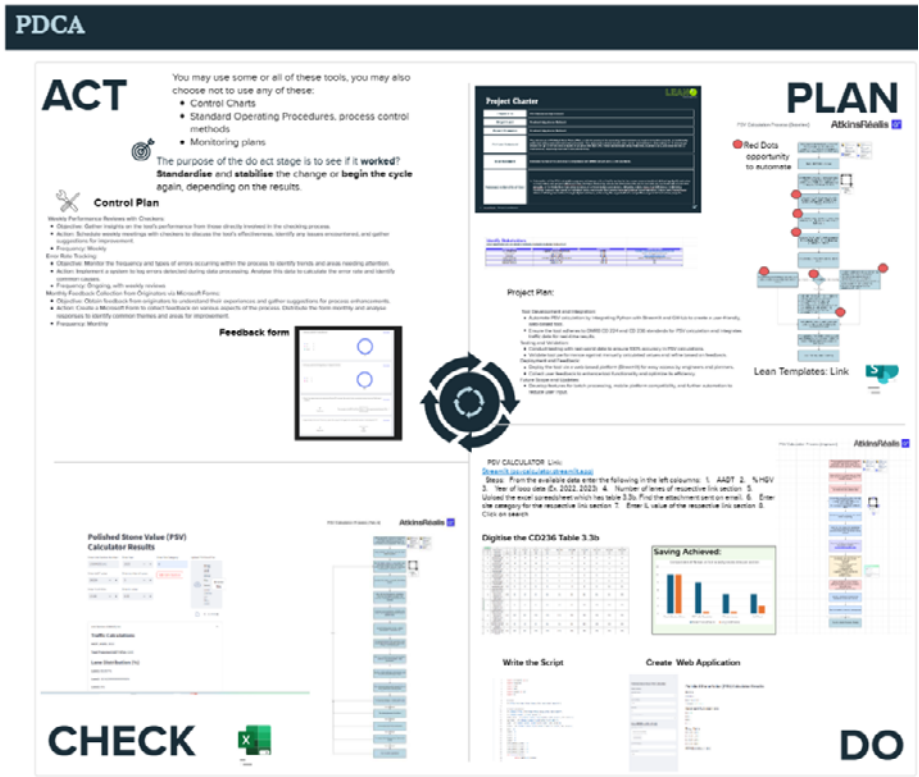
4.2.2 Benefits and Future Improvements from the PDCA Approach

The PDCA approach proved particularly advantageous due to its:

- **Iterative Nature:** The framework allowed the team to implement changes in phases, with each cycle building on feedback from the previous one.
- **Lean Focus:** It aimed to remove waste where automation was not possible. For example, the client's spreadsheet, provided in a specific format, only became valuable once the client adapted by submitting data in a more structured frame.
- **Flexibility:** During the "Check" phase, the team identified an opportunity to remove 90 percent of manual input within the improved process by enabling data uploads in a CSV format. This improvement will reduce manual effort significantly, saving time allowing the PSV value to be populated automatically for any number of resurfacing sites.

The iterative and flexible nature of PDCA also helped identify future opportunities for enhancement. These include:

- Further detailing processes to ensure clarity.
- Optimising automation using Dynamo to import CSV data directly into CAD, reducing manual entry time and minimising errors.

These opportunities will be incorporated into the "Plan" stage of the second PDCA cycle. Before initiating Cycle 2, the team will monitor the current process closely to capture errors, challenges, and stakeholder feedback. Addressing these findings will drive continuous improvement and ensure better alignment with stakeholder needs in the next iteration.

4.3   TECHNOLOGY STACK

The PSV calculation tool was developed using the following technologies:

1. **Python:** Python is a high-level, interpreted programming language known for its simplicity, readability, and versatility created by Guido van Rossum in 1991 (Python Software Foundation, 2024). Key features include:

    - **Easy to Read and Write:** Uses simple English-like syntax, making it beginner-friendly.
    - **Interpreted Language:** Code is executed line by line, simplifying debugging and testing.
    - **Cross-Platform:** Python runs seamlessly on Windows, macOS, and Linux.
    - **Open-Source:** Free to use and has a large supportive community.
    - **Extensive Libraries:** Python comes with an extensive collection of libraries that simplify development by offering pre-written code for tasks ranging from web development to scientific computing.

2. **Pandas and Math Libraries:**

    - **Pandas:** This powerful Python library is essential for data manipulation and analysis. It offers flexible data structures like Data Frames and Series, making it easier to work with structured data (such as tables or spreadsheets) (Pandas Development Team, 2024).
    - **Math:** This built-in library provides mathematical functions, supporting calculations like trigonometry, square roots, and logarithms.

3. **Streamlit:** Streamlit is an open-source Python library designed to create interactive web applications for data science and machine learning projects. It allows developers to quickly turn Python scripts into web apps without needing front-end development skills, providing an easy-to-use interface for the tool (Streamlit, 2025).

4. **GitHub:** GitHub is a cloud-based platform for version control, allowing developers to collaborate, manage code, and track changes using Git. It ensures smooth team collaboration and code management across different versions (GitHub, 2025).

A sample of the code used in the PSV calculation tool is displayed in Figure 6.

FIGURE 6

Code snippet for PSV
tool development

```
1    import streamlit as st
2    import requests
3    import time
4    import math
5    import pandas as pd
6    import os
7
8    # Title
9    st.title("Polished Stone Value (PSV) Calculator Results")
10
11   # Input parameters
12   st.sidebar.title ("Polished Stone Value (PSV) Calculator")
13   st.sidebar.header ("Enter values:")
14   aadt_value = st.sidebar.number_input("enter AADT value:", min_value=0)
15   per_hgvs = st.sidebar.number_input("enter % of HGVs:")
16   year = st.sidebar.number_input("enter Year", min_value=0)
17   lanes = st.sidebar.number_input("enter number of Lanes", min_value=1)
18   pcvl = 0
19   lane1 = 0
20   lane2 = 0
21   lane3 = 0
22   lane4 = 0
23   lane_details_lane1 = 0
24   lane_details_lane2 = 0
25   lane_details_lane3 = 0
26   lane_details_lane4 = 0
27   def roundup(value):
28           return math.ceil(value)
29
30
31   if year == 0 :
32           design_period=0
33
```

5.   Features of the Tool

5.1   USER-FRIENDLY INTERFACE
Built with Streamlit, this tool was designed with simplicity in mind, ensuring ease of use for anyone interacting with it. Users can:

- Enter traffic and design data via a streamlined sidebar.
- Upload an Excel file containing CD 236 Table 3.3b for PSV data.
- View results instantly through real-time calculations.
- Refer to Figure 3 for the visual representation of tool layout with output data.

5.2   CORE PYTHON LOGIC
At the core of the tool is Python, a powerful programming language known for its simplicity and efficiency. By utilizing libraries like Pandas and Math, the tool simplifies data handling and ensures reliable traffic projections and accurate PSV calculations.

> **The best part?** Since **Streamlit** is open source, the code developed to automate **PSV calculations** is available to everyone. Users can find it on **GitHub** at <u>highway/psvcalculator.py</u>, and can even contribute by adding new features to benefit collaboration of the wider civil and highway engineering community.

5.3   RESULTS DISPLAY
The tool delivers actionable insights:

a. **Traffic Projections**
   a. AADT for heavy vehicles
   b. Design period
   c. Projected AADT values over the design period

b. **Lane-Wise Distribution**
   a. Percentage of commercial vehicles per lane
   b. Lane-specific traffic values

c. **PSV Values**
   a. Calculated for each lane based on traffic and site-specific data

6. Testing Methodology

To ensure the tool operates as expected and provides a seamless user experience, a thorough testing process was carried out. The objective was to ensure the tool's accuracy, handle real-world challenges, and deliver optimal performance.

6.1 FUNCTIONAL TESTING

First, we tested the core functionality to ensure the tool accurately calculates PSV values based on the provided input. Over 100 different test cases, including varied lane numbers and site categories, were evaluated. We compared the tool's results with manually calculated PSV values to verify its accuracy. This was key in ensuring the tool adhered to all relevant standards.

6.2 BOUNDARY TESTING

Next, we pushed the tool to its limits by testing extreme values—both low and high. We also tested scenarios where data might be missing to see how the tool handles these outliers. This ensured that the tool remains stable and reliable under all conditions without crashing or malfunctioning.

6.3 USABILITY TESTING

To evaluate how user-friendly the tool is, we brought in actual end-users from the AtkinsRéalis GTC team and the CPS team. Their feedback helped confirm that the interface was intuitive, the tool was easy to navigate, and users could quickly input data and understand results without needing extensive training.

6.4 COMPLIANCE TESTING

Finally, the tool underwent compliance testing to ensure it met all relevant standards and guidelines required for the calculation as per DMRB CD 224 and CD 236. This was necessary to make sure the tool adhered to data handling and the project's technical requirements. The tool was also evaluated for compatibility with the overall system, ensuring it would integrate seamlessly.

7.   Results and Insights

The results from testing were promising, confirming that the tool was performing as expected:

- **Accuracy:** The tool consistently delivered accurate results, matching manual calculations in all test scenarios.
- **Stability:** Even with higher value inputs or with missing inputs the tool held up well, performing without errors or crashes notifying about the missing details.
- **User-Friendliness:** Feedback from usability testing showed that the tool's interface was easy to use and was intuitive. Users were able to navigate the system with minimal effort, which was a key success.

A bar chart comparing the time taken for each step in the manual process versus the automated tool reveals key insights, as shown in Figure 7:

- **Data Collection and Entry:** Time remains the same (~10 minutes) in both methods.
- **HGV Traffic Calculation:** The app is significantly faster (seconds vs. ~9 minutes manually).
- **PSV Value Lookup:** Nearly instant with the app, compared to ~5 minutes manually.
- **Self-Check:** Reduced from ~5 minutes manually to ~1.5 minutes using the app.

Overall, the app-based process saves substantial time, especially in calculations and PSV value lookup.

Comparison of Time Taken
for Manual vs. App-Based
PSV Calculation Process

Comparision of Manual vs Tool based process time per section

Legend: Manual Process (Minutes), Using Tool (Minutes)
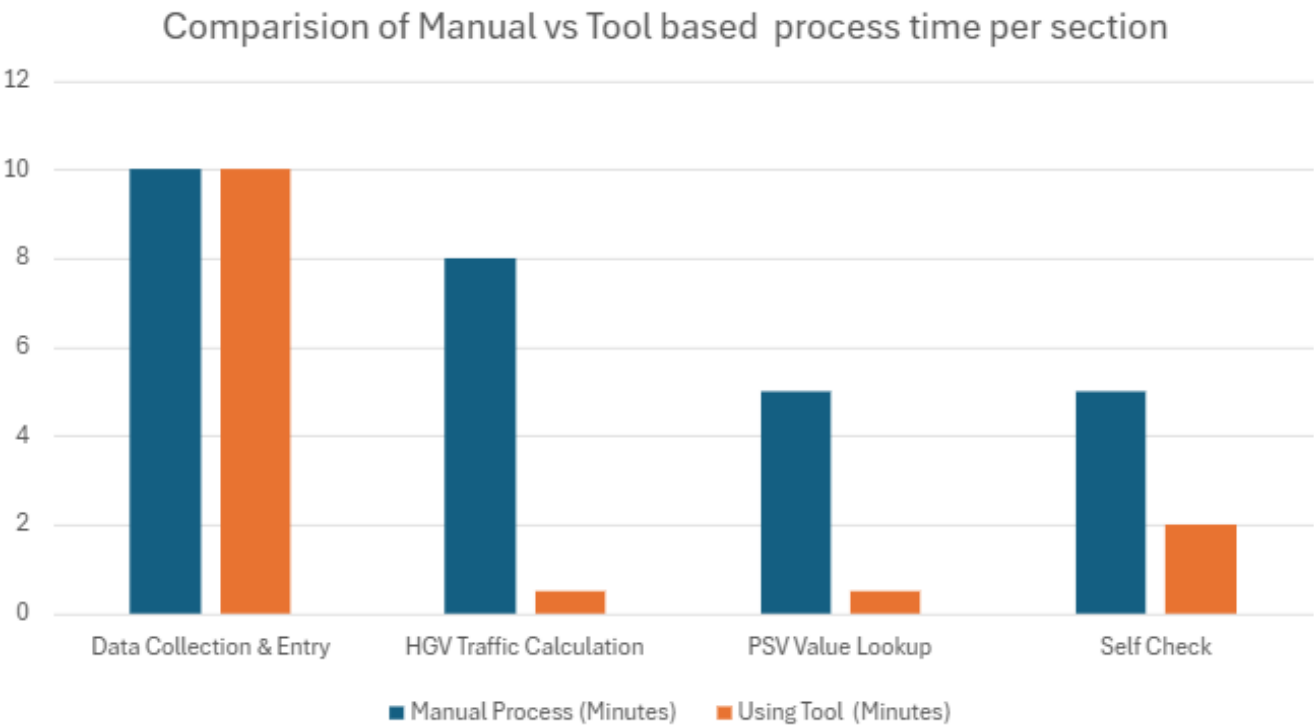
8.   User Feedback

The following feedback was received from the end user/client who used the tool:

Just writing regarding my experience with your PSV tool. It's been an absolute game changer for both fast calculations of PSV values and checking the calculated PSV values. I have used it last year and this for my packages, 24PP15 and 25PP04 to check my values and the results were accurate. A very convenient tool to have, so well done for your hard work in creating it.

Benjamin Osei Owusu, BEng GMICE
Assistant Highway Engineer
Connect Plus Services
Leatherhead, UK

I used PSV calculator couple of times and found it as an excellent tool for verifying the calculated values of PSV and to generate new values, ensuring accuracy and efficiency. The interface of the app is very user-friendly and the tool helps identify discrepancies in the calculation effectively with lots of time savings. With a few refinements, it has the potential to become an indispensable asset for PSV analysis. Overall, it's a valuable validation tool with great potential!

Jawad Amjad Ghauri, PMP, IntPE (Aus), CPEng (Aus), MCIHT, MCIArb
Senior Pavement Engineer
Connect Plus Services
Leatherhead, UK

I wished to comment on my impression on the Polish Stone Value (PSV) calculator developed by you. While working on the PSV sheet for 25PP29, I utilized the application to verify my traffic data and manually calculated PSV values. I am pleased to report that the results produced by the application aligned perfectly with my own calculations.

This feature proved to be extremely useful, as it allowed me to quickly identify any potential errors in my manual calculations. A couple of errors were identified by using the tool. The application significantly saved me time by providing an efficient means of cross-checking the given data and ensuring accuracy throughout my process.

Smriti Singh

Graduate Engineer

AtkinsRéalis, GTC Bangalore

9.   Conclusion

This Python-based PSV calculator truly showcases the power of technology in making civil engineering calculation more efficient and accurate. It's not just about simplifying complex calculations, it's also about improving road safety and encouraging learning across disciplines.

By reducing what used to take minutes down to just a few seconds, and eliminating the potential for human error, this tool marks a big step forward in how we work. Also, its compliance with DMRB CD 224 and CD 236 means it meets the standards required for today's infrastructure projects.

Whether you're a policymaker, a developer or a student, this tool invites you to dive into the exciting world where data and design come together.

The tool's efficiency becomes apparent when compared to traditional methods. A process that once took 10-15 minutes per road section is now completed in seconds, offering engineers a powerful advantage during review and decision-making.

Key Benefits:

- **Time Savings:** By automating the process, calculation time has been slashed by about 60 percent.
- **Error Reduction:** We've removed the human error factor to an extent, though care is still needed when entering the initial data.
- **Increased Productivity:** With less time spent on calculations, engineers can now devote their energy on other aspects of the project.

10.   Future Scope

As per the opportunities identified in the PDCA the second cycle of development should include:

1. **CSV Input and Output:** To enable the tool to receive inputs in a CSV format and produce the output in the downloadable format of CSV, further eliminating manual data entry errors.
2. **Dynamo Script Integration:** Developing a Dynamo script to automate the annotation of the calculated PSV values directly into CAD drawings. This will create an end-to-end solution, eliminating the need for manual entry and reducing human error at multiple stages of the workflow.

10.1   FUTURE CONSIDERATIONS

As automation, AI, and machine learning increasingly shape our design landscape, it's essential to pause and reflect on the responsibilities that accompany these tools. With platforms like the PSV tool and similar applications, we must focus on the *Voice of the Customer*. Ultimately, whether we rely on automation or manual calculations, the responsibility for delivering accurate outcomes—and the associated liability—remains with us, the supplier. This raises an important question: How do we ensure our tools are consistently fit for purpose and that their outputs are trustworthy? The answer lies in robust verification and validation processes that reinforce confidence in our deliverables.

The designer's role may be evolving. No longer burdened by repetitive calculations, the modern designer may increasingly take on the role of validating tools and ensuring process integrity. In doing so, we not only safeguard the quality of our outputs but also strengthen the trust our customers place in our solutions.

Acknowledgements

References

British Standards Institution (BSI). (2020). *Test for mechanical and physical properties of aggregates—Part 8 : Determination of polished stone value (BS EN 1097-8)*. BSI, London.

Connect Plus Services. *Documentation*. Retrieved February 7, 2025, from https://www.connectplusm25.co.uk/connectplusservices/

GitHub. (2025). *GitHub documentation*. Retrieved from https://docs.github.com/en

Impulse Geophysics. *Impulse Geophysics Roadshow*. Retrieved February 7, 2025, from https://connectplus.impulsegeo.com

National Highways. (2020). *Traffic Assessment* (DMRB CD 224, Revision 0). National Highways.

National Highways. (2022). *Surface course materials for construction* (DMRB CD 236, Revision 4.1.0). National Highways.

National Highways. *National Motorway Maintenance Manual – Part 2*. Retrieved February 7, 2025, from https://nationalhighways.co.uk/media/kenjqqp2/nmm_part_2.pdf

National Highways. (2025). *WebTRIS traffic data*. Retrieved from https://webtris.highwaysengland.co.uk/

Pandas Development Team. (2024). *Pandas documentation*. Retrieved from https://pandas.pydata.org/

Python Software Foundation. (2024). *Python Documentation (Version 3.x)*. Retrieved from https://docs.python.org/3/

Simplilearn. (2024). *Lean methodology article*. Retrieved from https://www.simplilearn.com/lean-methodology-article

Streamlit. (2025). *Streamlit documentation*. Retrieved from https://docs.streamlit.io/

03: Utilizing Vendor Data for Early Reliability Assessment in Rail and Transit Systems: Overcoming Sparse Data Issues

Significance Statement

Reliable rail and transit systems are essential for safe and efficient operations but estimating failure rates for high-reliability components often faces challenges due to sparse data, such as zero observed failures during truncated tests. This study compares three advanced statistical methods—Classical, Frequentist, and Bayesian—to address this issue using vendor test data from a critical rail component. Frequentist and Bayesian approaches provide conservative and realistic failure rate estimates that align with field data, unlike Classical methods that underestimate risks. These findings empower engineers to optimize maintenance schedules, improve safety margins, and reduce costs, offering clients robust tools for risk management and system design.

Énoncé d'importance

Des systèmes de transport ferroviaire et de transport en commun fiables sont essentiels à des opérations sûres et efficaces, mais l'estimation des taux de défaillance des composants à haute fiabilité présente souvent des défis en raison du manque de données, comme l'absence de défaillances observées pendant les essais tronqués. Cette étude compare trois méthodes statistiques avancées - classiques, fréquentistes et bayésiennes – pour aborder cette question, en se basant sur des données d'essai des fournisseurs issues d'un composant ferroviaire essentiel. Les approches fréquentistes et bayésiennes fournissent des estimations prudentes et réalistes du taux de défaillance qui correspondent aux données du terrain, contrairement aux méthodes classiques qui sous-estiment les risques. Ces résultats permettent aux ingénieurs d'optimiser les calendriers d'entretien, d'améliorer les marges de sécurité et de réduire les coûts, tout en offrant aux clients des outils robustes pour la gestion des risques et la conception des systèmes.

Behrooz Ebrahimi
RAMS Analyst, CPI
Canada – Rail, Transit & Mobility TPO
Montreal, Canada

Abstract

Reliability estimation in rail and transit systems is crucial for ensuring operational safety and cost efficiency. This paper addresses the challenge of estimating parts failure rate (λ) under sparse data conditions, a common issue in high-reliability components. We investigate three approaches: Classical (Maximum Likelihood Estimation), Frequentist (Chi-squared confidence bounds), and Bayesian inference with Jeffreys prior.

The study presents a case involving a critical rail component – the Controller and Contact Monitoring Board within a wayside controller – used in a light rail transit (LRT) project. Vendor-provided reliability data from a 500,000-hour time-censored reliability test with zero observed failures is analysed. We compare the three methods for estimating the failure rate and validate these estimates against field data collected from similar components in operating LRT systems. Our findings reveal that:

- The Classical method, even with a pseudo count, tends to underestimate the failure rate compared to field data.
- The Frequentist and Bayesian approaches provide more realistic estimates that align better with observed field performance, accounting for the uncertainty associated with sparse data.

This research provides RAMS engineers in the rail and transit sectors with robust analytical tools for reliability assessments, especially when dealing with limited failure data. The comparative analysis, validated with field data, enables more informed decision-making in system design, maintenance planning, and risk management under uncertainty, contributing to enhanced system efficiency and safety in rail and transit operations.

1. Introduction

The reliability of rail and transit systems is essential for ensuring safe, efficient, and cost-effective operations. These systems operate in complex environments where failures can lead to significant safety risks to the passengers and financial consequences. Reliability, Availability, and Maintainability (RAM) assessments provide a structured framework for understanding system performance and guiding decisions that balance operational safety with lifecycle costs [1, 2].

Over the past decades, improvements in manufacturing quality and process control have led to increasingly reliable components. However, a persistent challenge in RAM assessments is the accurate estimation of reliability metrics particularly under sparse data conditions. New or specialized systems often lack sufficient operational history, resulting in limited or zero-failure data during reliability tests or in-service operations.

Traditional reliability estimation methods, such as Maximum Likelihood Estimation (MLE), struggle in these scenarios because they rely heavily on extensive datasets. Sparse data can arise from factors such as rare failure events, limited testing durations, or incomplete data collection processes, leading to high uncertainty in reliability estimates [3]. Inaccurate reliability estimates can have significant consequences - overestimating failure rates may result in over-engineered designs, excessive preventive maintenance schedules, and increased costs. Conversely, underestimating failure rates can delay necessary maintenance actions, introduce latent risks during operations, and compromise safety margins [4]. Addressing these challenges requires advanced statistical methods capable of delivering meaningful results even with limited failure data.The consequences of inaccurate reliability estimates are significant- designers may struggle to make informed trade-offs between design alternatives, system specifiers may find it difficult to set achievable safety targets, potentially delaying regulatory approvals, and clients may face increased lifecycle costs due to underestimating failure rates.

When accelerated life testing (ALT) is not feasible or cost-effective, reliability tests are performed under normal operating conditions. These tests cannot continue indefinitely and are often truncated either by failure or time. In failure-truncated tests, data collection stops after a predefined number of failures, leaving uncertainty about the reliability of components that have not failed. In time-truncated tests, testing concludes after a fixed observation period, potentially without capturing sufficient failure data. Both scenarios result in censored data, which leads to biased estimates when analysed using classical methods that do not account for incomplete information. This censoring introduces a systematic underestimation of true reliability, as potential failures beyond the test duration are not considered.

Vendor-provided data offers a potential solution to mitigate sparse data issues by supplementing field observations with test results or warranty claims. However, vendor data is frequently incomplete or inconsistent with current designs and may also be truncated due to practical constraints during testing. These limitations necessitate robust analytical techniques capable of addressing sparse or censored data while integrating prior knowledge. Advanced statistical approaches such as Frequentist inference and Bayesian methods provide tools to overcome these limitations by incorporating prior knowledge and probabilistic modelling.

2.   Methodology

This section examines three approaches for reliability parameter estimation under sparse data conditions: Classical metrics, Frequentist approach, and Bayesian inference. Each method is analysed for its applicability to rail system components where few or zero-failure scenarios are common.

2.1   CLASSICAL RELIABILITY METRICS AND THEIR LIMITATIONS

Reliability analysis often relies on classical metrics such as the failure rate and Mean Time Between Failures (MTBF) to quantify system performance. These metrics provide fundamental insights into the expected reliability of engineering systems. The failure rate is defined as

$$\lambda = n/T$$

where T is the total observation time and n is the total number of observed failures. The MTBF is the reciprocal of the failure rate:

$$MTBF = 1/\lambda$$

MTBF is typically used for repairable systems and is widely applicable when the failure distribution follows an exponential model. In contrast, the Mean Time to Failure (MTTF) measures the expected time to the first failure and is primarily used for non-repairable products or systems.

These metrics assume a constant failure rate, which means that failure times for the component or system under investigation can be adequately modelled by the Exponential Distribution. For repairable systems, this means the Homogeneous Poisson Process (HPP) model applies where all infant mortality failures have been eliminated from the product through a rigorous Environmental Stress Screening (ESS) program [1]. The system or device is therefore considered operating in the flat portion or the "constant failure rate" region of the bathtub curve.

Despite their widespread use, classical reliability metrics exhibit significant limitations when applied to sparse or truncated data. These limitations become particularly evident in scenarios where failure observations are minimal or entirely absent, leading to unreliable reliability estimates. One major challenge arises in the case of zero observed failures. When no failures occur during the observation period, the classical failure rate calculation becomes zero, which can lead to misleading conclusions such as an infinitely high MTBF or a zero-failure rate. These interpretations do not accurately reflect the system's actual reliability and can result in overly optimistic assessments.

It is possible to relax this limitation by conservatively assuming that a failure occurs in the very next instant. Then, $n = 1$ can be used to evaluate an upper confidence limit of failure rate. This approach is often referred to as using a "pseudo count". The pseudo count method adds a small constant (typically 1) to the observed number of failures to avoid zero estimates. This conservative modification, although sometimes used by reliability engineering practitioners to allow a complete statistical analysis, lacks a firm statistical basis.

Similarly, when only a small number of failures are recorded, the estimated MTBFs are subject to substantial statistical uncertainty, making them highly unreliable for decision-making in safety-critical applications. The confidence intervals for these estimates become extremely wide, indicating a high degree of uncertainty in the true reliability parameters.

Given these limitations, alternative statistical methods such as Frequentist inference and Bayesian approaches are necessary to address the challenges posed by sparse or censored data. By leveraging such approaches, engineers can derive more meaningful insights into system reliability, ensuring more informed decision-making in design or maintenance planning and risk assessment. These advanced methods provide a means to quantify uncertainty in reliability estimates, allowing for more robust predictions and better-informed decisions in the face of limited failure data.

2.2 STATISTICAL METHODS FOR RELIABILITY ESTIMATION

Classical statistical inference, often referred to as the Frequentist approach, involves using statistical inference to derive confidence bounds for reliability parameters without incorporating any prior knowledge. This method assumes that observed failure data follows a probability distribution, from which confidence bounds on reliability metrics such as failure rate can be calculated.

Consistent with the previous section, we maintain the assumption of exponentially distributed failure times, which is fundamental to the applicability of the subsequent chi-squared analysis.

Confidence intervals can be constructed using either one-sided or two-sided bounds. A two-sided confidence interval provides both lower and upper limits for the failure rate, while a one-sided bound focuses only on the minimum or maximum possible value. In reliability assessments and industry practice, particularly in safety-critical applications, one-sided confidence bounds are often preferred, as they provide a conservative upper estimate to ensure compliance with reliability requirements.

Therefore, for the purpose of this study, we will use one-sided upper confidence bounds to estimate failure rate. Given a system tested for a cumulative time T with observed failures n, the one-sided upper confidence bound for the failure rate can be expressed as:

$$\lambda_{upper} = \frac{\chi^2_{1-\alpha,2n+2}}{T}$$

where $\chi^2_{1-\alpha,\nu}$ is the critical value of the chi-squared distribution with ν degrees of freedom and significance level α.

In the special case of zero failures ($n = 0$), which is particularly relevant for high-reliability components in rail and transit systems, the degree of freedom (ν) is 2 and the chi-squared distribution reduces to the exponential distribution. Therefore:

$$\lambda_{upper} = -\frac{\ln{(\alpha)}}{T}$$

As a result, the upper bound of failure rate can be estimated without referring to statistical tables. This provides a practical and conservative estimate for reliability assessment in safety-critical applications, ensuring compliance with stringent industry requirements.

2.3   BAYESIAN INFERENCE

Bayesian inference is a statistical framework that updates probability estimates as new data becomes available. In contrast to frequentist methods that rely solely on observed data, Bayesian methods combine prior knowledge from a variety of sources including historical records, experimental data, and expert judgment to deliver a more flexible and adaptive estimation process. This approach has been widely adopted in various scientific and engineering disciplines, including reliability engineering due to its ability to integrate expert judgment and historical data.

The foundation of Bayesian inference lies in Bayes' theorem, which expresses the posterior probability distribution as a function of the prior distribution and the likelihood of observed data. Mathematically, this is represented as:

$$P(\lambda|data) = \frac{P(data|\lambda)P(\lambda)}{P(data)}$$

Where:

- $P(\lambda\backslash data)$ is the posterior probability of λ given the observed data.
- $P(data\backslash\lambda)$ is the likelihood of observing the data given λ.
- $P(\lambda)$ is the prior probability distribution of λ.
- $P(data)$ is the marginal likelihood (or evidence).

For a system tested for time T with n failures, assuming a Poisson process, the likelihood function is:

$$P(data|\lambda) = \frac{(\lambda T)^n e^{-\lambda T}}{n!}$$

The choice of prior in Bayesian inference depends on our confidence in the available data - in scenarios where data quality is low, more informative priors incorporating trusted external evidence may be warranted, whilst when data is limited but we want an objective baseline, a non-informative choice like Jeffreys prior is appropriate. In our analysis, given the zero-failure vendor test results, we adopt Jeffreys prior to let the likelihood drive the inference without imposing additional external bias [5, 6]. For Poisson processes, the formal Jeffreys prior is:

$$\pi(\lambda) \propto \frac{1}{\sqrt{\lambda}}$$

This prior is derived from Fisher information and provides a theoretically sound basis for inference, even in zero-failure scenarios. Combining the Jeffreys prior with the Poisson likelihood using Bayes' theorem, the posterior distribution becomes:

$$\lambda | n, T \sim Gamma(n + 0.5, T)$$

This posterior distribution encapsulates our updated knowledge about the failure rate after observing the data.

As stated in the previous section, for reliability analysis, we often focus on the upper confidence bound. Given a confidence level α, the Bayesian upper bound λ is:

$$\lambda = \frac{\chi^2_{1-\alpha, 2n+1}}{2T}$$

where $\chi^2_{1-\alpha, \nu}$ is the critical value of the chi-squared distribution with ν degrees of freedom and significance level α.

3.   Case Study: Wayside Controller and Contact Monitoring Board

In railway signalling systems, the wayside controller is a critical component that manages trackside equipment such as signals, switches, and crossings, ensuring safe and efficient train operations by processing commands and relaying status information between the central control system and the physical railway infrastructure. Within the wayside controller, the controller and contact monitoring board plays a pivotal role by overseeing vital inputs like track circuit statuses and relay detections and storing essential software components necessary for system operation. The reliability and performance of this board are central to the overall safety and efficiency of railway signalling systems, making it a focal point in failure rate assessments, particularly when failure data is limited. Accurate evaluation of its failure rates is essential for determining appropriate maintenance and replacement intervals, as environmental factors such as temperature fluctuations can significantly impact the lifespan of electronic components in wayside signalling systems. This case study examines the application of three reliability estimation methods to a controller and contact monitoring board used in the wayside controller system of a light rail transit (LRT) project.

This case study highlights how conservative failure rate estimates derived from Frequentist and Bayesian Inference methods directly inform stakeholder decisions. Designers benefit from the upper confidence bound, which allows for a risk-aware comparison of alternative solutions, such as redundancy versus component upgrades. System specifiers can use these bounds to set achievable safety targets that account for sparse data limitations, ensuring compliance without over-engineering the system. Finally, clients gain confidence in lifecycle cost projections by validating vendor-provided data against field performance, which reduces financial uncertainty during system acceptance.

To illustrate the challenges of reliability estimation with sparse data, we analyse vendor-provided reliability data for the controller and contact monitoring board. As part of their standard reliability testing process, the vendor conducted a 500,000-hour time-censored test under operational conditions, during which zero failures were observed.

The vendor's pass/fail criterion may require this test duration to certify batch reliability. However, translating zero-failure results into meaningful reliability parameters remains a challenge due to the inherent limitations of sparse data. To address this, we employ three different methodologies to estimate the failure rate. The objectives of the analysis are to:

- Estimate the failure rate of the controller and contact monitoring board using three methods: Classical (MLE), Frequentist (Chi-squared), and Bayesian (Jeffreys prior).
- Compare the results of these three methods, given the zero-failure data after 500,000 hours of testing at a 90% confidence level.
- Compare the failure rate estimates obtained from these three methods with field data for the same component.
- Discuss the implications of these estimates in the context of rail system maintenance and risk management within the LRT project.

The results of the three failure rate estimation methods are summarised in Table 1.

TABLE 1	Method	Failure Rate (failures/hour)
	Classical (MLE)	2.0×10^{-6}
Failure Rate Estimates	Frequentist (Chi-squared)	4.60517×10^{-6}
from Vendor Test Data	Bayesian (Jeffreys prior)	2.30258×10^{-6}

3.1   COMPARISON WITH FIELD DATA AND DISCUSSION

To validate our failure rate estimates, we compared the results from the three methods with field data collected from several light rail transit projects using the same controller and contact monitoring boards. This field data is summarised in Table 2.

TABLE 2

Field Data from Light
Rail Transit Projects

No. of Boards	Operating Time (Hours)	No. of Failures	Failure Rate (failures/hour)
385	5100000	30	5.88235×10^{-6}
216	1900000	5	2.63158×10^{-6}
282	3700000	25	6.75676×10^{-6}
138	1200000	4	3.33333×10^{-6}

Based on the field data, the failure rates vary between 2.63158×10^{-6} and 6.75676×10^{-6} failures/hour. Comparing these values with our estimates from the vendor test data (Table 1), we observe the following:

- The Classical method estimate from vendor data (2.0×10^{-6} failures/hour) is lower than all of the field data points.
- The Frequentist method estimate from vendor data (4.60517×10^{-6} failures/hour) falls within the range observed in the field data.
- The Bayesian method estimate from vendor data (2.30258×10^{-6} failures/hour) is at the lower end of the range observed in the field data.

These results suggest that the Frequentist and Bayesian methods, which account for the uncertainty associated with sparse data, provide estimates that are more consistent with real-world field performance than the Classical method with pseudocount.

The Classical method, even with the pseudocount, produces a single-point estimate that doesn't reflect the uncertainty inherent in sparse data, often underestimating the true failure rate. The Frequentist approach provides a more conservative upper bound, which is valuable for regulatory compliance and risk management within the LRT project and tends to align more closely with the higher failure rates observed in some field deployments. The Bayesian approach with Jeffreys prior offers a balanced perspective by incorporating prior knowledge and providing a more nuanced estimate of the failure rate that also aligns reasonably well with the field data.

The estimated failure rates have practical implications for safety and reliability of the wayside controller and contact monitoring board within the LRT project. The more conservative Frequentist estimate may be used to set strict maintenance intervals and safety margins. The Bayesian estimate can inform decisions about component design and selection, balancing cost and reliability. This multi-faceted approach enables engineers to make more informed decisions about system design, maintenance planning, and risk management, ultimately contributing to enhanced system efficiency and safety in rail and transit operations. The accurate evaluation of the board's failure rates is essential for determining appropriate maintenance and replacement intervals, as environmental factors such as temperature fluctuations can significantly impact the lifespan of electronic components in wayside signalling systems.

The preceding sections have demonstrated the importance of careful analysis when dealing with sparse failure data, as is often encountered in the rail and transit industries. By comparing three different methodologies and validating them against field data, we are better equipped to make informed decisions based on an understanding of the strengths and limitations of each approach. In this case study, the Frequentist and Bayesian methods provided failure rate estimates that more closely aligned with the field data than the Classical method.

4.   Conclusion

This paper explored three methods for estimating failure rates under sparse data conditions, a common challenge in the rail and transit industry. Through a case study involving a critical component in a light rail transit project, we demonstrated the limitations of the Classical method (MLE) and the advantages of the Frequentist (Chi-squared) and Bayesian (Jeffreys prior) approaches.

Our findings, validated against field data, indicate that statistical methods that account for uncertainty, such as the Frequentist and Bayesian methods, provide more realistic and reliable failure rate estimates when dealing with sparse data. These methods offer a more balanced perspective for decision-making in system design, maintenance planning, and risk management, ultimately contributing to enhanced safety and efficiency in rail and transit operations.

Limitations and Future Works: Future research could explore the application of these methods to a wider range of rail and transit components and systems, as well as investigate the use of more informative priors in the Bayesian analysis to further refine the accuracy of the reliability estimates.

References

1. Mahboob, Qamar, and Enrico Zio, eds. Handbook of RAMS in railway systems: theory and practice. CRC Press, 2018.

2. CENELEC - CLC/TR 50126-3 - Railway applications – The specification and demonstration of Reliability, Availability, Maintainability and Safety (RAMS) – Part 3: Guide to the application of EN 50126-1 for rolling stock RAM

3. Leoni, Leonardo, et al. "Reliability estimation under scarcity of data: a comparison of three approaches." *Mathematical Problems in Engineering* 2021.1 (2021): 5592325.

4. Vališ, David, et al. "City Bus Reliability Measurement Based on Sparse Field Data Supported by Selected State Space Models." *Transportation Research Record* (2024): 03611981241263563.

5. Li, Haiyang, and Zeyu Zheng. "Reliability Estimation for Zero-Failure Data Based on Confidence Limit Analysis Method." *Mathematical Problems in Engineering* 2020.1 (2020): 7839432.

6. Keats, R. B., & Ashmore, A. D. (1997). Bayesian methods in reliability estimation: An overview. *IEEE Transactions on Reliability, 46*(2), 211–219.

04: Enhancing Infrastructure Resilience through Digital Twin Development: A Case Study of the Structures Moonshot Project

Significance Statement

The UK's ageing highways are vital but challenging to inspect and maintain due to hidden issues, causing safety risks and disruptive inspections that inconvenience the public. This research reveals how integrating data from various non-destructive testing (NDT) methods into a digital twin model can enhance bridge inspection and infrastructure management. By creating a unified 3D model, this approach improves how defects are visualised and analysed, leading to more informed maintenance and design decisions. This work represents an advancement in the interoperability gap towards digitising asset management for ageing infrastructure.

Énoncé d'importance

Les autoroutes vieillissantes du Royaume-Uni sont essentielles, mais difficiles à inspecter et à entretenir en raison de problèmes cachés, qui entraînent des risques pour la sécurité et nécessitent des inspections donnant lieu à des perturbations, au détriment du public. Cette étude montre comment l'intégration des données de diverses méthodes d'essais non destructifs (END) dans un modèle de jumeau numérique peut améliorer l'inspection des ponts et la gestion de l'infrastructure. En créant un modèle 3D unifié, cette approche améliore la façon dont les défauts sont visualisés et analysés, ce qui mène à des décisions d'entretien et de conception plus éclairées. Ce travail représente un progrès dans l'écart d'interopérabilité vers la numérisation de la gestion des actifs pour les infrastructures vieillissantes.
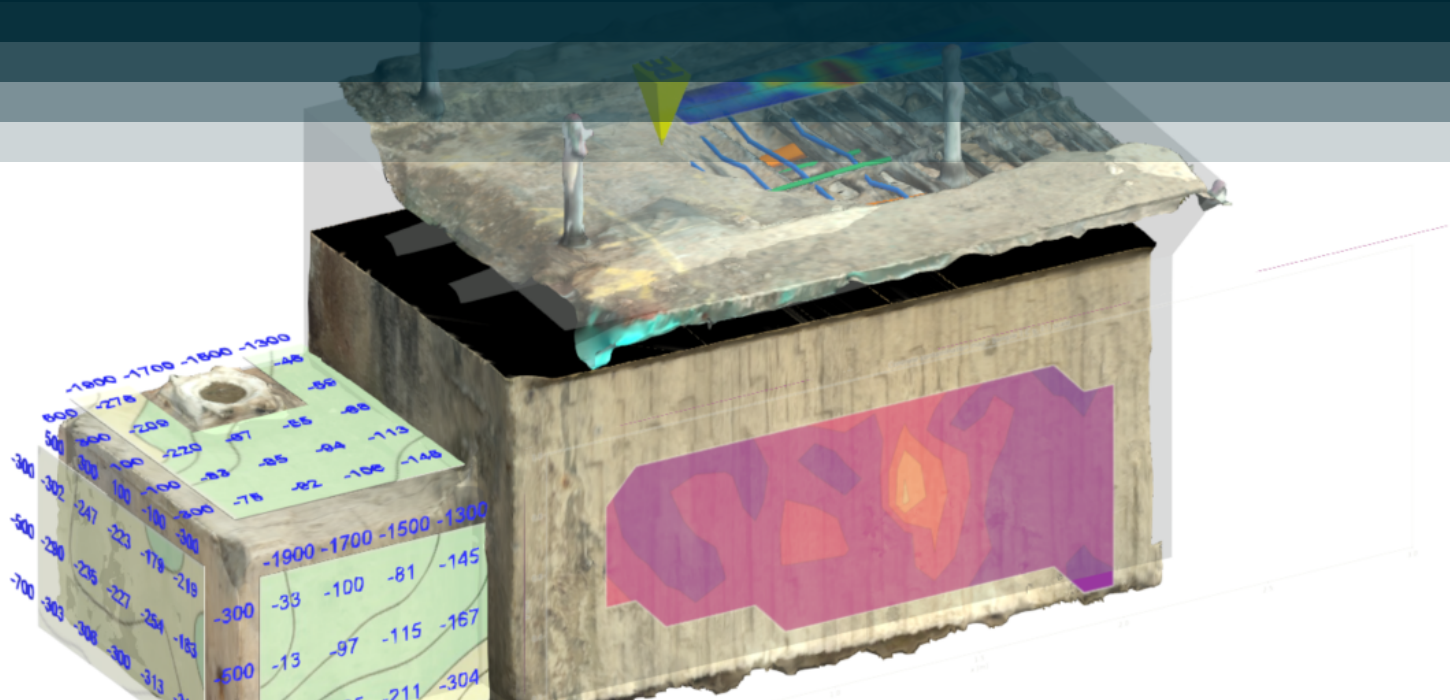
Shams Ghazy
Engineer
Transportation UK
Epsom, UK

Chris Mundell
Technical Director
Transportation UK
Bristol, UK

Tom Argyle
Chief Engineer
Transportation UK
Epsom, UK

Chris Hendy
Professional Head of Bridge
Engineering
Technical Director
Transportation UK
Epsom, UK

Abstract

This paper explores the integration of non-destructive testing (NDT) data into a digital twin framework to enhance bridge inspection and infrastructure resilience. The research aimed to address the challenge of federating data from various NDT - such as ultrasonic testing, ground-penetrating radar, and visual inspection data - into a unified 3D model with associated metadata. The primary results include the development of standardised data import workflows and the effective application of Revit for data visualisation and interpretation. The approach successfully met requirements for 3D representation, coordinate system integration, and data layering, though challenges with accessibility due to proprietary software remained. This work highlights the importance of improving asset and NDT data interoperability as well as integration with legacy systems to support intelligent asset management. The findings contribute to more resilient infrastructure by enabling better data visualisation, analysis, and decision-making in maintenance and inspection practices.

KEYWORDS
Digital twin; Non-destructive testing; Bridge inspection; Data interoperability; Infrastructure resilience

1.   Introduction

1.1   PROJECT BACKGROUND AND OBJECTIVES

The ageing infrastructure of the UK's highways presents a growing challenge for asset owners like National Highways (NH). With a significant portion of bridge stock exceeding 50 years of age, we face the challenge of having many structures with hidden critical elements that may be deteriorated or are deteriorating. The highest risk of these hidden critical elements is considered to be post tensioned structures or those with half joints - when sufficiently deteriorated these types of structures can pose an increased risk of catastrophic failure if not managed effectively. These types of structures are critical yet notoriously difficult to inspect and maintain because the most severe defects, such as voids, corrosion, and wire breaks within post-tensioned ducts, are entirely obscured. This not only poses a safety risk but also requires intrusive inspections that disrupt the network, leading to unintended closures and significant inconvenience to the public. National Highways has recognised these challenges and initiated the "Structures Moonshot" project, with an ambition to develop next generation self-maintaining structures. By enabling reliable condition monitoring and early issue detection, the project seeks to enhance safety while minimising the need for disruptive inspections and unplanned closures.

The current phase of the project, led by AtkinsRéalis, Jacobs, and supported by VSL, focuses on the evaluation of non-destructive testing (NDT) technologies. These include both mature technologies with high technology readiness levels (TRLs) and emerging technologies with lower TRLs, aimed at assessing their effectiveness in identifying various types of hidden defects (Mundell *et al.*, 2024a; Mundell *et al.*, 2024b). The aim is to enable early detection and intervention before defects necessitate major repairs, thereby extending the life of these critical assets and preventing unplanned network disruptions. For a more detailed discussion on the broader scope of the Structures Moonshot project, including the various activities and results of the NDT trials, refer to the works of Mundell *et al.* (2024a; 2024b).

1.2 THE NEED FOR DATA FEDERATION

To achieve the goals outlined by the Structures Moonshot project, an extensive series of NDT trials was conducted on large sections of the recently demolished A14 Huntingdon Viaduct shown in Figure 1. A diverse group of NDT specialists deployed a wide range of technologies, including Ground Penetrating Radar (GPR), Acoustic Emission, Impact Echo, and even cutting-edge techniques like Muon Tomography. The objective was to evaluate the accuracy and reliability of these technologies by comparing their results against actual, hidden defects within the bridge sections.

FIGURE 1

(Left to right) A14 HRV
Samples 1, 2 and 3

This evaluation required a meticulous process of validation. After the NDT trials, hydrodemolition was employed to progressively remove layers of the bridge sections while conducting LiDAR scans at regular intervals to document the visual state of the structure. This provided a detailed record of the internal conditions as they were revealed. Of particular interest, the hydrodemolition enabled the team to extract the post tensioned ducts - whole and intact - from the samples. These were removed to a separate laboratory where they could be carefully and meticulously opened, noting defects within the duct, grout and tendons themselves, to be compared against the findings of the NDT tests.

Each stage of this investigation generated a substantial volume of data, including high-resolution scans, detailed measurements, and defect locations. These datasets varied significantly in format, resolution, and scope as demonstrated in Figure 2, yet all were tied to a specific set of global coordinates and gridlines established for each of the bridge sections inspected. To accurately assess each NDT method's effectiveness and determine its role within a broader system of technologies, it was essential to not only compare their results individually but also to integrate them into a federated model. A holistic comparison would allow the evaluation of both the individual performance of each NDT and how they functioned together as a cohesive diagnostic system. Therefore, we looked at integrating this diverse data into a coherent, federated model which presented a significant challenge, especially since existing asset management software was not designed to handle such a wide variety of static and historic data in a seamless, machine-readable format.

FIGURE 2

Examples of the raw data
received from the suppliers
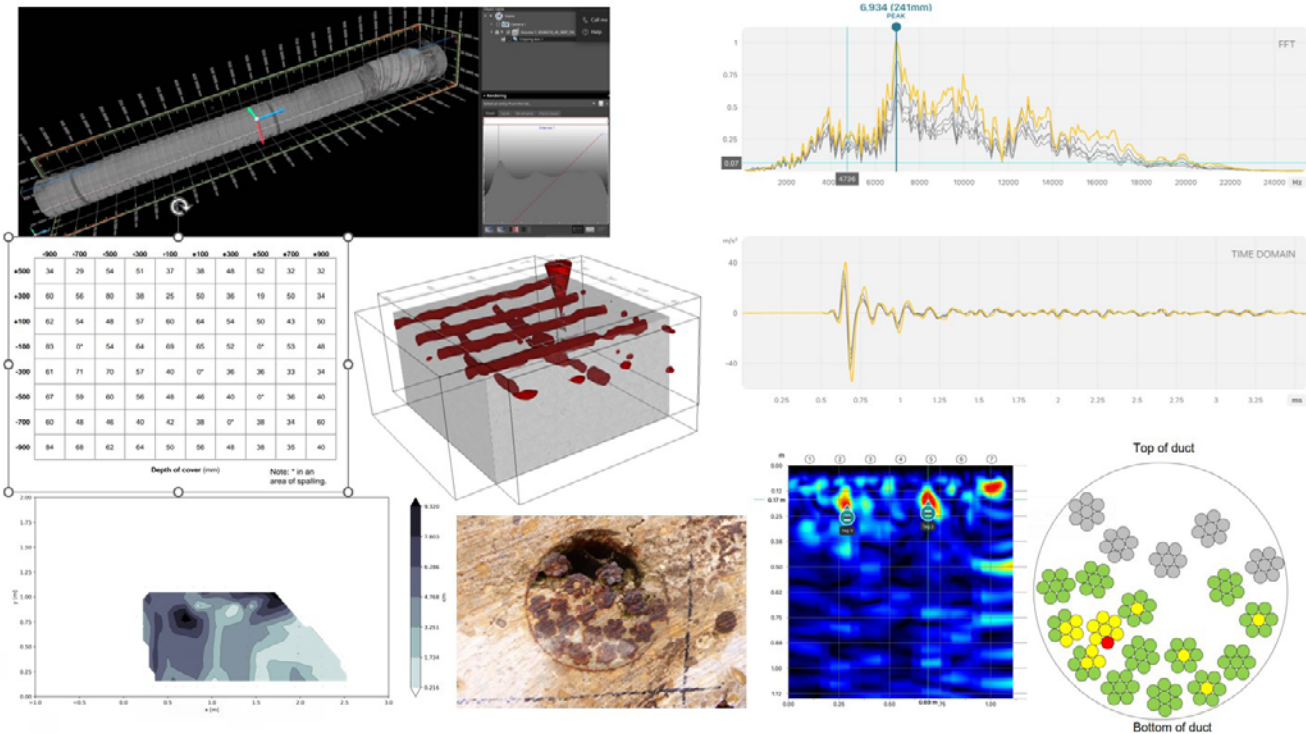
In this paper, we discuss the approach we took to effectively integrate and visualise the diverse set of data generated during these NDT trials in a way that allows for accurate analysis and meaningful conclusions about the performance of the NDT technologies. Through developing this solution, we considered how we can not only accurately represent the results but also provide an intuitive and accessible approach for day-to-day use by engineers and asset managers. This effort represents a critical first step towards improving how asset management data is stored, accessed, and analysed, moving beyond traditional, non-interoperable formats like PDFs and static images. This paper only focuses on the data interoperability challenge and does not discuss the analysis of the results of the different NDTs.

1.3   OVERVIEW OF THE LITERATURE

Asset management in infrastructure has traditionally relied on periodic inspections, maintenance logs, and manual record-keeping, often involving disparate data sources such as paper records, PDFs, and various digital formats. While these practices have been useful, they are increasingly seen as insufficient for meeting the demands of modern infrastructure, particularly given the ageing nature of many structures and the rising importance of predictive maintenance (Whitmore *et al.*, 2024).

Digital twins, which serve as virtual replicas of physical assets, represent a significant step forward, enabling real-time monitoring, simulation, and predictive analysis of infrastructure assets (Li *et al.*, 2024). However, the transition to digital twins is complex, involving the integration of vast and varied data types, including 3D models, LiDAR scans, and material condition data (Liu *et al.*, 2024). Moreover, when developing infrastructure digital twins (IDTs), interoperability is often achieved through standards like the Industry Foundation Classes (IFC). Yet, while IFC is widely adopted in some parts of the construction industry, such as building structures, it is still in its infancy when extending its use to manage transport infrastructure information, highlighting the limitations of existing models (Kwon *et al.*, 2021).

The integration of digital twin data with existing asset management systems presents a significant challenge, as many legacy systems are simple databases not designed to accommodate large, complex datasets such as 3D models, LiDAR scans, and real-time sensor data. Standard data models have been proposed to enhance interoperability and facilitate seamless data exchange between different asset management platforms, yet gaps remain in ensuring consistent and efficient integration (Halfawy et al., 2006).

The literature highlights the potential of digital twins to improve asset management outcomes, particularly in extending asset life and reducing maintenance costs through better-informed decision-making. Research has demonstrated how digital twins can unify various data sources into a cohesive model. Yet, significant challenges remain in integrating inspection data, especially when dealing with non-standard formats like static images or 3D DXF files (Yan et al., 2023). Furthermore, the integration of Building Information Modelling (BIM) with asset management has been explored, suggesting that BIM can be extended to develop more comprehensive digital twins that encompass the entire lifecycle of infrastructure assets (Desbalo *et al.*, 2024). However, even in these advanced models, integrating historical and static data remains a challenge, indicating a gap in current practices that requires innovative solutions.

Recent studies have also emphasised the need for deploying cloud and edge computing models in digital twin systems to enhance processing capabilities and reduce latency (Chen *et al.*, 2020b). When creating more complex IDTs that incorporate a wide range of IoT devices, semantic web technologies have gained significant attention due to their ability to store, share, and utilise heterogeneous data. Nevertheless, the integration of these technologies introduces issues such as data duplication, which remains a critical challenge to address (Zhao *et al.*, 2019; Gilbert *et al.*, 2018; Niknam *et al.*, 2019).

2.   Methodology

2.1   ESTABLISHING A GEO-REFERENCE SYSTEM

At the beginning of the project, it became clear that establishing a global reference system was essential for accurately correlating the results from the NDT tests with the actual defects identified during hydrodemolition. To facilitate this, a local coordinate system was implemented for each sample, enabling precise geolocation of defects and observations. This system was created by defining the (x, y, z) coordinates and orientation of the internal centroid of each test piece as the origin point (0, 0, 0), as depicted in Figure 3.

FIGURE 3

Sample geo-reference system
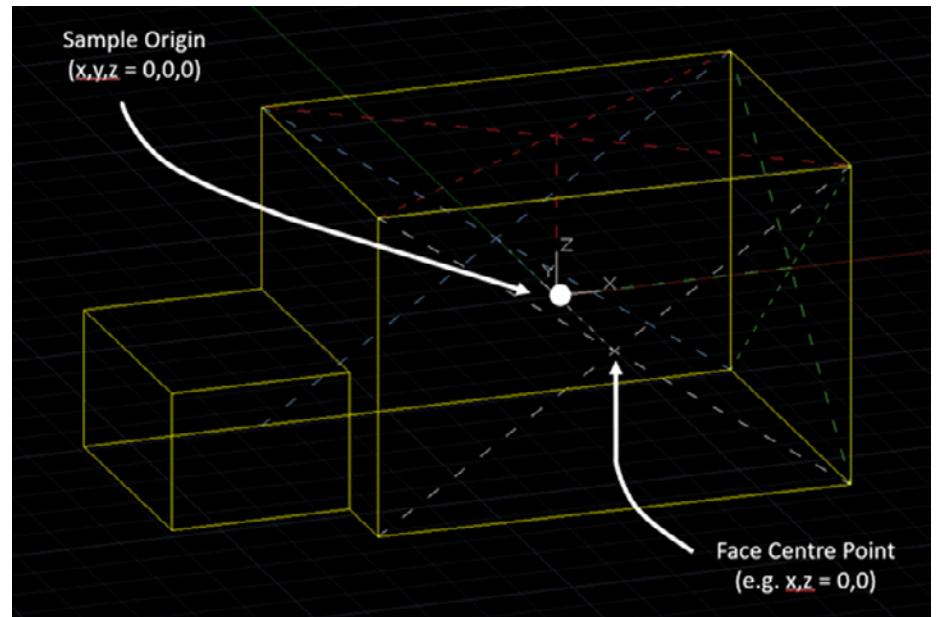
To ensure that suppliers could accurately define the location of their measurements relative to this central coordinate, a gridline system was implemented on each external face where testing occurred. These grids were physically drawn at 200mm intervals, as shown in Figure 4.

FIGURE 4

Physical grids on
sample faces

Aligning all data to this shared grid allowed for accurate comparison and overlay of information from various sources, maintaining spatial consistency within the digital twin model. This gridline system was crucial for the integrity of the federated model, ensuring that NDT results could be precisely matched with their corresponding physical locations within the bridge sections.

2.2   DEFINING SOLUTION REQUIREMENTS

To ensure the effective capture and federation of data from the various non-destructive testing (NDT) methods, a set of requirements needed to be defined to allow the digital twin to meet the project's objectives. Achieving a precise representation of complex internal conditions and enabling intuitive visualisation for engineers and asset managers were key priorities. Additionally, the solution had to be interoperable with existing asset management tools, scalable to incorporate additional data types or structures, and capable of handling large volumes of data efficiently.

To refine these requirements and collaboratively approach the federation of data, a suppliers' workshop was hosted. This workshop served as a platform for engaging with key NDT suppliers to discuss their data environments and explore how the digital twin could be tailored to accommodate the wide range of data formats they worked with. The collaborative insights gained during these discussions were key in shaping the digital twin's design, ensuring it met the practical needs of the project and the technical capabilities of the suppliers.

Table 1 outlines the solution requirements identified during the workshop, along with their corresponding purposes:

Requirement	Purpose
3D Representation of each Sample	To enable the overlay of diverse data types in a shared 3D space, facilitating accurate visualisation and comparison.
Coordinate System Integration	To ensure data can be accurately imported and aligned with the predefined geo-reference system for precise location mapping.
Flexible Data Import Capabilities	To accommodate various data formats, ensuring the system can handle unexpected or diverse data types provided by suppliers.
Compatibility with Existing Expertise	To ensure the software could be utilised without requiring new expertise, allowing for immediate application and efficiency.
Data Layering and Toggle Functionality	To allow the comparison of multiple data sets simultaneously, aiding in both individual and holistic NDT analysis.
Accessibility	To enable multiple stakeholders, including those from different parts of the supply chain to access and interpret the data.

These requirements were carefully considered to ensure that the final digital twin solution not only met the technical demands of the project but also aligned with the practical needs of all stakeholders involved.

2.3 DATA ACQUISITION, CLEANING, AND PROCESSING

Integrating diverse NDT datasets into a unified digital twin required careful data preparation and standardisation. The following subsections will describe the strategy taken to prepare and import the data into the digital twin.

2.3.1 Data Preparation and Standardisation

Given the complexity and variety of the data formats, a critical step in this process was standardising data imports into manageable workflows. Autodesk Revit was selected as the primary platform due to its advanced 3D modelling capabilities, which allowed for precise visual representation of the samples. Revit's interoperability with various file formats made it an ideal choice for integrating the diverse data generated by the NDT methods. Additionally, Revit is an industry-standard tool, so our team's existing expertise with the platform reduced the learning curve and ensured smooth project progression.

While Revit was well-suited for bringing data into a unified model, it is primarily an engineering design platform, optimised for experienced modellers and requiring a significant amount of computational power, especially for complex models. This makes it effective for managing federated data from diverse file formats where data manipulation is often required. However, it is less intuitive for those unfamiliar with 3D modelling software, and for this reason, we considered exploring other platforms that would offer a more accessible environment for inexperienced users to review the data.

Data preparation also required handling data manipulation tasks such as scaling, rotating, and cleaning, which were essential to prepare the data for federation. Typical federation tools, such as Navisworks, were not viable as standalone solutions, as they lack the necessary features to directly process raw data into usable formats. This limitation reinforced the need for a modelling tool like Revit, which supports these kinds of modifications and prepares the data for seamless integration.

Raw data was collected from various NDT methods, each producing data in different formats, ranging from numerical grids to complex 3D scans. Given the diversity of data, we undertook a systematic data cleaning process to ensure consistency and accuracy across all datasets. This involved working closely with the suppliers to identify the key data points of interest, verify the data, removing irrelevant or erroneous data points, and converting files into compatible formats for integration into Revit. In addition, a review of the alignment of each data point to the geo-reference system was crucial for maintaining the integrity of the federated model and ensuring accurate comparisons.

2.3.2   Establishing Import Workflows

To manage the complexity of the data integration, we developed standardised import workflows that cover most of the data formats we received from the suppliers. Table 2 presents a list of the NDT methods undertaken on the samples and a corresponding description of the data formats received for each.

TABLE 2

NDT methods and their
corresponding data formats

NDT Method	Number of data formats	Data formats description
NDT Visual Inspection (VI-NDT)	2	▪ Defect images, locations, dimensions ▪ Videos
Carbonation Test (CBT)	1	▪ Values at specific locations
Cover Meter Survey (CMS)	3	▪ Numerical Grid ▪ Values at specific locations ▪ Heat map / Contour / Scans / Graph Overlay
Dust Sampling (DS)	1	▪ Values at specific locations
Electrical Resistivity (ER)	1	▪ Numerical Grid
Half-cell Potential Survey (HPS)	3	▪ Numerical Grid ▪ Values at specific locations ▪ Heat map / Contour / Scans / Graph Overlay
GPR (GPR)	2	▪ Heat map / Contour / Scans / Graph Overlay ▪ 3D DXF Files
Muon Tomography (MUON)	2	▪ Heat map / Contour / Scans / Graph Overlay ▪ Point Cloud
Impact Echo (IE)	2	▪ Graphs at specific locations ▪ Numerical Grid
Pulse Echo (PE)	1	▪ Heat map / Contour / Scans / Graph Overlay
Ultrasonic Tomography (UT)	1	▪ Heat map / Contour / Scans / Graph Overlay
Hydrodemolition Visual Inspection (VI-HDM)	1	▪ LiDAR Scans
Intrusive Visual Inspection (VI-INT)	2	▪ Tendon condition per length ▪ Values at specific locations
FITR Gas Monitoring (FITR)	1	▪ Graph for a specific location / tendon
Portable Xray Fluorescence (PXF)	1	▪ Values at specific locations
Ultrasonic Wire Inspection (UW)	1	▪ Strand condition per length
XCT Scan (XCT)	1	▪ Non-interoperable format (.vgl, .vgp, .raw)

2.3.3 Defect Naming Conventions and Metadata Schema

To enable effective layering and toggling of data within the federated model, we developed a consistent naming convention for defects, as well as a standardised metadata schema. The naming convention ensured that each defect could be uniquely identified across datasets, while the metadata schema provided a structured description of each defect's attributes. The attributes considered were specific to the project's objectives and setup as described in Table 3.

TABLE 3

Defect metadata schema

	Sample	Zone	Provider	Source	Tool	Element -Type	Confidence
Description	Bridge Sample on which test was conducted	Face or Tendon on which test was conducted	The NDT supplier that conducted the test	The type of NDT method	The specific equipment used for the test	The structural element which the NDT is targeting and the type of Measurement it is taking	The supplier's confidence level in the accuracy of the result
Example	Sample 1	Face A	Bridgology	Ground Penetration Radar (GPR)	Proceq GP8000	Concrete - Cover	Medium

2.4   EVALUATION OF INTEGRATION SOLUTIONS

Several approaches were explored for federating the diverse datasets into a single digital twin model. This process involved preparing data for import into Revit, exploring alternative software solutions, and assessing their suitability for our project's needs. As Revit is not developed particularly for the case of visualising asset management data, especially static images and inspection scans, further solutions were explored to enable importing data into Revit.

Different formats required different adjustments, for example the heatmaps required creating an inverted image to allow the white space to be cut out, and the values at specific locations required setting up Dynamo scripts to import bulk values into the model. The importing process required advanced knowledge of Autodesk Revit, CAD, and Dynamo, limiting accessibility for less technical users.

To enhance the user friendliness of the digital twin given the range of users anticipated to work with it, we explored coupling Revit with other software to improve its accessibility. Table 4 summarises the advantages and disadvantages of the different solutions trialled.

TABLE 4

Comparison between

software solutions

		BIM Track	Autodesk Tandem	Revit Schedules
Pros		• **Color-Coded System:** Aligned with the metadata schema, BIM Track allowed for developing a unique identifying system for the defects. • **Clash Detection:** Originally designed for clash detection, it offered a structured way to pin metadata to defects in the model.	• **Web-Based Accessibility:** Tandem provided a highly accessible platform, allowing multiple stakeholders to view the model without specialised software. • **Ease of Use:** Being web-based, Tandem was user-friendly, making it easier for non-technical users to interact with the model.	• **Customisability:** Revit schedules enabled the creation of on/off toggles for each scan, significantly improving the model's usability. • **Integrated Solution:** Since this method remained within Revit, it maintained data integrity and compatibility.
Cons		• **Limited Usability:** BIM Track required creating a family for each defect, which did not add much benefit to using Revit on its own. • **Visualisation Challenges:** Defects were represented by partially transparent circles that changed size depending on zoom, leading to poor visualisation of actual defect locations.	• **Static Data Integration Issues:** Tandem was designed for live-stream data, making it unsuitable for handling static data and linked materials, such as LiDAR scans, which were crucial for our project. • **Material Loss:** None of the material data from Revit (e.g., scans and overlays) carried over, reducing its effectiveness for visualisation and comparison.	• **Accessibility:** This approach did not address the issue of Revit's limited accessibility, as users still needed a Revit license and expertise to interact with the model.

3.   Results

The following results showcase an approach for managing and visualising infrastructure asset data, with a particular emphasis on data generated from inspections. This section details the workflows developed for various data types and presents the final setup of the digital twin, highlighting how these methods facilitate comprehensive management and analysis of diverse asset data.

3.1   IMPORT WORKFLOWS

The datasets received from the suppliers required specific workflows for effective integration into the digital twin. To ensure all data could be standardised, imported, and visualised seamlessly within Revit, eight distinct workflows were developed. These workflows, as detailed in Figure 5, address the various data types and ensure a consistent approach to managing and visualising the information in the digital twin. The presented workflows only show the data flow after it has been cleaned from any noise, aligned to the geo-referencing grid, and undergone export iterations with the suppliers to generate an interoperable format.

FIGURE 5

Eight data import

workflows into

Autodesk Revit

Workflow			Data Cleaned and uploaded to BIM360	Pre-Processing	Import into Revit	Revit Processing	Integrated in Digital Twin
Workflow	1	**3D DXF**		1. Check DXF data within AutoCAD and extrude any lines which need to be solids for easy viewing within Revit.		1. Import DXF file into a Revit family 2. Position DXF files within Revit correctly 3. Position family on model	1. Verify data in digital twin with Supplier
Workflow	2	**Image / Video Attachment**				1. Locate created family for specific data 2. Position on grid for given co-ordinates 3. Fill out metadata and attach BIM360 link to Image / Video attachment	1. Verify data in digital twin with Supplier
Workflow	3	**Image Overlay**		1. Work out scaling of image 2. Create black and white silhouette image		1. Create surface for material within family 2. Set up material and apply to surface 3. Position family on model	1. Verify data in digital twin with Supplier
Workflow	4	**LiDAR Scan**		1. Open .obj file within Autodesk ReCap photo 2. Orientate correctly and export		1. Import .obj file 2. Position using similar location points 3. Update Material name and re-apply	1. Verify data in digital twin with Supplier
Workflow	5	**Numerical Grid**		1. Organise data in Excel, in order of import for Dynamo script		1. Create numerical grid family, mirroring Excel sheet 2. Run Dynamo script to import data from Excel	1. Verify data in digital twin with Supplier
Workflow	6	**Tendon Condition**				1. Create extrusion along tendon, using chainage for length and location 2. Add data to family containing extrusion	1. Verify data in digital twin with Supplier
Workflow	7	**Values at Specific Locations**				1. Locate created family for specific data 2. Position on grid for given co-ordinates 3. Fill out metadata	1. Verify data in digital twin with Supplier
Workflow	8	**Point Cloud**		1. Check point cloud data within Recap 2. Clean up point cloud if required		1. Attach point cloud file saved from Autodesk ReCap 2. Position point cloud in model	1. Verify data in digital twin with Supplier

3.2 THE DIGITAL TWIN

The final digital twin integrates all NDT data into a cohesive 3D model within Autodesk Revit, with the primary objective of layering the NDT data alongside the actual defects recorded during hydrodemolition and intrusive inspections. For hydrodemolition, each LiDAR scan was organised within individual Revit Views, enabling users to easily navigate through different stages of hydrodemolition when examining specific NDT scans. For data from NDT suppliers and the intrusive inspections, the workflows outlined in Section 3.1 were applied, with each dataset linked to a schedule line that allows toggling the data on or off.

FIGURE 6

Screenshot of the digital twin interface
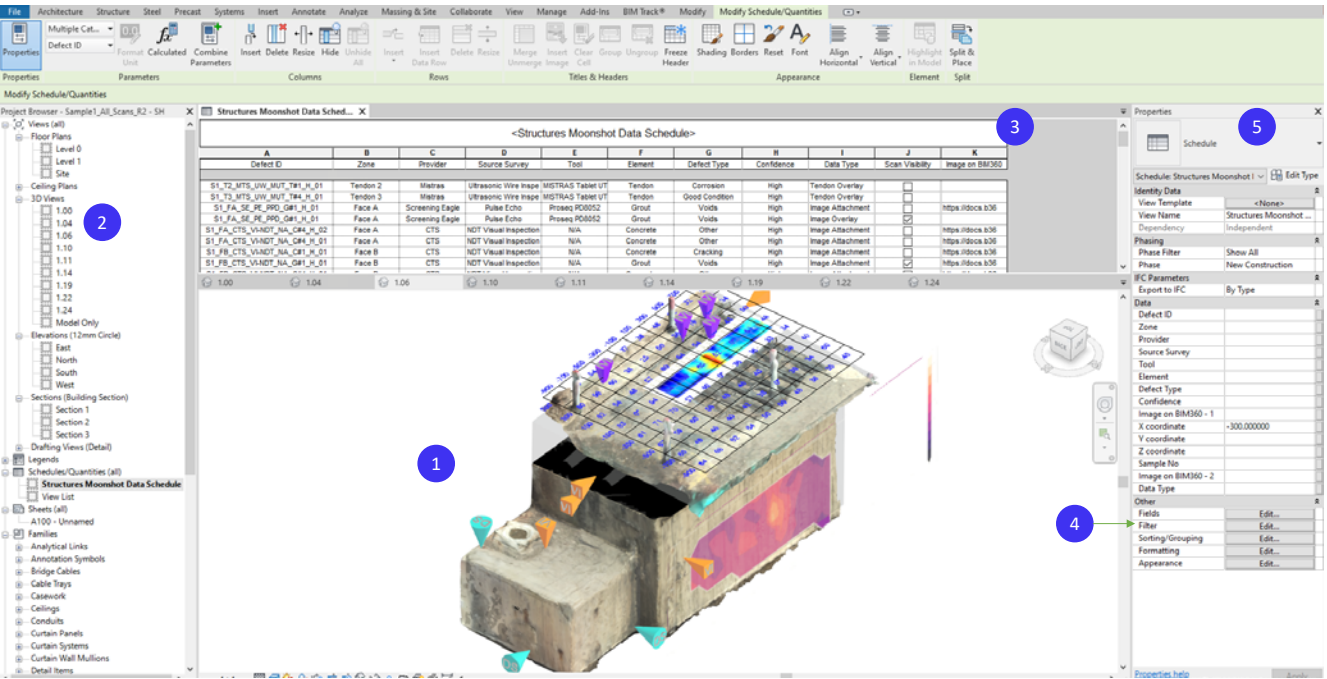
Figure 6 provides a detailed snapshot of the user interface for the digital twin in Autodesk Revit, highlighting the following key elements:

1. **3D Model Viewer** – This area allows users to visualise the 3D model of the sample, with various data points and overlays integrated directly onto the model.
2. **Hydrodemolition Views** – Users can access different stages of the hydrodemolition process via the 3D views in Revit. These stages are organised sequentially, from the initial state of the sample before hydrodemolition to the final stage of material removal.
3. **Data Schedule** – The schedule enables users to toggle the visibility of different results and scans, as well as access their associated metadata.
4. **Schedule Filters** – The Data Schedule can be filtered based on metadata categories, facilitating quicker and more efficient data access.
5. **Properties Panel** – This panel displays the full metadata set when any data point in the 3D space is selected.

4.   Discussion

4.1   CHALLENGES IN DATA INTEGRATION AND STANDARDISATION

The integration and standardisation of diverse datasets from Non-Destructive Testing (NDT) methods into a unified digital twin model presented several challenges, primarily related to data interoperability and consistency. Addressing these challenges required a multi-faceted approach, and the results of our efforts provide insights into both the obstacles encountered and the solutions implemented. This section will discuss the key challenges faced, the strategies employed to overcome them, and the implications for real-world applications.

4.1.1   Challenges in Data Interoperability

1. **Diverse Data Formats:** A significant challenge was the variety of data formats from different NDT methods, including point clouds, meshes, numerical grids, heat maps, and 3D DXF files. The heterogeneity of these formats complicated efforts to standardise and integrate the data into a cohesive model. Deciding on the most appropriate file formats for each technology required trial and error. For example, LiDAR data collected with an iPhone 14 Pro provided both a point cloud and a mesh, with the mesh being more useful to compare against.

2. **Inconsistent Data Resolution and Precision:** Different NDT methods provided data at varying levels of resolution and precision. For example, Ground Penetrating Radar (GPR) produced detailed 3D .dxf files, while Impact Echo (IE) provided numerical grids and graphs. This disparity meant that aligning data from various sources in a manner that preserved their individual qualities while allowing for accurate comparison was challenging.

04: Enhancing Infrastructure Resilience through Digital Twin Development: A Case Study of the Structures Moonshot Project

104

3. **Geo-Referencing Issues:** Ensuring that all data was accurately aligned with the established geo-reference system was crucial. Misalignment between data sets could lead to erroneous interpretations and unreliable conclusions. Such issues could arise not only from technical challenges but also from human error during data recording or translation. For example, lack of familiarity with the tests or the object's geometry could lead to misalignments, which in real-world applications could have significant consequences. This was especially critical when integrating LiDAR scans with other forms of NDT data.

4. **Data Standardisation and Cleaning:** Raw data from NDT methods required extensive cleaning and standardisation to ensure consistency. This involved removing irrelevant data, converting formats, and verifying the accuracy of measurements. Without a robust standardisation process, the risk of integrating erroneous or inconsistent data into the digital twin model was high.

4.1.2   Strategies and Solutions

1. **Developing Import Workflows:** To manage the diversity of data formats, we developed standardised import workflows tailored to each NDT method. These workflows streamlined the data preparation and import processes, ensuring that various types of data were effectively integrated into Autodesk Revit. For instance, workflows for heat maps and numerical grids included specific steps for formatting and aligning data before import.

2. **Utilising Autodesk Revit's Capabilities:** Autodesk Revit was selected as the primary platform due to its advanced 3D modelling capabilities and compatibility with various file formats. Custom scripts in Dynamo were used to handle bulk data imports, while Revit schedules facilitated the toggling of data layers, improving accessibility and usability.

3. **Creating a Unified Metadata Schema:** A consistent naming convention and metadata schema were developed to ensure that each defect could be uniquely identified and described across different datasets. This approach enhanced the ability to layer and compare data from multiple sources effectively, as demonstrated by the data schedules and filters implemented in the digital twin.

4.1.3   Application in Real Life

While the controlled methods used in this project provided a solid foundation, real-world implementation of these techniques requires adaptation to practical constraints. While drawing physical grids on a bridge is impractical, alternative methods for geo-referencing can be employed. Using high-precision GPS and laser scanning technologies can create a digital coordinate system without the need for physical markings. However, as demonstrated, many NDT methods are not yet advanced enough to seamlessly integrate with GPS, often still relying on more traditional, manual methods for recording locations.

In practice, engineers and NDT specialists will need to import their data directly into an interoperable system. This requires significant automation between the NDT proprietary software and the software hosting the digital twin. While the research project allowed time for thorough verification of data import accuracy, real-world applications demand robust import workflows and spatial correlation to ensure data is stored and interpreted correctly. This would be crucial as the digital twin would be used to derive maintenance and design decisions.

4.2 BEST PRACTICES AND LESSONS LEARNED IN DATA MANAGEMENT

One of the key challenges we encountered was the lack of use of interoperable data formats, such as .nii, .nrrd, and .vgl. These formats, mostly proprietary to specific software, created barriers to seamless data integration. In addition, in the presence of interoperable formats, trial and error was required to decide on the appropriate format to be integrated. To overcome this, we worked together with the suppliers to export formats that could be integrated into Autodesk Revit. This experience underscored the importance of advocating for more open and standardised data formats in the industry, which would reduce the need for such workarounds and enhance the efficiency of data management processes.

The use of a comprehensive metadata schema was invaluable in categorising and accurately identifying defects across the dataset. This structured approach facilitated better organisation and retrieval of data, leading to more effective analysis and decision-making. Moving forward, developing a standard vocabulary using semantic web technologies could further enhance interoperability by providing a unified language for asset management data. This would bridge many of the current interoperability issues, allowing for more seamless data exchange and integration across different platforms and stakeholders.

A significant lesson learned from this project was the value of collaboration. All suppliers were willing to contribute their data in an open format and work together towards the collective learning of the group, and hence the industry. This collaborative approach, though often rare in typical competitive projects, was crucial in overcoming data integration challenges and achieving the project's goals. Encouraging such collaboration in future projects can lead to better outcomes and foster innovation, as it allows for the pooling of resources and expertise.

4.3   EVALUATION OF SOFTWARE SOLUTIONS

Throughout the project, various software solutions were explored to meet the complex requirements of managing and analysing bridge inspection data. Ultimately, Autodesk Revit was chosen due to its robust capabilities, which aligned with the project's goals. Revit's 3D modelling environment allowed the creation of a digital model, enabled geo-referencing, and the ingestion of a range of data formats. The use of Revit Schedules was particularly beneficial for developing the layering system required to visualise the data.

However, despite its strengths, Revit is a proprietary software that requires specialised skills and expertise to operate effectively. This presents a challenge in terms of accessibility, as not all stakeholders may have the necessary knowledge or resources to engage with the software directly. For instance, the model could not be easily shared with the client for independent exploration. Instead, we had to extract insights and guide them through the data during presentations, limiting their ability to interact with the information firsthand.

To address these limitations, integrating Revit with a web-based interface would be an ideal solution. Such an interface would democratise access to the model, allowing any stakeholder to view and interact with the data without needing specialised software or expertise. Furthermore, there is a need to consider how this solution could be integrated with existing asset management systems, such as IAMIS for National Highways. As IAMIS is a legacy system with limited functionality, significant development would be required for this integration.

4.4   COMPLEMENTARY NATURE OF LAYERED NDT TECHNIQUES

The creation of a digital twin played a crucial role in enabling a comprehensive assessment of various non-destructive testing (NDT) techniques. By integrating data from multiple NDT methods into a unified digital model, the project allowed for both individual analysis of each technique and a holistic evaluation of their combined effectiveness. The digital twin provided a practical platform for evaluating the strengths and limitations of each NDT technique in a real-world context. It revealed how different defects - from surface anomalies to deep-seated structural issues - correlate across various layers of the bridge. For example, surface-level defects identified through visual inspections could be compared with internal issues detected by ultrasonic testing or ground-penetrating radar, offering a clearer understanding of the bridge's condition and the progression of defects.

Additionally, the layered approach enabled by the digital twin demonstrated the complementary nature of combining multiple NDT techniques. The integration of data from various sources results in a more comprehensive dataset, supporting more informed decision-making and better prioritisation of maintenance actions. From a practical standpoint, the digital twin offers significant advantages in repeat inspections over time. As data is collected in subsequent years, the model allows for easy comparison of new inspections against previous ones, enabling the detection of subtle changes and trends. This continuous monitoring helps identify root causes of defects, making long-term asset management more efficient and ensuring that maintenance is based on real, up-to-date insights.

5.   Conclusions and Future Recommendations

5.1   CONCLUSIONS

This paper highlights the key contributions of the data federation approach taken under the National Highway Structures Moonshot project. The development of a comprehensive solution for data federation represents a significant advancement in managing and storing inspection data within asset management systems for infrastructure. Through the development of robust and standardised import workflows and creating a unified digital twin model, the project effectively integrated various data from non-destructive testing (NDT) methods, enabling both individual and holistic assessments of the technologies.

The solution successfully addressed the requirements set out to meet the project's objectives. The digital twin provided a 3D representation which allowed for the integration of a coordinate system, ensuring accurate alignment and spatial correlation of data. Autodesk Revit provided the flexibility to accommodate different data formats, however, the majority of the datasets received required pre-processing in order to import into Revit. Autodesk Revit was compatible with existing expertise which reduced the learning curve and time to complete the deliverables. Revit Schedules allowed the layering of data and toggle functionality which facilitated comparison of multiple datasets. However, the requirement for broad accessibility was less effectively met due to Revit's proprietary nature, which limits the ease of sharing the digital model with external stakeholders. This highlights an area for improvement in ensuring that future solutions provide greater accessibility to a wider audience. Further collaboration with Autodesk and Bentley is currently ongoing to explore ways to improve accessibility of the model.

The contributions discussed in this paper along with the best practices, lessons learned, and insights on interoperability underscore the value and impact of this work. They demonstrate how innovative approaches to data federation can enhance infrastructure asset management and provide a clearer understanding of structural conditions.

5.2 IMPLICATIONS ON INFRASTRUCTURE ASSET MANAGEMENT

The data federation approach implemented in the National Highways Structures Moonshot project presents a method towards an enhanced ability to overlay and integrate diverse datasets into a unified digital twin model. One of the most immediate benefits observed was the capacity to overlay a LiDAR scan onto an as-built 3D model. This functionality enables asset managers to verify whether the constructed infrastructure aligns with the original design specifications or if there have been any deviations. This is particularly valuable in assessing construction accuracy and identifying any modifications that may have occurred during or after construction.

For example, during a bearing replacement inspection where multiple bearings are aligned, the ability to model the soffit in 3D and perform a LiDAR scan offers an effective method to detect any potential settlement. By overlaying the LiDAR data on the 3D model, engineers can accurately identify shifts or misalignments, which would be difficult to detect using traditional methods. This integration ensures that any necessary maintenance or corrective measures can be promptly addressed, thereby enhancing the reliability and safety of the infrastructure.

Moreover, the digital twin's ability to layer inspection data from visual surveys provides a more intuitive and comprehensive view of infrastructure conditions over time. Instead of sifting through multiple PDF reports to track the progression of a specific defect, engineers can visualise the defect's development directly within the 3D model. This layered approach not only saves time but also reduces the likelihood of missing critical information, thereby improving decision-making processes. However, it's important to recognise that asset owners still have a duty to report on their infrastructure in accordance with current standards. As such, the digital twin must also support the ability to produce standardised reports, ensuring compliance with regulatory requirements while benefiting from the enhanced insights the model provides.

The inclusion of non-destructive testing (NDT) data into the digital twin further amplifies the benefits of data federation. By integrating multiple NDT sources, the model can cross-verify findings, thereby increasing the confidence in defect identification. For instance, if multiple NDT methods indicate a potential issue in the same location, the likelihood of a genuine defect increases. This capability is crucial for predictive maintenance strategies, as it allows for more accurate forecasting of potential failures and the development of proactive maintenance plans.

Additionally, the integration of various data sources - such as LiDAR, visual inspections, and NDT - into a single, federated model enhances the overall understanding of the infrastructure's condition. This holistic view facilitates more informed decision-making and allows asset managers to prioritise maintenance activities based on the most accurate and comprehensive data available.

These enhancements underscore the transformative impact that data federation and digital twin technology can have on infrastructure asset management. By enabling a more detailed, accurate, and accessible understanding of asset conditions, these technologies provide a foundation for more resilient and efficient infrastructure management practices.

5.3   FUTURE RECOMMENDATIONS

To enhance the use of digital twins and NDT in infrastructure management, a few key recommendations should be considered. Developing and adopting standardised data formats and metadata schemas across the industry will help streamline data integration and improve interoperability between different systems. Creating web-based interfaces for digital twins will also improve accessibility, enabling all stakeholders, including clients and external users, to interact with and utilise the data effectively.

It is also important to explore methods for integrating digital twins with existing legacy asset management systems to ensure comprehensive data utilisation and support informed decision-making. Additionally, continuing to refine and combine NDT techniques will enhance defect detection and analysis, contributing to more effective predictive maintenance strategies. Investing in training programmes for engineers and asset managers will support the effective use of digital twins and NDT tools, promoting broader adoption and consistent application.

These recommendations aim to build on the project's successes and address areas for improvement, advancing the application of digital twins and NDT in infrastructure management.

Acknowledgements

References

Chen, Y., Hou, F., Li, X. & Liu, Y. (2020b) 'Deploying data-intensive applications with multiple services components on edge', Mobile Networks and Applications, 25, pp. 426–441. doi: 10.1007/s11036-019-01400-y.

Desbalo, M.T., Woldesenbet, A.K., Habtu, T.M., Bargstädt, H.-J. & Yehualaw, M.D. (2024) 'BIM-enabled built-asset information management conceptual framework: A case of public university buildings in Addis Ababa, Ethiopia', Heliyon, 10(12), p. e33026. doi: 10.1016/j.heliyon.2024.e33026.

Gilbert, T., Zhang, X., Wu, X. & Moore, A. (2018) 'Software systems approach to multi-scale GIS-BIM utility infrastructure network integration and resource flow simulation', ISPRS International Journal of Geo-Information, 7(8), p. 310. doi: 10.3390/ijgi7080310.

Halfawy, M., Vanier, D. & Froese, T. (2006) 'Standard data models for interoperability of municipal infrastructure asset management systems', Canadian Journal of Civil Engineering, 33(12), pp. 1453–1463. doi: 10.1139/l06-086

Kwon, T.H., Kim, J.H., Park, S.H. & Kim, Y.W. (2021) 'Building Information Modeling-based bridge health monitoring for anomaly detection under complex loading conditions using artificial neural networks', Journal of Civil Structural Health Monitoring, 11, pp. 1301–1319. doi: 10.1007/s13349-021-00512-9.

Li, Y., Wang, Q., Pan, X., Zuo, J., Xu, J. & Han, Y. (2024) 'Digital Twins for Engineering Asset Management: Synthesis, Analytical Framework, and Future Directions', Engineering. doi: 10.1016/j.eng.2023.12.006.

Liu, L., Zeng, N., Liu, Y., Han, D. & König, M. (2024) 'Multi-domain data integration and management for enhancing service-oriented digital twin for infrastructure operation and maintenance', Developments in the Built Environment, 18, p. 100475. doi: 10.1016/j.dibe.2024.100475.

Mundell, C., Hendy, C., Argyle, T. & George, C. (2024a) 'Advancements in Bridges NDT: National Highways' "Structures Moonshot"', in Jensen, F., Frangopol, D.M. & Schmidt, F. (eds) Bridge Maintenance, Safety, Management, Digitalization and Sustainability. Open Access: www.taylorfrancis.com, pp. 1-8. doi: 10.1201/9781003483755-431.

Mundell, C., Hendy, C., Argyle, T. & George, C. (2024b) 'Advancements in Bridges NDT: National Highways' "Structures Moonshot"', in Jensen, F., Frangopol, D.M. & Schmidt, F. (eds) Bridge Maintenance, Safety, Management, Digitalization and Sustainability. Open Access: www.taylorfrancis.com, pp. 9-16. doi: 10.1201/9781003483755-432.

Niknam, M., Jalaei, F. & Karshenas, S. (2019) 'Integrating BIM and product manufacturer data using the semantic web technologies', Journal of Information Technology in Construction, 24, pp. 424–439. doi: 10.36680/j.itcon.2019.025.

Whitmore, D., Krystallis, I., Papadonikolaki, E., Ford, J., Cleaver, M. & Alexander, D. (2024) 'Digital twins in the asset life cycle: are we there yet?', Proceedings of the Institution of Civil Engineers - Management, Procurement and Law. doi: 10.1680/jmapl.23.00003.

Yan, B., Yang, F., Qiu, S., Wang, J., Cai, B., Wang, S., Zaheer, Q., Wang, W., Chen, Y. & Hu, W. (2023) 'Digital twin in transportation infrastructure management: a systematic review', Intelligent Transportation Infrastructure, 2, p. liad024. doi: 10.1093/iti/liad024.

Zhao, L., Liu, Z. & Mbachu, J. (2019) 'Highway alignment optimization: An integrated BIM and GIS approach', ISPRS International Journal of Geo-Information, 8(4), p. 172. doi: 10.3390/ijgi8040172.

05: Advancing Deep Soil Mixing Techniques for Organic Soils: A Multi-Code Approach

Significance Statement

Soft soils complicate construction due to their tendency to compress and settle. Deep soil mixing is a ground improvement technique where soil is mixed with a binder to make it stronger and more stable. The technique is underutilized and lacks a well-established design methodology and clear construction guidelines. This paper aims to fill that gap by combining recommendations from various codes into a unified approach. It also presents a literature review with laboratory tests and field trials on cement-mixed soft soil, exploring how cement mixtures impact soil strength. The findings provide valuable insights for future ground improvement projects, offering a reliable reference for practitioners and guiding future developments in this area.

Énoncé d'importance

Les sols meubles complexifient la construction en raison de leur tendance à se comprimer et à se tasser. Le malaxage des sols est une technique d'amélioration du sol où le sol est mélangé à un liant pour le rendre plus solide et plus stable. La technique est sous-utilisée et ne dispose pas d'une méthodologie de conception bien établie et de lignes directrices claires en construction. Cet article vise à combler cette lacune en combinant les recommandations de divers codes dans une approche unifiée. Il présente également une revue de la littérature avec des essais en laboratoire et des essais sur le terrain sur un sol meuble mélangé à du ciment, explorant comment les mélanges de ciment influencent la résistance du sol. Les résultats fournissent des renseignements précieux pour les futurs projets d'amélioration du sol, offrant une référence fiable pour les praticiens et guidant les futurs développements dans ce domaine.

Anand Kori
Assistant Geotechnical Engineer
Office of the COO - GTC
- Ground Engineering
Bangalore, India

S Venkata Reddy
Geotechnical Engineer
Office of the COO - GTC
- Ground Engineering
Bangalore, India

Alexander Chmoulian
Technical Director
UK & Ireland – Infrastructure,
Ground Engineering and
Tunnelling
London, UK

Abstract

Construction on soft soils poses significant challenges due to their low load-bearing capacity, high compressibility, and susceptibility to settlement and instability, which can compromise safety and durability of structures. To address these issues, ground improvement techniques may sometimes be employed, which involve adding materials or energy to enhance soil performance. Key methods include void filling, grouting, densification, replacement, or soil mixing.

One of available ground improvement options is Deep Soil Mixing (DSM), which is an advanced technique that involves adding a binder to enhance soil properties, particularly in challenging environments like organic peaty soils. This paper discusses DSM methods for peaty soils, emphasizing recent advancements and addressing significant challenges. It reviews the DSM methodology discussed in various design guidelines such as those discussed in EuroSoilStab, BS14679, and FHWA manual, and their limitations. The paper emphasizes critical design principles, including meeting Ultimate Limit State (ULS) and Serviceability Limit State (SLS) criteria, selecting appropriate binders, and ensuring robust quality control. It also discusses the risks associated with the use of DSM, like insufficient column strength or creep settlements, recommending mitigation options through quality assurance and continuous monitoring, and integrating various design methods to advance DSM techniques in organic soils.

1.   Introduction

Ground improvement involves adding materials or energy to soils to enhance their performance, ensuring they function more reliably and can be effectively integrated into the design process. This crucial aspect of geotechnical engineering tackles the challenges posed by weak or problematic soils, allowing for safe and cost-effective construction on otherwise unsuitable ground. The major forms of ground improvement include:

- **Void filling:** The process of filling cavities within the soil to stabilize and enhance its load-bearing capacity.
- **Grouting:** This technique includes permeation, compaction, and jet grouting techniques, which all involve injecting materials into the soil to increase strength.
- **Improvement through densification or replacement:** Methods such as vibro compaction, dynamic compaction, and stone columns are used to densify or replace loose soils, enhancing their structural integrity.
- **Controlled Modulus Columns (CMCs):** This technique involves reinforcing the ground using rigid inclusions, such as piles, to transfer the applied load to deeper, more stable strata. To ensure effective load distribution, this method requires the implementation of a load transfer platform.
- **Soil mixing:** The technique involves mixing binding agents into the soil to create a restructured stronger composite material, which is particularly effective in treating soft or unstable soils.

Choosing an appropriate ground improvement method is a crucial aspect of project planning. This paper specifically examines ground improvement using deep mixing techniques. When soil is combined with a binder, the binder absorbs the moisture present in the soil, initiating the hydration process. As the binder hydrates, it dissolves into the diffused water around the clay particles and reacts with clay minerals like silica and alumina. This reaction leads to the formation of a strong, water-insoluble gel composed of calcium silicate and calcium aluminate. This reaction is commonly referred to as the pozzolanic reaction, which will impact the index properties of soil by reducing the liquid limit, increasing the plastic limit and eventually reducing the plasticity index. For this reaction to proceed effectively, it is crucial to maintain a high pH level and ensure the presence of excess calcium ions (Masaki Kitazume, 2012). Organic peaty soils pose challenges due to their high moisture content, low shear strength, and acidic nature. The acidity of peat complicates its reaction with cement or lime, making it difficult to initiate the hydration process necessary for achieving the desired strength.

Given these complexities, project design decisions and material selection are crucial for achieving the required performance of the improved ground. It is essential that these decisions are validated through comprehensive laboratory tests and field trials conducted at appropriate stages of the project. The complex behaviour of soil-cement mixed ground under these conditions highlights the importance of careful planning and thorough testing.

This paper focuses on the design method for deep mixing and the associated performance testing requirements. It also highlights the significant risks involved in this design, especially in challenging soil conditions like peat. Understanding and mitigating these risks is crucial for the successful implementation of deep soil mixing techniques in such environments.

2.   Literature Review

Nigel Pye's paper, "Deep Dry Soil Mixing to Stabilize a Live Railway Embankment Across Thrandeston Bog," discussed the application of Deep Dry Soil Mixing (DSM) to stabilize a live railway embankment across Thrandeston Bog, United Kingdom. The case study involved a 5-meter-high railway embankment resting on up to 9m of very soft peat and clay, which had required maintenance for over 150 years. Field investigations revealed undrained shear strengths of 2 to 20kPa for peat and 15 to 50kPa for clay. The embankment required frequent surface maintenance due to ongoing settlements, significantly driving up maintenance costs. The long-term settlements of up to 2.6m were estimated, unless additional ground improvement measures would be implemented. To mitigate this, 600mm diameter DSM columns were installed in a panel arrangement with 100mm overlap and spacing between 0.14m and 0.44m, replacing 40 to 50 percent of the soil (Figure 2.1). The DSM columns used Portland cement (BS EN 197-1 CEM1) at 275kg/m^3 for peat and 175kg/m^3 for clay. Post-installation, long-term settlements reduced from the originally estimated 2.6m to 0.15m.

FIGURE 2.1

Plan and cross-section of ground treatment at Thandenston Bog, UK (Nigel Pye, Deep Dry Soil Mixing to Stabilize a Live Railway Embankment Across Thrandeston Bog, 2012)
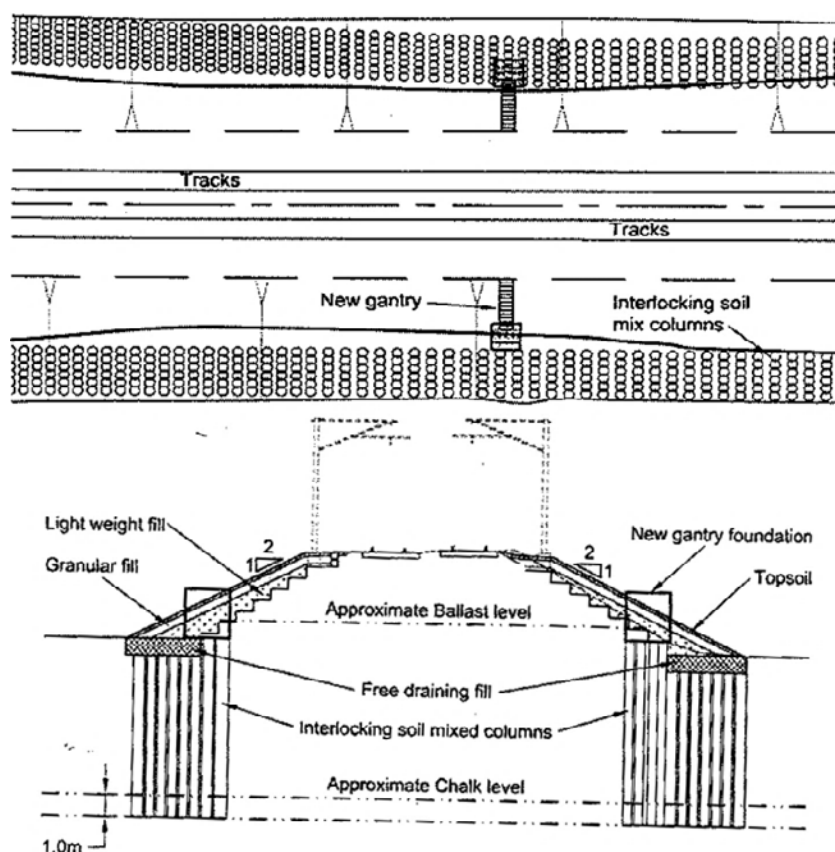
Pye reported laboratory and field trials for DSM column design and construction. Laboratory tests on peat and clay mixed soils with varying cement binder content followed EuroSoilStab (EuroSoilStab, 2000) guidelines, using multistage triaxial compression tests with binder content from 150kg/m^3 to 300kg/m^3. Laboratory results showed increased shear strength with higher binder content and curing time. For the peat material with the binder dosage of 250kg/m^3, 14-day laboratory strengths were typically in the range of 140kPa to 170kPa. The columns were constructed onsite and column push-in tests (CoIPT) and reverse column pull-out tests (RCoIPT) were conducted. The test results indicated undrained shear strengths of 200kPa to 220kPa for the binder dosage of 250kg/m^3 and 14-day curing period. The historic published data shows the laboratory strengths being two to three times higher than field strengths. However, it was concluded that the relative mix energy used in the laboratory and field, empirical correlations used to derive field strength, confining pressures during curing in the laboratory and field, temperature in the laboratory, and field during curing may have influenced the obtained results in this case (Nigel Pye, Laboratory and Field Trials for Deep Dry Soil Mixing to Stabilize a Live Railway Embankment Across Thrandeston Bog, 2012).

The CoIPT is an in-situ means of verifying the strength of stabilized soil columns. During the test, a winged penetrometer penetrated the stabilized column at a constant rate and the column strength was estimated from the recorded probing resistance using a bearing capacity factor (N). CoIPT offers a number of conceptual advantages over the popular cone penetration test (CPT). CPT cones only probe at a point location within the column cross section and tend to follow the weakest path, whereas in the case of CoIPT, a chord of the column is probed. In addition, CPT cones are more prone to deviation from vertical than the winged penetrometer, particularly in strong columns. In RColPT, a probe attached to the wire is placed at the bottom of the treated soil column during production and left there until testing. The probe is withdrawn from the column and the continuous record of resistance can be made.

Dennes and Glen conducted a comprehensive full-scale study on the application of Deep Cement Mixing in soft Bangkok Clay (Indraratna & Chu, 2005), underlying a 6-metre-high reinforced-earth trial embankment. The site consists of about 6.5m thick soft clay deposits with undrained shear strength of 15kPa. The objective of the full-scale study was to evaluate and compare the performance of the existing reinforced earth embankment on soft ground with that of an embankment constructed on improved ground. Jet mixing was the technique employed to install DSM columns. The column diameter was 0.5m and they were constructed in a square pattern with spacings of 1.5m and 2m (Figure 2.2).

FIGURE 2.2

Plan and cross-section
of ground improvement
in Bangkok Clay
(Indraratna & Chu, 2005)

The settlements of the embankment were reduced by 70 percent when underlain by the improved ground, compared to the unimproved soft clay foundation. In addition, the rate of consolidation of the clay was significantly increased due to the improved soil conditions, providing further evidence of the benefits of the DSM method in enhancing the overall stability and performance of the embankment. It was concluded that the DSM process, combined with jet grouting, leads to increased pore water pressures not only at the site of improvement but also in the surrounding areas near the improvement zone.

In the context of the literature reviewed, it is evident that the DSM method has significant potential to enhance organic soils. However, for successful implementation, it is crucial to conduct thorough laboratory and field trials. Additionally, appropriate measures must be taken to ensure that the required target strength is achieved when the method is applied on a full-scale construction project.

3. Materials

In any ground improvement project, one of the most crucial aspects is achieving the desired design strength of the materials when mixed with cementitious binders. The effectiveness of the DSM process, particularly in organic peaty soils, depends significantly on the choice of binder and their interaction with the in situ soil.

The selection of appropriate materials is guided by extensive research and available literature. A key reference in this process is Table 6.1 of the EuroSoilStab guidelines [2] (Table 3.1), which provides detailed specifications for choosing the type of binder based on the organic content of the soil. This table serves as an essential tool in making informed decisions regarding the most suitable binder for various soil conditions.

TABLE 3.1

Selection of binder
(EuroSoilStab, 2000)

Binder	Silt Organic content 0-2%	Clay Organic content 0-2%	Organic Soils, e.g., Gyttja Organic Clay Organic Content 2-30%	Peat Organic Content 50-100%
Cement	XX	X	X	XX
Cement + Gypsum	X	X	XX	XX
Cement + Furnace slag	XX	XX	XX	XXX
Lime + Cement	XX	XX	X	-
Lime + Gypsum	XX	XX	XX	-
Lime + Slag	X	X	X	-
Lime + Gypsum + Slag	XX	XX	XX	-
Lime + Gypsum + Cement	XX	XX	XX	-
Lime	-	XX	-	-

XXX	Very good binder in many cases
XX	Good in many cases
X	Good in some cases
-	Not suitable

For soils with high organic content, such as peat, selecting the appropriate binder is crucial due to the soil's acidic nature and its effect on the hydration process of cementitious materials. Choosing the wrong binder can result in insufficient strength development, jeopardizing the stability and safety of the entire project.

To verify the binder selection, a series of laboratory tests can be conducted on laboratory mix samples. Tests such as Unconfined Compressive Strength (UCS) tests, triaxial tests, and oedometer tests are essential for evaluating the mechanical properties of the soil-cement mixtures. These tests should include samples with varying binder contents and water-binder ratios to gain a comprehensive understanding of material behaviour and determine the requirements for further field trials.

Engineering codes often indicate that there can be significant variability between the strength of laboratory mix samples and field mix samples. This underscores the importance of constructing trial columns and collecting core samples to correlate with the laboratory findings. Additionally, Cone Penetration Tests (CPTs) should be performed to assess the in situ conditions and the results from these tests should be compared with the core laboratory findings to validate design parameters of the stabilised soil.

4.   Design Principles

4.1   DEEP MIXED COLUMNS

The design and implementation of ground treated through deep mixing must be approached with care to ensure that the supported structure remains fit for its intended purpose throughout its lifespan. This design should balance reliability with cost-effectiveness considering all potential actions and influences during both construction and operation. It is essential to address both the serviceability and ultimate limit states during this process.

The geo-mechanical philosophy for deep stabilization is to produce a stabilised soil that mechanically interacts with the surrounding unstabilised soil. The applied load is partly carried by the columns and partly carried by the unstabilised soil between the columns, with strain compatibility maintained consistently across the entire depth of the stabilized soil at all levels (EuroSoilStab, 2000).

The initial step in the design process involves selecting the appropriate arrangements and locations based on the expected stress conditions. Different types of DSM column arrangements are shown in Figure 4.1. For instance, the ground beneath embankment side slopes experiences increased horizontal stress, and the shear strength mobilized is less due to the reduced overburden. The stability of side slopes against deep seated/base failure can be improved by proposing an appropriate arrangement of DSM columns as shown in Figure 4.2.

FIGURE 4.1

Deep Soil Mixing
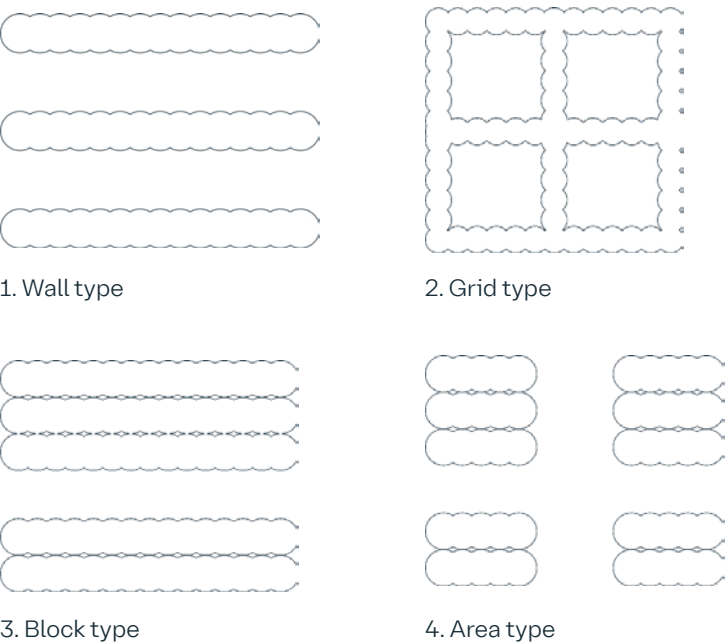patterns / arrangements
(BS 14679, 2005)

1. Wall type

2. Grid type

3. Block type

4. Area type

FIGURE 4.2

Deep Soil Mixing pattern for embankment project (Federal Highway Administration, 2013)

Embankment

Deep-mixed shear walls within the deep mixed zone

- Cross Section -

Deep Mixed Zone

Isolated columns within the deep mixed zone

- Plan View -
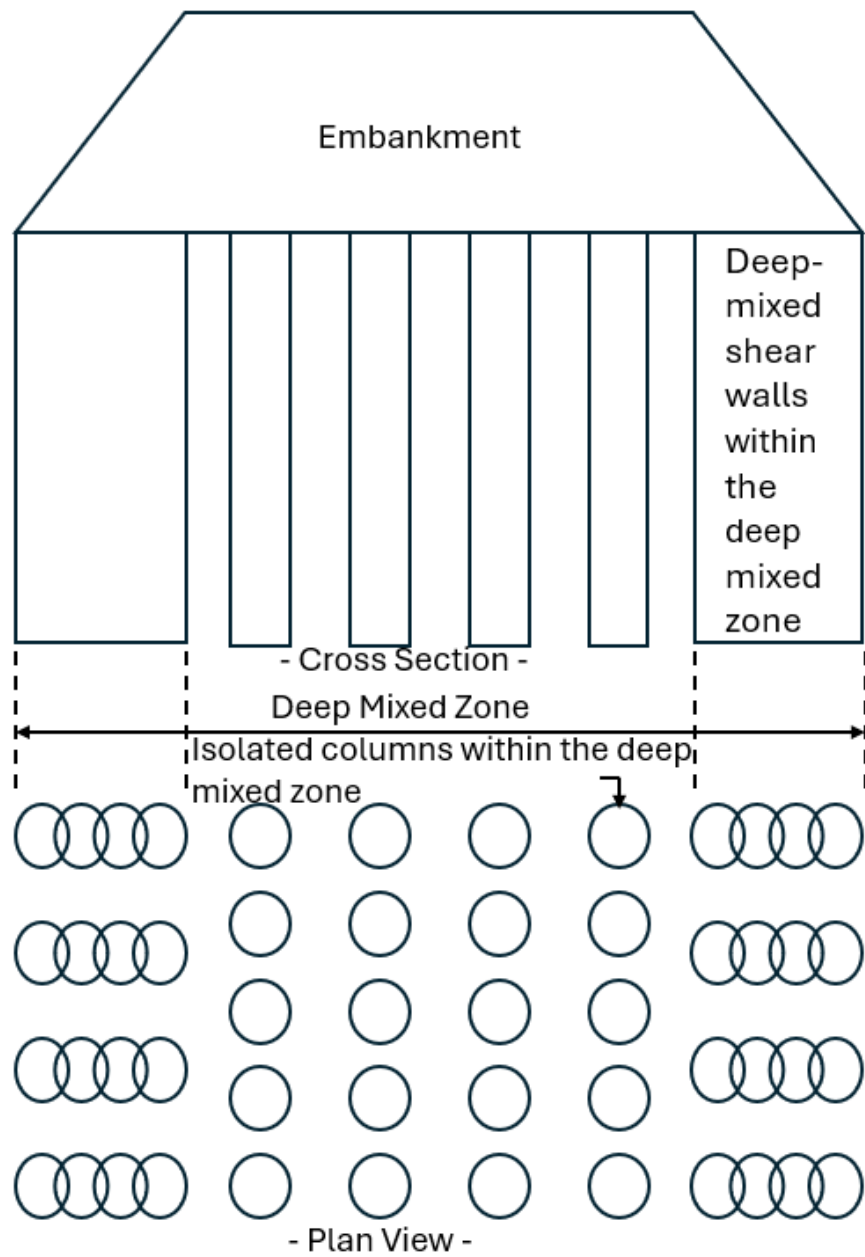
One effective solution under slopes of overlying earthworks is to employ a panel arrangement perpendicular to the toe line of the embankment. In this configuration, the DSM columns within the sloped zone act as shear walls, significantly enhancing the stability of the embankment. However, these shear walls must be thoroughly assessed for several potential slope failure modes (see Figure 4.3):

- **Overturning or sliding:** Shear panels experience overturning and sliding forces due to the higher horizontal stresses present beneath the embankment slopes. The design must ensure that the panels can resist these forces to maintain structural integrity.
- **End Bearing:** The panels' base must have sufficient bearing capacity to support the imposed loads without causing excessive settlement or failure.
- **Shearing of Vertical Planes:** The overlap between columns is particularly susceptible to shearing forces, which could compromise the stability of the entire structure if not adequately addressed in the design.
- **Extrusion of Unstabilised Soil Between Columns:** There is a risk of unstabilised soil extruding between the columns. This extrusion must be controlled by carefully considering the spacing and arrangement of the columns, as well as the properties of the surrounding soil.

FIGURE 4.3

a) Overturning/sliding criteria for panel arrangement, b) Shearing of vertical planes in panel arrangement (Federal Highway Administration, 2013) c) End bearing criteria for panel arrangement d) Extrusion of unstabilised soil between DSM panels (Masaki Kitazume, 2012)
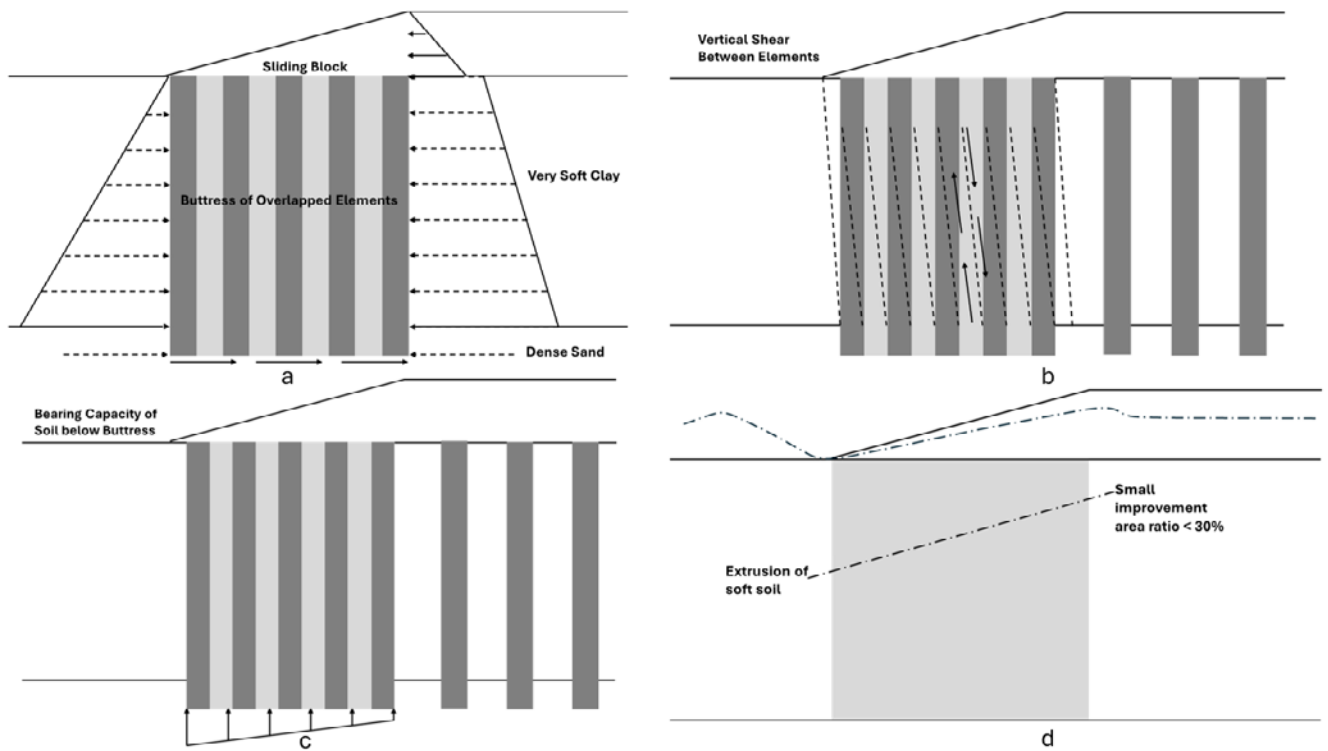
In addition, isolated DSM columns beneath the embankment should be checked for their load-bearing capacity. There are various approaches that exist with the EuroSoilStab recommendations often adopted as codal guidelines. A key consideration is the potential degradation of the DSM column surfaces over time. EuroSoilStab recommends limiting the ultimate strength of DSM columns to 75 to 90 percent to account for this degradation with adjustments made based on the chemical conditions of the surrounding unstabilised soil. The decline in strength of the soil-cement mix due to degradation can be predicted through uniaxial compression tests, needle penetration resistance tests, and thermogravimetric analysis (Vanngoc Pham, 2017). It is crucial to assess the depth of deterioration and the change in strength over time. A conservative reduction factor for the ultimate strength of DSM columns should be applied. Additionally, the smaller diameter cement mix columns exposed to seawater experience a higher rate of deterioration. The diameter of deep mixed columns should be carefully selected in such environments (Vanngoc Pham, 2017).

The overall stability of the combined ground, including both treated and untreated zones, must also be assessed. The parameters used in this stability assessment are crucial, often relying on the area ratio between treated and untreated soil. However, it is important to recognize that the strength of unstabilised soil is fully mobilised at much higher strains, when the DSM columns may have already reached their maximum stress state. Therefore, assuming the full strength of unstabilised soil can result in an overestimation of the combined ground properties. This issue can be mitigated by applying an appropriate mobilisation factor. For very soft soils, such as organic peats, it is recommended to disregard the strength of the unstabilised soil altogether to avoid overestimation.

FIGURE 4.4

Stability of Deep Mixed
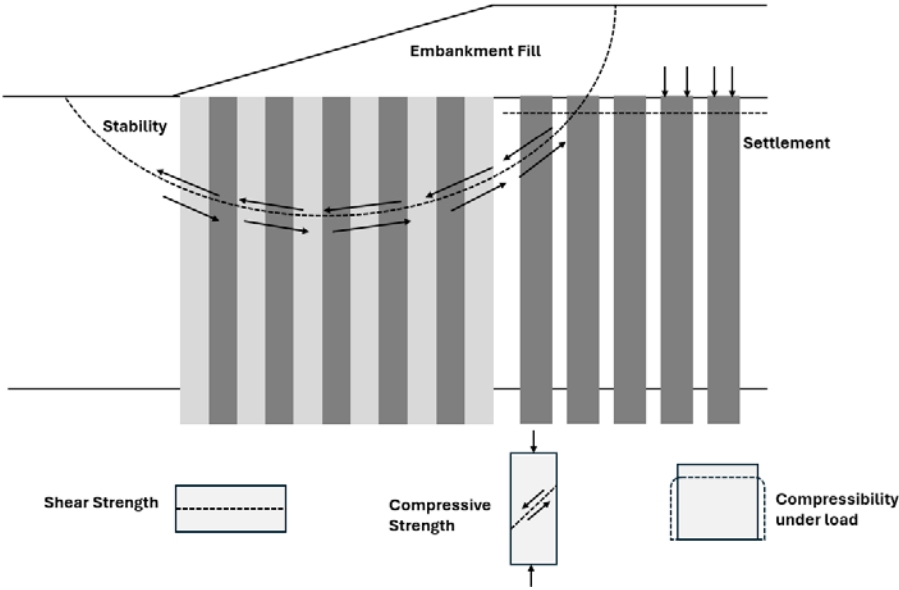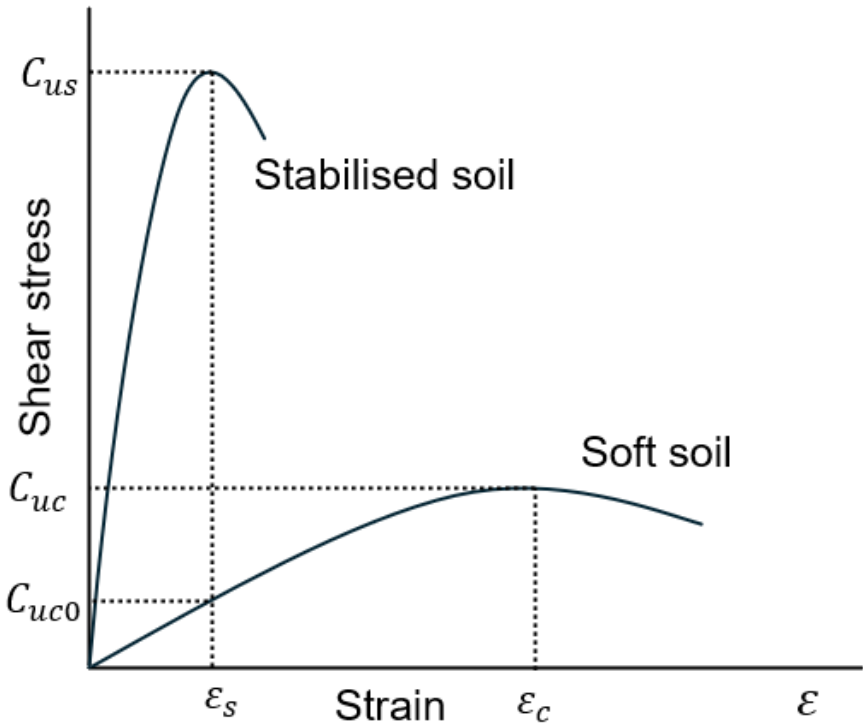columns (Federal Highway
Administration, 2013)

FIGURE 4.5

Strain levels in DSM
columns and unstabilised
soil (Federal Highway
Administration, 2013)

$$T = a_s . C_{us} + (1 - a_s).k.C_{uc}$$

$$k = \frac{C_{uc0}}{C_{uc}}$$

Where,

- a_s: improvement area ratio.
- C_{uc}: undrained shear strength of soft soil (kN/m²).
- C_{uc0}: undrained shear strength of soft soil mobilised at the peak shear strength of stabilised soil (kN/m²).
- C_{us}: undrained shear strength of stabilised soil (kN/m²).
- k: mobilization factor of soil strength. The value of k is less than 1.
- T: average shear strength of improved ground (kN/m²)

The other parameters could be considered based on the similar approach demonstrated above.

4.2   SETTLEMENT CONSIDERATIONS

The settlement of the improved ground under serviceability limit states is a crucial performance requirement for numerous projects. Accurate estimation of settlement is necessary to ensure the long-term functionality of the structure. It is recommended that settlement to be estimated by assuming strain compatibility at the surface of the improved ground.

FIGURE 4.6

Distribution of loads
in DSM columns and
strain compatibility
(EuroSoilStab, 2000)
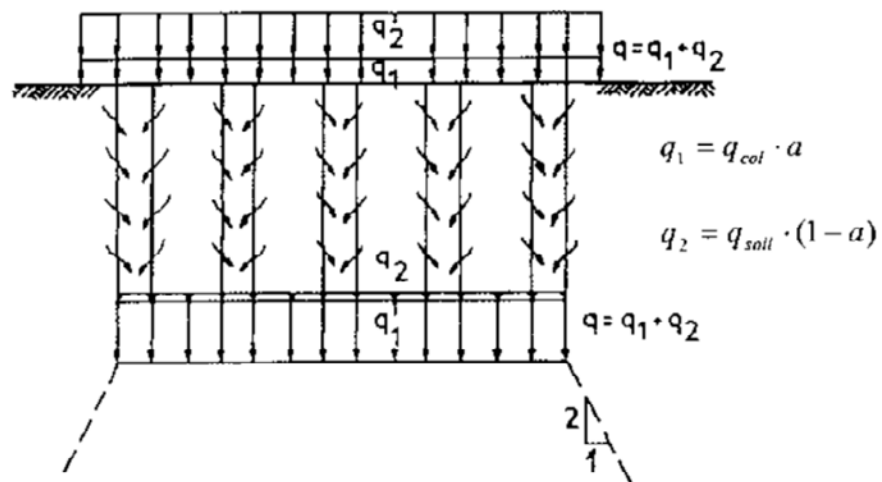
Various methods are available for assessing strain compatibility, including the Finite Element Method. An example of one approach to evaluating strain compatibility is illustrated below.

Settlement in the DSM columns could be determined using the equation provided below:

$$S_1 = \sum \frac{\Delta h}{a} \cdot \frac{q_1}{E_{col}}$$

Where,

- S_1 = Settlement in the column
- Δh = Stratum thickness
- q_1/a = Load on column
- a = Improvement area ratio
- E_{col} = Young's modulus of column

Settlement in the unstabilised soil could be determined using the equation provided below:

$$S_2 = \sum \frac{\Delta h}{1-a} \cdot \frac{q_2}{M_{soil}}$$

Where,

- S_2 = Settlement in unstabilised soil
- $q_2/(1-a)$ = Load on unstabilised soil as above
- M_{soil} = Compression modulus of unstabilised soil

A first calculation should be made by assuming that $q_1 = q_{1max}$. The calculated settlement S_1 in the columns is compared with the calculated settlement S_2 in the unstabilised soil. If $S_1 > S_2$, the load q_1 is gradually reduced and correspondingly q_2 is increased, so that finally $S_1 = S_2$.

When the ground is treated with a cementitious binder, the binder effectively retains water within the DSM columns, promoting the hydration process. Under these conditions, the water pressure within the DSM columns is assumed to be hydrostatic, which may help prevent consolidation settlements within DSM columns.

However, when the improved ground is subjected to loading it may result in excess pore water pressure in the unstabilized soil mass, potentially causing long-term settlements that need to be carefully evaluated. The DSM method (Masaki Kitazume, 2012) provides guidance for rough estimates of such long-term settlements, but these estimates must be verified through continuous instrumentation and monitoring throughout the project lifecycle.

4.3   LOAD TRANSFER PLATFORM

The load transfer platform (LTP) is a vital component in DSM projects, particularly when it is preparing the ground for structures like embankments. The primary function of the LTP is to distribute the load effectively across the DSM columns, preventing future surface settlements that could compromise the integrity of the structure.

When an embankment is proposed over DSM columns, it is essential to assess the potential for arching within the embankment. If arching is anticipated, the special requirement for an LTP may be reduced, as the natural load distribution would already mitigate the settlement risks. However, the assumption that arching will sufficiently transfer the loads onto the DSM columns must be verified through the construction of trial embankments, especially in large-scale projects. These trials provide essential data on the actual performance of the ground improvement system and assist in validating or adjusting the design assumptions. It is also crucial to consider the feasibility of constructing the embankment, as arching effects are expected to become significant once the embankment reaches a certain height.

The arching potential within the embankment and the reinforcement requirements for the load transfer platform can be evaluated according to the recommendations provided in BS 8006 (BS 8006-1:2010+A1, 2016), which offers guidance on piled embankments. Additionally, the FHWA code recommends that if the height of the embankment is greater than two times the clear spacing between the DSM columns, there is no special requirement for a load transfer platform. By adhering to these standards and recommendations, it can be ensured that the LTP meets the necessary criteria for stability and load distribution, reducing the risk of unforeseen issues during the service life of the structure.

5. Construction Requirements

Choosing the right deep mixing method is crucial and should align with specific project requirements. Depending on the ground conditions, either the dry or wet mixing method may be proposed. In the dry mixing method, the binder is added in powder form, whereas in the wet mixing method, the binder is introduced in slurry form. It's important to note that in cases where the soil moisture content is very high, the wet mixing method may take longer for the treated soil to gain strength. Conversely, the dry mixing method may raise environmental concerns, such as dust and noise, which are significant factors to consider.

The binder content should be selected based to the strength gain requirements determined through laboratory and preliminary field tests. Ensuring that all constructed columns achieve the specified design strength is crucial. To ensure this, a comprehensive testing regime must be implemented to validate that the strength requirements are consistently achieved.

In addition to binder content, other critical factors in deep soil mixing include binder type, soil type, moisture content, and curing period, the mixing time and method. Auger rigs are commonly used to install DSM columns. Key variables such as the number of mixing blades, the placement of grout outlets, the volume of binder injected during both penetration and extraction, and the choice between an open or closed mixing head all significantly influence the homogeneity of the DSM columns. The typical mixing blades employed for wet mixing are shown in Figure 5.1. The binder penetration rate, rotational speed during penetration and extraction, and binder injection rate must be carefully monitored and controlled by the rig's monitoring system to ensure the quality and consistency of the columns. The Blade Rotation Number (BRN) which is the function of above-mentioned parameters shall be greater than 300 to achieve efficient mixing.

FIGURE 5.1

Typical mixing blades
employed for wet
deep mixing method
(Masaki Kitazume, 2012)
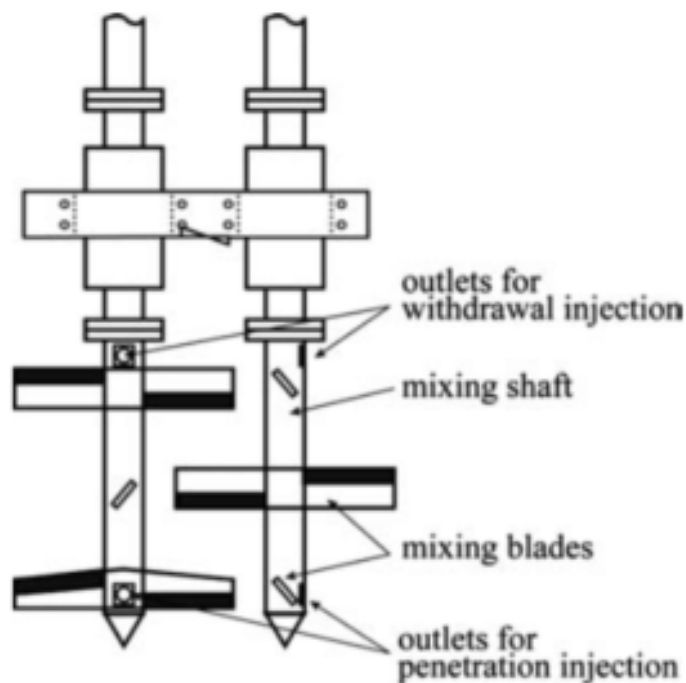
Accurate positioning of DSM columns is crucial for achieving optimal composite behaviour. Tolerances for positioning should be clearly defined in the project specifications. It is recommended that the deviation in position of DSM columns shall be less than 100mm in any direction. It is essential to maintain the verticality of the mixing shaft during the penetration and extraction process, and appropriate instrumentation must be employed to monitor and control the vertical alignment. The deviation in verticality, during installation of the DSM column, shall not be greater than 1 percent. The mixing process used in the CDM (Cement Deep Mixing) method is illustrated in Figure 5.2.

FIGURE 5.2

Execution process
of CDM method
(Masaki Kitazume, 2012)

Positioning Penetration Bottom treatment Withdrawal Completion
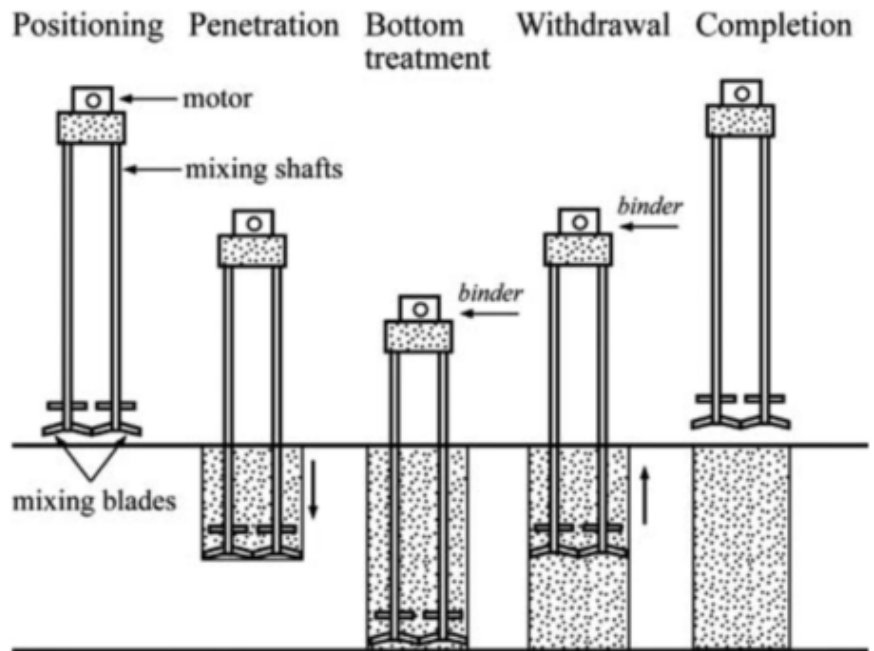
To validate the strength requirements of DSM columns, various tests can be conducted, including UCS testing on cured grab samples and rotary cored samples, as well as consolidated drained (CD) and consolidated undrained (CU) triaxial tests. The CD tests help determine the long-term stiffness modulus, drained cohesion, and friction angle, which can be analysed using stress path concept or MIT plots. The CU triaxial tests and the UCS tests allow to estimate the undrained shear strength of the stabilized soil. The CPT tests are also crucial for validating DSM column parameters. The undrained shear strength from CPT could be obtained as shown in the following equation,

$$C_u = \frac{(q_t - \sigma_{v0})}{N_k}$$

Where,

- q_t = the corrected total cone resistance obtained from CPT test
- σ_{v0} = vertical effective stress
- N_k = cone factor, whose value varies from 17 to 25

The N_k value, used to derive the undrained shear strength of DSM columns from CPT cone resistance, should be carefully calibrated against UCS test results to ensure optimal accuracy. It is important to recognize that the CPT cone may become misaligned (popping out), potentially leading to misinterpretation of results. To alleviate this, pre-boring can be carried out up to a certain distance above the expected deviation zone, followed by redoing the CPT to obtain reliable data.

The frequency of these tests should be determined based on recommendations from relevant standards, the conditions of the parent ground, and insights from various case studies. For the testing process, one wet grab sample will be collected for every $50m^2$ of the improved area or once per working shift. Full depth continuous coring is recommended for 2 percent to 4 percent of the elements produced, depending on the project's criticality or the importance of the proposed location. In large-scale projects, one CPT should be conducted for every 10 DSM columns during the construction of the first 200 DSM columns. This frequency may be increased to one test per $100m^2$ of improved area. From each recovered core, four UCS tests and four triaxial tests should be performed to confirm the strength achieved. The wet grab samples shall undergo testing during the initial curing periods to verify if the expected strength gain is being achieved. If the required strength is not attained, the contractor must revise the mix to enhance the strength. A minimum of two slurry density tests are recommended per batching plant to verify the target density such that the target water and binder ratio is proved for the binder type specified.

It is crucial to ensure that deep mixed columns are sufficiently embedded into the underlying competent soil strata, to efficiently transfer the imposed loads. The embedment depth can be monitored during construction using plant monitoring equipment that records the increase in torque required to rotate the mixing blades as they penetrate the soil. This increase in torque can serve as an indicator of proper embedment. The final embedment criteria should be determined based on site trials.

6.   Design Risks

DSM is a complex ground improvement technique, and it is essential to manage various design risks to ensure project success. Key risks associated with DSM include:

- ▪ **Inadequate Strength of DSM Columns:** A major risk in DSM projects is the potential for inadequate strength of the DSM columns due to inappropriate quality control measures. If the mixing process or materials are not carefully monitored and controlled, the resulting columns may fail to meet the required strength specifications. This risk can be mitigated by implementing robust quality assurance programs that ensure consistency and reliability in the mixing process and material properties.

FIGURE 6.1

Various failure modes
of group of individual
DSM columns
(Masaki Kitazume, 2012)
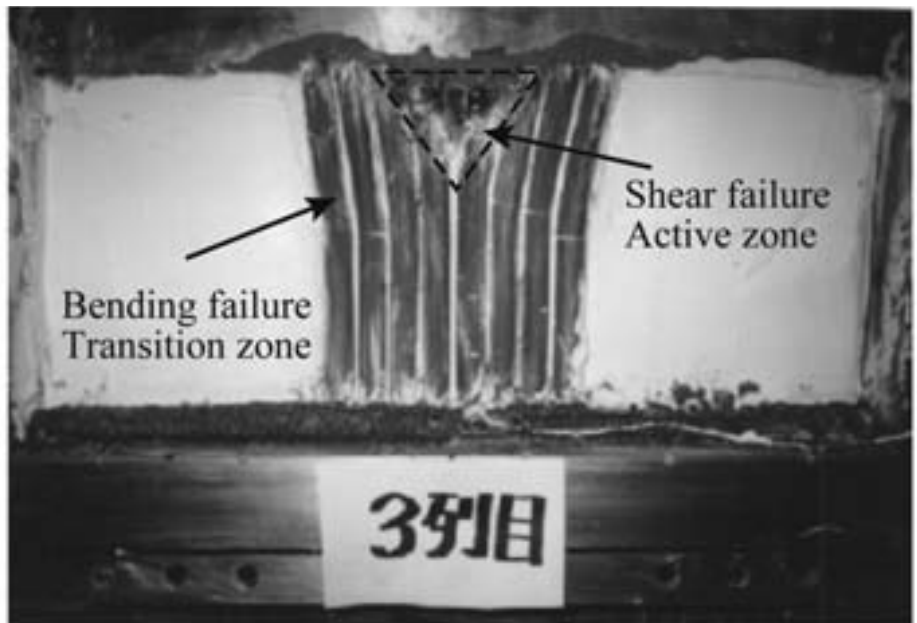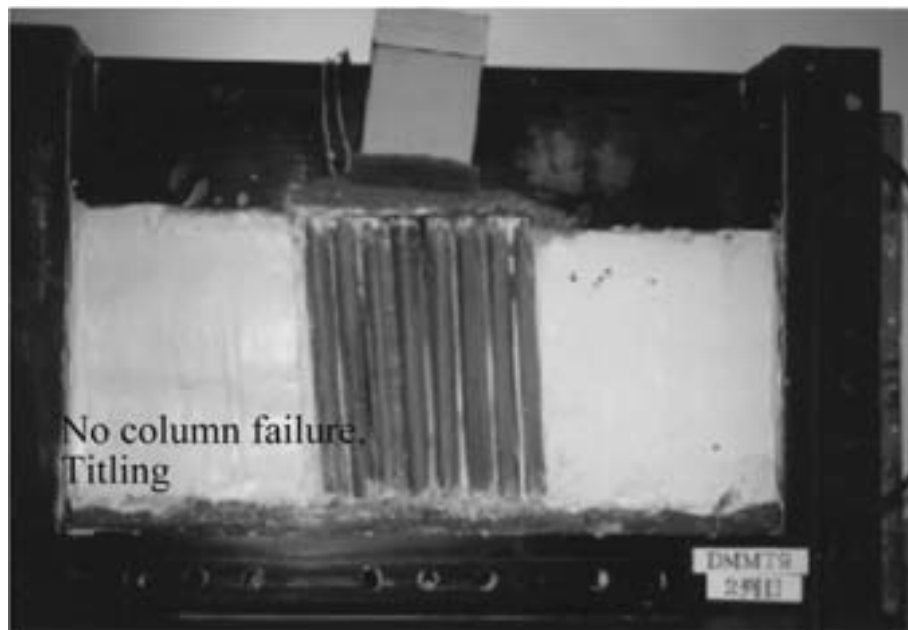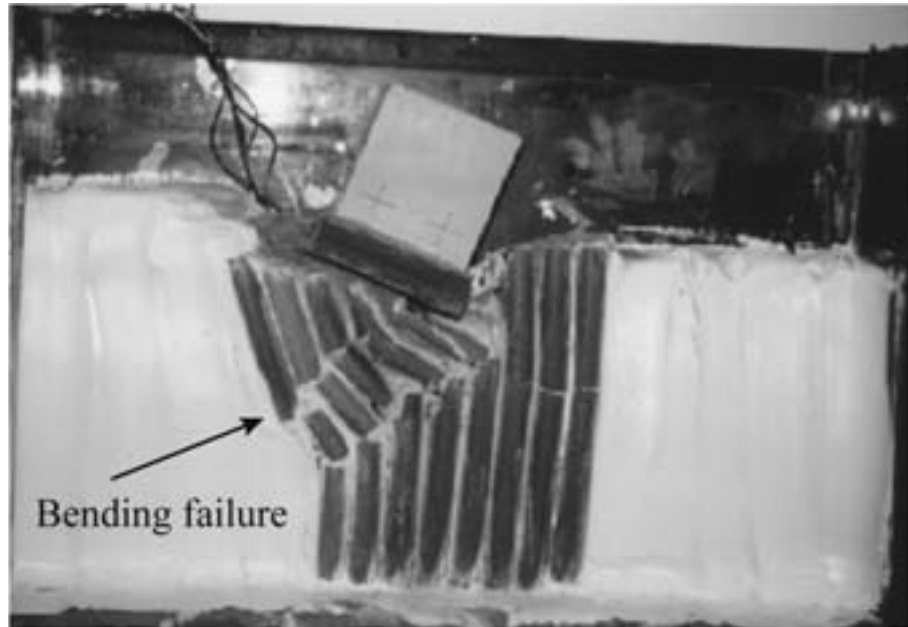
- **Unidentified Competent Bearing Layer:** Another significant risk is the inadequate embedment of DSM columns in the underlying bearing stratum. If the columns do not penetrate deeply into the bearing layer, the overall performance of the improved ground can be compromised, leading to potential failures or excessive settlements. It is crucial to carefully assess the nominal depth of ground improvement to ensure that the toe of the DSM columns rests in a competent bearing stratum. Proper design and verification during construction are essential to ensure adequate embedment and to mitigate this risk.
- **Creep Settlements:** The improved ground can be subject to creep settlements over time, particularly in soft or organic soils like peat. Creep settlements can occur gradually and may impact the long-term performance of the structure. Continuous instrumentation and monitoring of the improved ground are vital for detecting and assessing any creep behaviour.
- **Complex Behaviour of Improved Ground:** The behaviour of the improved ground with DSM can be complex, especially when dealing with very high strength DSM columns at wider spacings. In these cases, the columns may behave more like rigid piles rather than as part of a homogeneous improved ground mass. The capacity of these rigid columns should be assessed differently, rather than following the standard design approach outlined in this paper.

7.   Conclusions

DSM may be an effective technique for improving ground conditions, particularly in challenging soils such as peat. However, the success of DSM projects depends on several critical factors:

- **Binder Content Selection:** The choice of binder content is a fundamental aspect of DSM projects. It is essential to verify the selected binder through appropriate laboratory and field tests at different stages of the project. This ensures that the desired properties are achieved in the final ground improvement.
- **Design for ULS and SLS:** The design of ground improvement must adequately address both the ULS and the SLS to ensure that stability and performance requirements are consistently met. Proper design practices help prevent structural failures and ensure the long-term viability of the project.
- **Risk Mitigation:** The inherent risks associated with DSM, such as inadequate column strength or creep settlements, should be proactively managed. Field trials are crucial for validating design assumptions and preventing potential future failures. These trials may include load tests on individual DSM columns, groups of DSM columns, and, if necessary for large-scale projects, trial embankments.
- **Quality Control and Assurance:** Achieving the appropriate assumed ultimate strength of DSM columns on-site is key to the success of the project. This can be accomplished through a well-established quality control and quality assurance program that monitors and verifies all aspects of the mixing process and material properties.

Acknowledgements

References

BS 14679. (2005). *BS 14679: Execution of special geotechnical works - Deep mixing.* BSI.

BS 8006-1:2010+A1. (2016). *BS 8006-1:2010+A1 Code of practice for strengthened/reinforced soils and other fills.* BSI Standards Publication.

EuroSoilStab. (2000). *Design Guide Soft Soil Stabilisation (Project No: BE 96-3177).* BRE.

Federal Highway Administration . (2013). *Design Manual: Deep Mixing for Embankment and Foundation Support.* FHWA.

Indraratna, B., & Chu, J. (2005). *Ground Improvement Case Histories.* ELSEVIER GEO-ENGINEERING BOOK SERIES - Volume 3.

Institution of Civil Engineers. (2012). *ICE manual of geotechnical engineering.* ICE.

Masaki Kitazume, M. T. (2012). *The Deep Mixing Method.* CRC Press (Taylor and Francis Group).

Nigel Pye, O. A. (2012). Deep Dry Soil Mixing to Stabilize a Live Railway Embankment Across Thrandeston Bog. *Grouting and Deep Mixing 2012.*

Nigel Pye, O. A. (2012). Laboratory and Field Trials for Deep Dry Soil Mixing to Stabilize a Live Railway Embankment Across Thrandeston Bog. *Goruting and Deep Mixing 2012.*

Vanngoc Pham, B. T. (2017). Long-term strength of soil-cement columns in coastal areas. *Soils and Foundations - Tokyo.*

06: Study of the Overprovision of Cement and Emissions in a Reinforced Concrete Structure

Significance Statement

Cement, a constituent of concrete, significantly contributes to global greenhouse gas emissions. Using more cement generally makes concrete stronger, but it also increases emissions. This case study investigated cement overprovision. The results showed that the structural design specified a concrete strength higher than required, whilst the concrete produced was stronger than needed. In this case, a reduction of cement content of 12.5% was acceptable, which has considerable emissions implications on the project. Careful consideration of cement content throughout design and construction could play a crucial role in reducing overall concrete emissions.

Énoncé d'importance

Le ciment, un composant du béton, contribue considérablement aux émissions mondiales de gaz à effet de serre. L'utilisation d'une plus grande quantité de ciment renforce généralement le béton, mais augmente également les émissions. Cette étude de cas portait sur l'imposition de spécifications trop strictes pour le ciment. Les résultats ont démontré que la conception structurale spécifiait une résistance du béton plus élevée que nécessaire, alors que le béton produit était plus résistant que nécessaire. Dans ce cas, une réduction de la teneur en ciment de 12,5 % était acceptable, ce qui entraîne des répercussions considérables sur les émissions du projet. Un examen attentif de la teneur en ciment tout au long de la conception et de la construction pourrait jouer un rôle crucial dans la réduction des émissions globales du béton.

Fenella Ross
Senior Civil Engineer
Infrastructure – UK & Ireland
London, UK

Abstract

In this case study, the efficient use of cement is explored through the reduction in concrete strength because there is typically a positive correlation between cement content and concrete strength. This was explored through two means: analysis of concrete mix strengths achieved (efficient use of materials) and investigation of over-design (underutilised section design). The impact of using a concrete mix with a specified strength 20% lower than that considered in design is investigated through analysis of the compressive test results and reanalysis of the structural design for the specific building. The results showed that both the provided and specified strength was higher than required; consequently over 99% of the analysed structure was acceptable with a lower design strength. This lower provided strength resulted in greenhouse gas emissions savings of 150kg per m^3 of concrete, indicating that the design was inherently overly conservative. Main longitudinal (flexure) reinforcement was not sensitive to the change in concrete strength for the ultimate limit state design but showed more variation for serviceability limit states. The design for shear was shown to the most sensitive to a lower concrete strength with unacceptable results for shear requiring some local rework. Additionally, discussions with project stakeholders enable understanding into the principle causes of this initial over-requirement for cement content.

145

1.   Introduction

The International Energy Agency (IEA, 2019) identifies that the buildings and construction sector is a key area to target for decarbonisation, however the sector is not currently decarbonising at the rate needed to meet Net Zero targets. Currently, decarbonisation of the sector is focused on the reduction of greenhouse gas emissions (hereafter referred to simply as emissions) produced during operation of an asset such as decarbonisation of energy and transport supplies. However, as these operational emissions reduce, the proportion of embodied emissions will increase towards 100% of total emissions (Drewniok *et al.,* 2023b; Purnell and Black, 2012). Therefore, reduction of these embodied emissions will become an increasing area to target.

Cement, which acts as the main component to the concrete binder, accounts for approximately 90% of concrete emissions (Miller, 2020a) and contributes to 7-8% of global anthropogenic emissions (Shah *et al.,* 2022). Coincidently, the production and consumption of cement is growing; cement production has more than doubled over the past 2 decades (Shah *et al.,* 2022) and there is expected to be a continued growth in developing countries (Uratani and Griffiths, 2023) due to a strong positive correlation between economic growth and cement consumption (Griffiths *et al.*, 2023). Therefore reduction of cement emissions is a key target area; it has been identified as the third largest source of difficult to eliminate emissions globally (Shah *et al.,* 2022).

In the manufacture of cement, 60% of emissions are generated by the decomposition of limestone ($CaCO_3$) to produce lime (CaO) and carbon dioxide (CO_2) whilst 40% of emissions are generated from the heating of limestone (Uratani and Griffiths, 2023). Globally, however, methodologies to reduce cement emissions have focused on easier to implement interventions through emissions reduction in the heating of limestone (Miller *et al.,* 2021), (Parmenter and Myers, 2021), (Watari *et al.*, 2022). Reducing the volume of cement through material efficiency (ME) is the most effective solution to reducing manufacture emissions as there is currently no commercially viable solution to produce cement with no emissions (Miller *et al.* 2021).

Although ME forms a key component of global decarbonisation strategies (European Commission, 2018; IEA, 2019; IRP, 2020; Material Economics, 2019), there is typically limited direction on how to achieve ME and many strategies only focus on the introduction of new materials and re-use and recycling of existing materials. It is noted in literature that there are many barriers to ME covering industry, technology, government policy and standards. Within industry, emissions mitigation is typically relatively low priority (Balsara *et al.*, 2021). The principal barriers are generally cost and risk; relatively low cement cost leads to over-specification of material and adoption of standardised construction processes (Rissman *et al.*, 2020), (Miller *et al.*, 2021). In addition, there can be difficulties for new technologies to enter the market due to concerns over these being unproven (Balsara *et al.*, 2021) and standards not maintaining pace with new cement technologies (Griffiths *et al.*, 2023). Further, there has historically been limited policy to support adoption of new technologies. For example, the UK has typically overlooked ME in policy, instead only capturing a circular economy approach (Parmenter and Myers, 2021) whilst government policy and regulation barriers were shown to be the most dominating in the cement industry in India (Balsara *et al.*, 2021). Actions to reduce emissions and improve ME must be implemented immediately, therefore ready to adopt solutions must be developed and more work to understand industry blockers is required.

Moreover, there are limited practical methods which are not currently impacted by ME blockers. Within literature, research into decarbonisation strategies for cement and concrete highlights the importance of ME such as Rissman *et al.* (2020), Parmenter and Myers (2021), Watari *et al.* (2022), Drewniok *et al.* (2023a), Miller *et al.* (2021) and Shanks *et al.* (2019). These strategies generally focus on methods to reduce the concrete volume which include the use of precast concrete, post-tensioning of reinforcement and 3D printing. Much of this work covers reducing the percentage cement content of concrete through reduction in over-design and mix tailoring, however practical methods to achieve this are not explored in detail beyond the use of cement replacements such as ground granulated blast-furnace slag (GGBS) and fly ash produced in the blast furnace for steel manufacture and coal-fired power-stations respectively. However, the provision of these commonly used cement replacements is expected to decrease as these industries decarbonise (Drewniok *et al.*, 2023a).

Therefore, further research is required into strategies to reduce the percentage cement content in concrete. Research has generally focused on optimising the mix design for specified concrete strengths, such as work carried out by Fan and Miller (2018), DeRousseau *et al.* (2018), Reis *et al.* (2021) and Purnell and Black (2012). These papers generally investigated the optimisation of concrete constituent components to minimise carbon emissions for a given strength. However, the research did not investigate the overprovision of strength for certain mix designs. Further, the research generally showed that increased strengths are achieved through increased cement binder volume and consequently emissions. Therefore, although optimisation of mix design forms a key aspect of reducing cement content, it misses the most impactful solution of reducing the cement content to achieve the lowest acceptable compressive strength for specified designs.

Literature investigating alterations to concrete strength to reduce emissions typically focuses on increasing rather than reducing concrete strength. The investigation focuses on reducing required volume of concrete with the higher provided concrete compressive strength. Purnell and Black (2012) and Habert and Roussel (2009) show that increasing the compressive strength reduces the cross-section and embodied emissions for cross-sections acting in compression. Habert *et al.* (2012) and Tae *et al.* (2011) investigate increasing the compressive strength of concrete for a bridge and high-rise apartment building respectively; both show that the increase in strength reduces concrete volume and embodied emissions. However, increasing the compressive strength of concrete will only reduce emissions where the decrease in volume outweighs the increase in emissions intensity of the concrete. Habert and Roussel (2009) discuss that increasing the compressive strength for horizontal load-carrying members does not bring a benefit of emissions reductions and Tae *et al.* (2011) noted that the increased concrete strength only led to reductions in element sizes for vertical members.

Kourehpaz and Miller (2019) have presented calculation methods to assess the effect of concrete strength on different types of concrete elements. Their work shows that the lowest emissions are achieved by increasing concrete strength for compressive members (such as columns).

However, the opposite behaviour is shown for members in flexure (such as beams) with the lowest emissions achieved by reducing concrete strength. Miller (2020b), Watanabe *et al.* (2021a) and Watanabe *et al.* (2021b) show similar trends; typically designing with higher compressive strength has a positive effect on emissions for columns with axial load but a negative effect on elements in flexure. The Concrete Centre (2020) show similar results by calculating that increasing concrete strength reduces emissions for vertical elements but increases emissions for slabs. Miller *et al.* (2015) investigated different methods to reduce emissions from a concrete frame building design to provide practical solutions to reducing embodied emissions such as increasing cement replacement, altering column sizes and reducing column strengths at higher floors. Although this is a positive step in providing practical methods to reduce emissions in building design, the authors did not investigate the effect on strength of members acting in flexure (such as slabs) despite the same work showing that beams with higher cement content result in higher emissions. Additionally, Torelli and Lees (2019) showed that it is feasible to grade concrete properties across a structure element (i.e., considering layers of different concrete compositions within the same elements). The authors acknowledged the benefit of this approach for optimisation of cement content in the structural element as strength capacity is only reached in certain parts of the element. It is assumed that this refers to flexure, where typically the compressive strength is only required for less than half the cross-section thickness.

Therefore, although literature presents a good indication for the influence of strength on emissions for members in flexure, it is apparent that no proven industry examples have been documented. Additionally, the impact of other design criteria, such as shear have not been captured. Watanabe *et al.* (2021b) noted that the effects of lateral reinforcement should be explored in future work. Therefore, this case study will investigate the impact of concrete strength for members acting in flexure by reducing the design strength from that originally analysed. Additionally, the case study will identify the industry drivers behind the over-specification of concrete strength by designers and contractors.

2.   Case Study Background

This case study focuses on a reinforced concrete structure on large-scale infrastructure project. It is a partially buried 5-storey structure with plan dimensions of approximately 1000m^2. Two different concrete compressive strengths have been allowed by the client across the construction site: C40/50 and C60/75, the respective properties are shown in Table 1. The below-ground structure (~2,500m^3) and above-ground structure (~4,500m^3) were designed with different concrete strengths: C60/75 and C40/50 respectively. Three of the below-ground concrete pours with a combined volume of 350m^3 (indicated in Figure 1) used a lower strength C40/50 concrete rather than the specified higher strength C60/75 concrete considered in the design. Due to the high lateral loading on the structure, the wall and slab elements within these concrete pours were shown to primarily act in flexure. The reinforcement arrangement for these elements is shown indicatively in Figure 1.

Two opportunities were investigated to identify if a lower concrete strength was acceptable: the actual strength test data for the mixes poured and the reanalysis of the design with lower strength.

TABLE 1

Concrete Mix Properties

Strength Class	Mix Reference	Design Cylinder Compressive Strength (MPa)	Design Cube Compressive Strength (MPa)	Binder Content			
				Cement - CEMI (kg/m^3)	GGBS (kg/m^3)	Total Binder (kg/m^3)	Proportion GGBS
C40/50	6F and 6S	40	50	120	280	400	70%
C60/75	3F and 3S	60	75	135	315	450	70%

FIGURE 1

Typical reinforcement
arrangement in Pour A and
C (top) and Pour B (bottom)

Typical Wall Section

60mm external cover
12mm link
45mm internal cover
32mm horizontal reinforcement
32mm vertical reinforcement
200mm spacing
450mm thick

Typical Slab Section

45mm cover
12mm link
45mm cover
25mm horizontal reinforcement
25mm horizontal reinforcement
200mm spacing
500mm thick
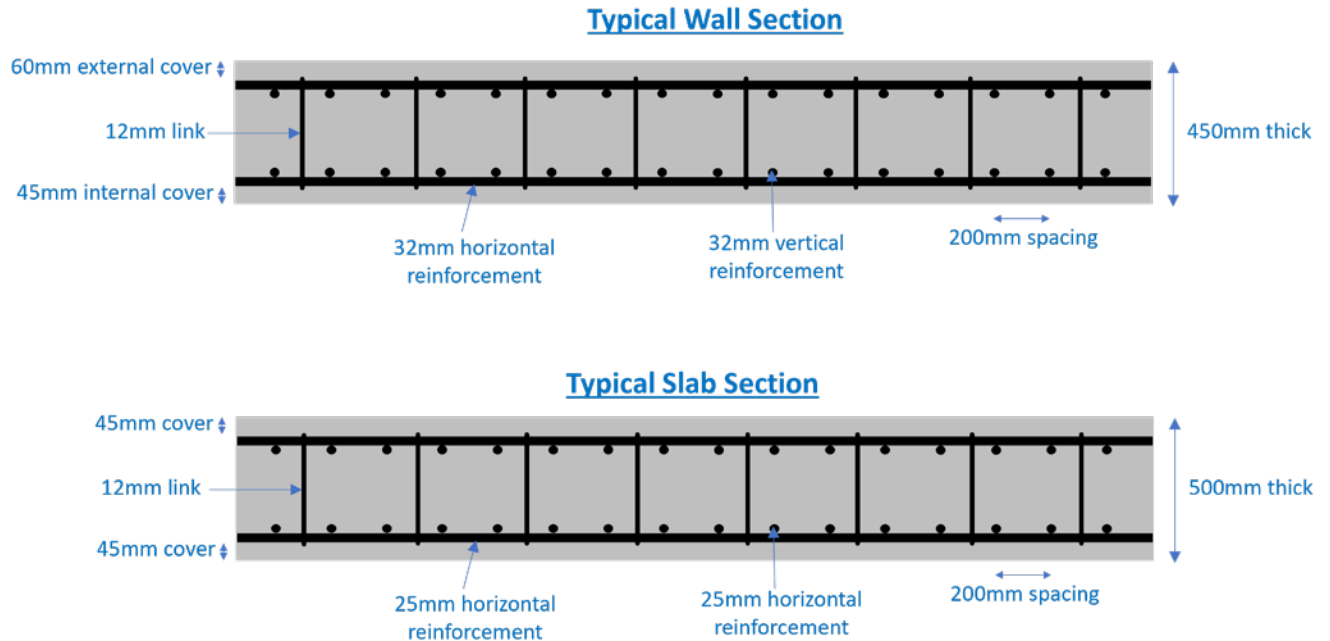
2.1 ANALYSIS OF THE POURED CONCRETE

Cube samples are taken for every concrete pour across the site and their compressive strength is tested at the following intervals: 7-days, 28-days, 56-days and 91-days. The concrete cubes test results were collated for Pour A to C and every pour for the same period (approximately 800 samples). The two different mix designs (6S and 6F) were used for slab and wall pours; these contained the same binder mass but with admixture alterations due to differing workability requirements.

The difference in embodied emissions was then compared between the two different concrete strengths. As the cement accounts for approximately 90% of concrete emissions (Miller, 2020a), the difference in emissions for the concrete mixes was evaluated using the inventory of carbon and energy database v3 (Jones, 2019) considering the cement content only.

2.2   REDESIGN WITH REVISED STRENGTH

The building had been modelled in Finite Element (FE) modelling software Simula Abaqus to determine the section forces and moments for the relevant load combinations. An automated script was developed for the project to resolve the FE analysis section forces and moments into reinforcement design forces by using the sandwich model approach from Eurocode 2 Part 2 (British Standards Institution, 2010). The required reinforcement is determined for each FE based on Eurocode 2 Part 1 (British Standards Institution, 2015). The provided reinforcement is an input for each FE analysis to determine a Utilisation Ratio (UR).

The original analysis showed that the FE analysis results were not sensitive to the ~10% change in stiffness between the concrete strengths, consequently the original FE analysis was carried out considering properties for C40/50 strength class throughout. Therefore, only local calculations to determine revised reinforcement URs were required for each longitudinal reinforcement direction and shear. The maximum UR from the 7no. panels considered in the analysis was compared between the different concrete strengths used. Additional design checks were performed including those to verify interface shear, punching shear and reinforcement anchorage lengths with the lower concrete strength, however the results of these are outside of the scope of this case study.

Elements primarily acting in flexure were reanalysed for another large-scale infrastructure project (case 2) which used hand-calculations to evaluate if the same conclusions would be reached through an alternative analysis methodology. The compressive strength used across the project of C40/50 was specified by the client. In this case study, the plank was reanalysed to identify the lowest acceptable compressive strength for design (i.e. yielding a UR less than 1).

3.   Results

3.1   ANALYSIS OF THE POURED CONCRETE

The historical cube test data shows high strength is achieved for both concrete mixes: the mean concrete strength of 58MPa at 28-days for both mixes exceeds the design strength by over 10% as seen in Figure 2. The minimum strength achieved at 28-days across the 800 samples was within 5% of the design value. All samples reached 55MPa by 91-days; thus achieving the required strength for the next strength class of C45/55.

Results for the specific pours analysed in this case study lie within the expected range from the historical data. All samples exceed the design strength at 28-days and fall within 1MPa of the required strength for C45/55 at 56-days.

FIGURE 2

The cube strength results for C40/50 strength
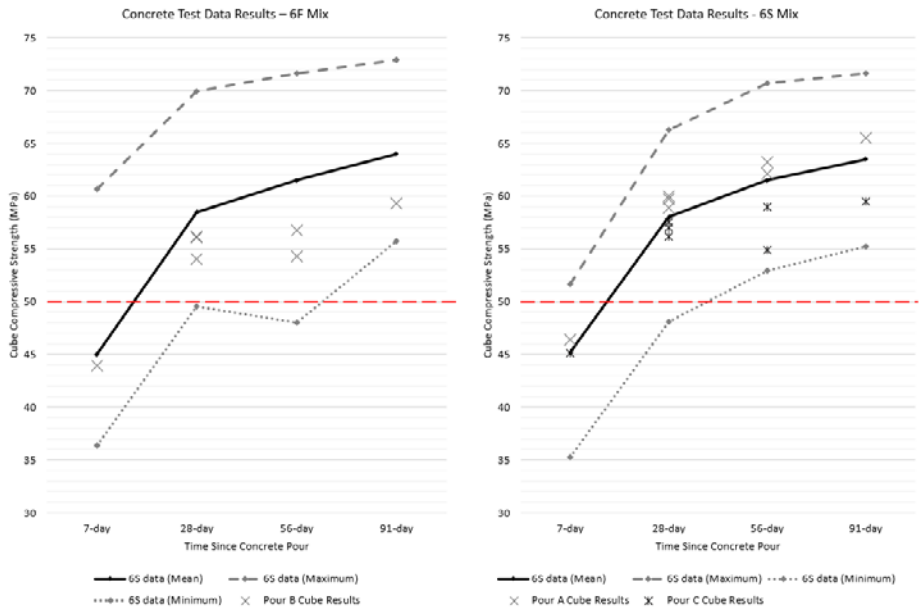
The cement (CEMI) content increased with increasing strength class; the C60/75 mix design contained 12.5% more CEMI and overall binder than the C40/50 mix design. The increase in emissions is proportional to the increase in binder, with CEMI contributing significantly more than GGBS to emissions. Nevertheless, despite the high GGBS binder content, the higher strength concrete still led to an additional 150kg of emissions per m^3 of concrete or 5,250kg for the area of this case study.

3.2   REDESIGN WITH REVISED STRENGTH

The analysis showed that the majority of the building could be verified considering the strength properties for the C40/50 strength class. The original analysis was governed by the Ultimate Limit State (ULS) and crack-width with low URs for the Serviceability Limit State (SLS), as shown in Table 2.

TABLE 2

Percentage of results with high utilisations (UR > 0.8) for accidental ULS (ULS$_a$), frequent ULS (ULS$_f$), characteristic SLS (SLS$_c$), frequent SLS (SLS$_f$) and quasi-permanent SLS (SLS$_{qp}$)

	Longitudinal Reinforcement						Shear Reinforcement	
	ULS$_a$	ULS$_f$	SLS$_c$	SLS$_f$	SLS$_{qp}$	Crack-Width	ULS$_a$	ULS$_f$
Percentage of URs > 0.8	13%	67%	0%	7%	0%	54%	44%	41%

Figure 3 shows the percentage change in UR for each limit state. For the longitudinal reinforcement, ULS and SLS_c did not show a significant change in UR with the lower strength class with no change for the mean and median. In some cases, a decrease in utilisation of up to 0.04 with the lower strength was observed. It is expected that this minor difference is due to small changes in the iterative sandwich layer thicknesses determination in the analysis. The impact of the lower strength class was more significant for the longitudinal reinforcement URs for SLS_f, SLS_{qp} and crack-width with the mean change in UR varying between 10-20%. The impact on shear reinforcement was the most significant, with a mean percentage change of 13% for ULS_f and 28% for ULS_a. The more significant change for ULS_a is expected to be due to the lower safety factors and higher loading experienced.

Percentage Changes in UR
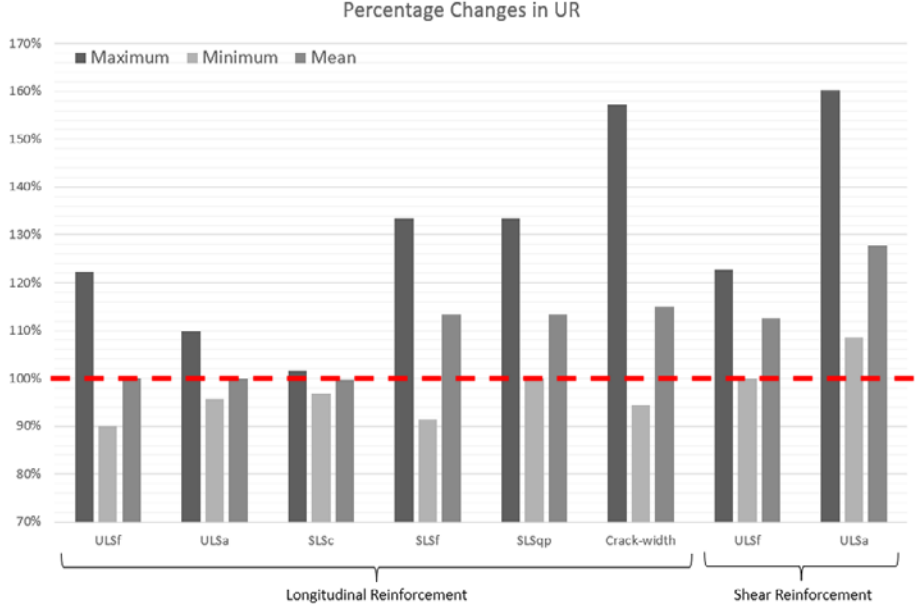
Discussions with the designers yielded the reasons for the selection of concrete strength on the project. The initial input data specified for C40/50 strength class for the entire building. However, the analysis results of this original design showed that the reinforcement for multiple buried walls could not be practically designed due to high demand. This unsuccessful analysis run delayed the delivery of the building design. As resolution, multiple measures were implemented in parallel to ensure successful results for the design next iteration. These measures included increasing element thicknesses, additional wall elements and increasing the strength class for the below ground structure. As only C40/50 and C60/75 strength classes were approved, the only viable higher strength class was C60/75. Conversations with wider project stakeholders yielded the general opinion that the additional concrete strength gain past the required strength was positive and provided additional margin.

The results from Case 2 showed similar trends in the change in utilisation ratios, with an increase of 5% for ULS longitudinal reinforcement and crack-with and an increase in 24% for shear reinforcement.

4.   Discussion

4.1   CONCRETE MIX DESIGN

The compressive strength test results showed that concrete strength is consistently exceeded for the concrete poured across the site. Considering the 217,000m³ of concrete poured per year at the construction site, this leads to a significant overprovision of cement and additional emissions. This exceedance is not expected to be localised to this construction site; Miller *et al.* (2021) presented that it is commonplace for contractors to order higher cement content to reduce risk. As noted by Griffiths *et al.* (2023), reducing cement use by 15% by 2050 could avoid 604Mt emissions per year globally. This case study showed that a 12.5% cement reduction was acceptable, therefore suggesting this 15% reduction could be achieved ahead of 2050.

Generally, this additional strength gain is considered by the project stakeholders to be positive to provide additional structural margin. This further confirms the risk adverse attitude of stakeholders presented in earlier work (Rissman *et al.*, 2020; Miller *et al.,* 2021). Further, it confirms the hypothesis of Balsara *et al.* (2021) that a lack of environmental awareness exists in the construction industry. Although additional strength may provide additional margin on design, this margin is not well understood or targeted.

Further, it is noted that additional concrete strength is not always favourable for the structure design. For example, higher strength would require higher minimum reinforcement (British Standards Institution, 2015) and could increase differential drying shrinkage strains. Therefore, amendments to the specification of concrete mixes are needed to unnecessary avoid additional emissions and ensure that the design is appropriately bounded. This could include recommending a maximum strength value, which if exceeded would require discussions between stakeholders and amendments to mix design. Alternatively, concrete strength could be specified at 56-day strength as presented by Miller *et al.* (2015) and Jones (2020) which enables lower cement content due to the increase in cement gain over the longer time period. This is especially key for cements with high GGBS content where strength gain is slower. However, it is noted that this benefit may not be achieved in all design codes. For example, the second generation of the Eurocodes (British Standards Institution, 2023) a factor is applied on the compressive strength of concrete to account for the effect of high sustained loads and the time of loading on concrete compressive strength. For concrete with slow or normal strength development, this factor can only be taken as 1 where 28-day strength is specified; otherwise, a factor of 0.85 must be applied. This may negate any benefit in specifying a 56-day strength.

The concrete strength results showed a large disparity in strengths achieved; with variations of up to 25MPa between the maximum and minimum strength values. Batching of the concrete is undertaken with strong quality control processes, therefore the variety of strengths achieved is expected to be due to the differences in raw ingredients and climatic conditions during pouring. The introduction of additional measures to improve the conditions for curing of concrete could lead to significantly improved strength gain and consequently lower required cement content. The increased adoption of pre-cast concrete, as suggested in literature such as Parmenter and Myers (2021), could enable optimum climatic conditions to be achieved during curing. Further, as noted by Uratani and Griffiths (2023), 42% of the global cement market uses bagged products and on-site mixing. This results in quality control issues and likely more variation in concrete strength which could further benefit from concrete batching and use of pre-cast.

4.2   CONCRETE STRENGTH ON DESIGN

Although the concrete strength was increased to resolve design issues during the ULS flexure calculations (for longitudinal reinforcement), the impact on the ULS flexure URs due to the change in strength was relatively minor. The strength of concrete influences the depth of the outer sandwich layer (British Standards Institution, 2010); thinner outer layer thicknesses are enabled by higher concrete strength and consequently the reinforcement lever-arm increases. The same relationship can be observed from more typical hand calculations, as demonstrated in Equation 10 of Kourehpaz and Miller (2019) where concrete strength only contributes to the determination of the reinforcement lever-arm. The equation is derived based on American design codes, however a very similar relationship is derived based on British Standards Institution (2015) shown in Equation 1 where f_{cd} is the design concrete strength, M_{Ed} is the design moment, A_s is the area of reinforcement, f_{yd} is the design reinforcement strength and b is the section width.

$$UR = \frac{M_{Ed}}{A_s f_{yd}\left(d - 0.63\frac{A_s f_{yd}}{b f_{cd}}\right)} \qquad (1)$$

The impact on concrete strength for the SLS varied. The UR for SLS was determined by comparing the maximum reinforcement and concrete stress to their allowable limiting values. The SLS_c load combination considers the highest factor on actions and all SLS combinations considered the same limit on concrete stress: 60% of the compressive strength. Therefore, as SLS_c results displayed limited change in UR it can be assumed that SLS URs were governed by the stress in the reinforcement. For SLS_c, this reinforcement stress was limited to 80% of the steel tensile strength. The impact on UR for SLS_f and SLS_{qp} was more significant as the limiting reinforcement stress considered the tensile strength of the concrete, which increases with increasing compressive strength (British Standards Institution, 2015), for strength classes C40/50 and above. Although the UR increases for SLS_f and SLS_{qp} were up to 33%, these limit states did not typically govern the design and could be accommodated. Other elements may be more sensitive to changes in concrete strength for SLS; examples include where the element is governed by concrete stress rather than steel stress or where SLS loading is more closely aligned to ULS loading thus increasing the SLS URs.

Cracks form in concrete where the tensile stress exceeds the tensile strength of concrete. Therefore, it is expected that crack-width was also influenced by the change in concrete strength, with maximum and mean increases in UR of 57% and 15% respectively. Concrete tensile strength contributes to the calculation of mean strain in the concrete between cracks which is a component of the crack-width calculation. The impact of this component increase appears to align with the 15% mean increase in UR, however it is not expected to lead to the maximum increase in UR of 57% observed. It is expected that this large increase is due to minor changes to the considered elements, but further investigation may be required to confirm this assumption.

The impact of concrete strength is the most significant for shear where utilisation ratios increased by up to 60%. Designed shear reinforcement is only provided where the section properties are not sufficient to resist shear. The key properties used to determine the requirement for shear reinforcement include the depth of section, provided longitudinal reinforcement, axial force and concrete compressive strength. Where reinforcement is provided, the design followed a modified equation in Eurocode 2 (British Standards Institution, 2010) which considers the shear resistance provided by both the shear reinforcement and the concrete strength. Therefore, concrete strength is a key component in determining the provision of shear reinforcement and the overall shear resistance. The significant impact was observed during the reanalysis for the revised design strength; the change in shear UR could not be justified in some areas and was the only cause of rework required. Additionally, a large increase in UR of 24% was also observed for the element analysed using hand-calculations for case 2. Therefore, this case study shows that concrete strength has a significant impact on shear design, this must be considered when selecting concrete strength. However, there is currently limited research into the relationship between ME and shear provision as noted by Watanabe *et al*. (2021b).

As higher strength concrete has a lower porosity and consequently reduces concrete carbonation (Habert *et al.*, 2012), most national standards contain a minimum binder content (Damineli *et al.*, 2010). In the design codes used in case study, strength class is considered in the determination of the minimum cover to reinforcement where cover must be increased by 5 mm where lower concrete strength classes are used below (British Standards Institution, 2015; British Standards Institution, 2020). However, in this case, the change in concrete strength class did not impact the required cover and effective section depths. Table 3 represents the impact on design, had the reduced strength class led to a higher minimum cover. Here, it is shown that the change in minimum cover value has a minor impact considering no change to element thickness and a decrease in structural capacity (option 1) or an increase in thickness proportional to the increase in cover (option 2) for two element configurations considered in this case-study and an additional onerous element. It is noted that this effect may increase with requirements provided in other codes. Where concrete class does significantly impact the required cover, this may increase the overall concrete volume and consequently cement emissions. Where non-corrosive reinforcement is adopted, such as basalt fibre reinforced polymer presented in a previous edition of this Technical Journal (Gowda and Hendy, 2024), this effect could be negated.

TABLE 3

Impact of any increase to cover requirements in accordance with Eurocode 2 (British Standards Institution, 2015)

			Wall	Slab	Additional Onerous Element
Original values	Thickness (mm)		450	500	300
	Cover (mm)		60	45	30
	Lever-arm (mm)*		326	384	218
Revised values	Cover (mm)		65	50	35
	Option 1	Lever-arm (mm)*	321	380	213
	Option 2	Revised thickness (mm)	460	510	310
Comparison	Option 1	Change in lever-arm and capacity	-1.4%	-1.2%	-2.1%
	Option 2	Change in thickness	2.2%	2.0%	3.3%

*Considering link diameter of 12 mm and main bar diameter of 32 mm. As shown in Equation 1, lever-arm is dependent on concrete compressive strength $\left(d - 0.63\frac{A_{sf}\,y_d}{b f_{cd}}\right)$. However, for simplicity, the lever-arm has been considered in this case as 0.9 x section effective depth in accordance with Section 6.2.3 of Eurocode 2 (British Standards Institution, 2015)

5.   Limitations and Considerations for Further Work

This case study investigates elements designed for high loads and subsequently have high reinforcement density. Additionally, the elements investigated in this case study were primarily acting in flexure. Further research is required into different element and structure types to investigate the impact of different structural behaviour and reinforcement demand on the selection of concrete compressive strength.

Additionally, more investigation into the balance between concrete strength and provided reinforcement is required. Concrete strength class was shown to impact additional aspects of design including the required lap and anchorage lengths of reinforcement. Increasing concrete strength enables lower lap and anchorage lengths to be provided thus reducing embodied carbon of reinforcement. Furthermore, as discussed above, the reducing concrete strength class can lead to an increase in shear reinforcement required, thereby partially offsetting any potential overall reduction in emissions.

6.   Conclusion

This assessment explored two aspects of the design; the compressive test results for the concrete mix used and reanalysis of the structure considering lower strengths. For the first it was shown that the strength of concrete provided exceeded the strength required from the mix, thus enabling a higher strength class to be considered of C45/55. For the second it was shown that there was a limited impact on flexural ULS URs but a more significant impact on SLS and shear ULS URs. A combination of these measures was used to justify over 99% of the poured concrete. This holistic assessment through both design and construction has enabled improved understanding into industry behaviours and the emissions savings gains which could be achieved through efficient use of concrete strength. Key findings from this work include:

- Higher strength concrete was introduced on the structure in parallel with other design measures to resolve issues with the ULS flexural design under tight time pressure. However, as shown in this case study, the introduction of higher concrete strength was not required as it did not significantly contribute to the ULS flexural resistance. This suggests that more time is required to enable designers to iterate towards a more sustainable and efficient solution.
- Shear was shown to be the critical design case in this case study, however due to the numerous interdependencies shown in the case study, this cannot be considered to be the case for all structural elements. Nonetheless, this highlights the risk with existing literature which has typically focused on longitudinal reinforcement only. Additionally, further research is needed into determining optimal ratios between concrete strength and provided shear links to resist shear loading.

References

Balsara S., Jain P.K. & Ramesh A. (2021) 'An integrated methodology to overcome barriers to climate change mitigation strategies: a case of the cement industry in India', *Environmental Science and Pollution Research* **28**, pp. 20451–20475. Available at: https://doi.org/10.1007/s11356-020-11566-6

British Standards Institution (2010) BS EN 1992-2:2005: *Eurocode 2 – Design of concrete structure – Part 2: Concrete bridges – Design and detailing rules.* BSI Standards [Online]. Available at: https://doi.org/10.3403/BSEN1992 [Accessed: 22 October 2023]

British Standards Institution (2015) BS EN 1992-1-1:2004+A1:2004: *Eurocode 2 – Design of concrete structure – Part 1-1: General rules and rules for buildings.* BSI Standards [Online]. Available at: https://doi.org/10.3403/BSEN1992 [Accessed: 22 October 2023]

British Standards Institution (2020) BS 8500-1:2015+A2:2019 *Concrete – Complementary British Standard to BS EN 206 Part 1: Method of specifying and guidance for the specifier.* BSI Standards [Online]. Available at: https://www.bsigroup.com/en-GB/industries-and-sectors/construction-and-building/bs-8500-concrete-complementary-british-standard-to-bs-en-206/ [Accessed: 22 October 2023]

British Standards Institution (2023) BS EN 1992-1-1:2023 *Eurocode 2. Design of concrete structures. General rules and rules for buildings, bridges and civil engineering structures.* BDI Standards [Online]. Available at: https://doi.org/10.3403/30430557U

Concrete Centre (2020) *Specifying Sustainable Concrete.* Available at: https://concretecentre.com/Publications-Software/Publications/Specifying-Sustainable-Concrete.aspx [Accessed: 28 October 2023]

Damineli B.L., Kemeid F.M., Aguiar P.S. and John V.M. (2010) 'Measuring the eco-efficiency of cement use', *Cement and Concrete Composites* **32(8)**, pp. 555-562. Available at: https://doi.org/10.1016/j.cemconcomp.2010.07.009

DeRousseau M.A., Kasprzyk J.R. and Srubar III W.V. (2018). 'Computational design optimization of concrete mixtures: a review'. *Cement and Concrete Research* **109(6)**, pp. 42–53. Available at: https://doi.org/10.1016/j.cemconres.2018.04.007

Drewniok M.P, Manuel Cruz Azevedo J., Dunant C.F., Allwood J.M., Cullen J.M., Ibell T. and Hawkins W. (2023a) 'Mapping material use and embodied carbon in UK construction', *Resources, Conservation and Recycling* **197**, 107056. Available at: https://doi.org/10.1016/j.resconrec.2023.107056

Drewniok M.P., Dunant C.F., Allwood J.M., Ibell T. and Hawkins W. (2023b) 'Modelling the embodied carbon cost of UK domestic building construction: Today to 2050', *Ecological Economics* **205**, 107725. Available at: https://doi.org/10.1016/j.ecolecon.2022.107725

European Commission (2018) *A Clean Planet for all: A European strategic long-term vision for a prosperous, modern, competitive and climate neutral economy.* Brussels: Communication from the Commission to the European Parliament, the European Council, the Council, the European Economic and Social Committee, the Committee of the Regions and the European Investment Bank.

Fan C. and Miller S.A. (2018) 'Reducing greenhouse gas emissions for prescribed concrete compressive strength', *Construction and Building Materials* **167**, pp. 918-928. Available at: https://doi.org/10.1016/j.conbuildmat.2018.02.092

Griffiths S., Sovacool B.K., Furszyfer Del Rio D.D., Foley A.M., Bazilian M.D., Kim J. and Uratani J.M. (2023) 'Decarbonizing the cement and concrete industry: A systematic review of socio-technical systems, technological innovations, and policy options', *Renewable and Sustainable Energy Reviews* **180**, 113291. Available at: https://doi.org/10.1016/j.rser.2023.113291

Gowda C. and Hendy C. (2024) 'Basalt FRP as Embedded Reinforcement and its Embodied Carbon Comparison Against Steel RC', *AtkinsRéalis Technical Journal* **6(1)**, pp. 9-37. Available at: https://www.atkinsrealis.com/en/media/technical-journals [Accessed: 07 July 2024]

Habert G., Arribe D., Dehové T., Espinasse L. and Le Roy R. (2012) 'Reducing environmental impact by increasing the strength of concrete: quantification of the improvement to concrete bridges', *Journal of Cleaner Production* **35**, pp. 250-262. Available at: https://doi.org/10.1016/j.jclepro.2012.05.028

Habert G. and Roussel N. (2009) 'Study of two concrete mix-design strategies to reach carbon mitigation objectives', *Cement and Concrete Composites* **31(6)**, pp. 397-402. Available at: https://doi.org/10.1016/j.cemconcomp.2009.04.001

IEA (2019) '2019 Global Status Report for Buildings and Construction, IEA, Paris https://www.iea.org/reports/global-status-report-for-buildings-and-construction-2019, License: CC BY 4.0

IRP (2020) Resource Efficiency and Climate Change: *Material Efficiency Strategies for a Low-Carbon Future.* Hertwich E., Lifset R., Pauliuk S. and Heeren N. A report of the International Resource Panel. United Nations Environment Programme, Nairobi, Kenya. Available at: https://doi.org/10.5281/zenodo.3542680 [Accessed: 28 October 2023]

Jones, C. (2019) 'The Inventory of Carbon and Energy (ICE) Database V3.0'. Available at: https://circularecology.com/embodied-carbon-footprint-database.html [Accessed: 25 September 2023]

Jones T. (2020) 'Using 56-day concrete strengths', *Concrete*, June. Available at: https://www.concretecentre.com/TCC/media/TCCMediaLibrary/News/2021/06_Concrete-Magazine-56-day-concrete-strength-(TJ).pdf [Accessed: 28 October 2023]

Kourehpaz P. and Miller S.A. (2019) 'Eco-efficient design indices for reinforced concrete members'. *Materials and Structures* **52**, 96. Available at: https://doi.org/10.1617/s11527-019-1398-x

Material Economics (2019) *Industrial Transformation 2050 - Pathways to Net-Zero Emissions from EU Heavy Industry.* Available at: https://materialeconomics.com/publications/publication/industrial-transformation-2050 [Accessed: 28 October 2023]

Miller S.A., Horvath A., Monteiro P.J.M. and Ostertag C.P. (2015) 'Greenhouse gas emissions from concrete can be reduced by using mix proportions, geometric aspects, and age as design factors' *Environmental Research Letters* **10**, 114017. Available at: http://dx.doi.org/10.1088/1748-9326/10/11/114017

Miller S.A. (2020a) 'The role of cement service-life on the efficient use of resources', *Environmental Research Letters* **15**, 024004. Available at: https://doi.org/10.1088/1748-9326/ab639d

Miller S.A. (2020b) 'Life cycle environmental impact considerations for structural concrete in transportation infrastructure', *Pavement, Roadway and Bridge Life Cycle Assessment 2020.* London: Taylor & Francis Group

Miller S.A., Habert, G. Myers, R.J. and Harvey, J.T. (2021) 'Achieving net zero greenhouse gas emissions in the cement industry via value chain mitigation strategies', *One Earth* **4(10)**, pp. 1398-1411. Available at: https://doi.org/10.1016/j.oneear.2021.09.011

Parmenter S. and Myers R.J. (2021) 'Decarbonizing the cementitious materials cycle: A whole-systems review of measures to decarbonize the cement supply chain in the UK and European contexts', *Journal of Industrial Ecology* **25(2)**, pp. 359-476. Available at: https://doi.org/10.1111/jiec.13105

Purnell P. and Black L. (2012) 'Embodied carbon dioxide in concrete: Variation with common mix design parameters', *Cement and Concrete Research* **42(6)**, pp. 874-877. Available at: https://doi.org/10.1016/j.cemconres.2012.02.005

Reis D.C., Quattrone M., Souza J.F.T., Punhagui K.R.G., Pacca S.A. and John V.M. (2021) 'Potential CO_2 reduction and uptake due to industrialization and efficient cement use in Brazil by 2050', *Journal of Industrial Ecology,* **25**, pp. 344–358. Available at: https://doi.org/10.1111/jiec.13130

Rissman J., Bataille C., Masanet E., Aden N., Morrow III W.R., Zhou N., Elliott N., Dell R., Heeren N., Huckestein B., Cresko J., Miller S.A., Roy J., Fennell P., Cremmins B., Koch Blank T., Hone D., Williams E.D., de la Rue du Can S., Sisson B., Williams M., Katzenberger J., Burtraw D., Sethi G., Ping H., Danielson D., Lu H., Lorber T., Dinkel J. and Helseth J. (2020) 'Technologies and policies to decarbonize global industry: Review and assessment of mitigation drivers through 2070', *Applied Energy,* **266**, 114848. Available at: https://doi.org/10.1016/j.apenergy.2020.114848

Shah I.H., Miller S.A., Jiang D. and Myers R.J. (2022) 'Cement substitution with secondary materials can reduce annual global CO_2 emissions by up to 1.3 gigatons', *Nature Communications* **13**, 5758. Available at: https://doi.org/10.1038/s41467-022-33289-7

Shanks W., Dunant C.F., Drewniok M.P., Lupton R.C., Serrenho L.A. and Allwood J.M. (2019) 'How much cement can we do without? Lessons from cement material flows in the UK', *Resources, Conservation and Recycling* **141**, pp. 441-454. Available at: https://doi.org/10.1016/j.resconrec.2018.11.002

Tae S., Baek C. and Shin S. (2011) 'Life cycle CO_2 evaluation on reinforced concrete structures with high-strength concrete', *Environmental Impact Assessment Review* **31(3)**, pp. 253-260. Available at: https://doi.org/10.1016/j.eiar.2010.07.002

Torelli G. and Lees J.M. (2019) 'Fresh state stability of vertical layers of concrete', *Cement and Concrete Research* **120**, pp. 227-243. Available at: https://doi.org/10.1016/j.cemconres.2019.03.006

Uratani J.M. and Griffiths S. (2023) 'A forward looking perspective on the cement and concrete industry: Implications of growth and development in the Global South', *Energy Research & Social Science* **97**, 102972. Available at: https://doi.org/10.1016/j.erss.2023.102972

Watanabe S.I., Kamau-Devers K., Cunningham P.R. and Miller S.A. (2021a) 'Material Efficiency as a Means to Lower Environmental Impacts from Concrete,' *UC Davis: National Center for Sustainable Transportation.* Available at: http://dx.doi.org/10.7922/G2RJ4GS8. Retrieved from: https://escholarship.org/uc/item/88f4b2w9

Watanabe S.I., Kamau-Devers K., Cunningham P.R. and Miller S.A. (2021b) 'Transformation of Engineering Tools To Increase Material Efficiency of Concrete' *UC Davis: National Center for Sustainable Transportation.* Available at: https://doi.org/10.7922/G2W957H0. Retrieved from: https://escholarship.org/uc/item/2zn128b8

Watari T., Cao Z., Hata S. and Nansai K. (2022) 'Efficient use of cement and concrete to reduce reliance on supply-side technologies for net-zero emissions', *Nature Communications* **13**, 4158. Available at: https://doi.org/10.1038/s41467-022-31806-2

07: Space to Breathe: How We're Helping to Deliver Air Quality Improvements in UK Cities

Significance Statement

Air pollution can cause and worsen health conditions, including cardiovascular and respiratory diseases. The vehicles on our roads are a major contributor to pollutants, and thus to poor air quality. This paper describes how AtkinsRéalis has been working with several city authorities and UK government to implement 'clean air zones', which charge high-emitting vehicles a fee to enter. Using our expertise in engineering, consultancy, project management and technology, we have supported multiple successful implementations. Enabling councils to integrate their disparate systems, liaise with stakeholders, and achieve their goals, we are making a difference to lives affected by poor air quality.

Énoncé d'importance

La pollution atmosphérique peut causer et empirer certains problèmes de santé, y compris les maladies cardiovasculaires et respiratoires. Les véhicules qui circulent sur nos routes contribuent grandement à la production de polluants et, par conséquent, à la mauvaise qualité de l'air. Cet article décrit la façon dont AtkinsRéalis collabore avec plusieurs autorités municipales et avec le gouvernement du Royaume-Uni pour mettre en œuvre des « zones d'air pur », qui imposent des frais d'entrée aux véhicules à émissions élevées. Grâce à notre expertise en ingénierie, en consultation, en gestion de projet et en technologie, nous avons appuyé de multiples mises en œuvre réussies. En permettant aux conseils d'intégrer leurs systèmes disparates, d'assurer la liaison avec les parties prenantes et d'atteindre leurs objectifs, nous changeons la donne dans la vie des personnes touchées par la mauvaise qualité de l'air.

Jonathan Burns
Principal Consultant
UK & Ireland - Digital Advantage,
Aerospace, Defence, Security
and Technology
London, UK

Ian Sadler
Senior Consultant
UK & Ireland - Technology
Solutions, Aerospace, Defence,
Security and Technology
Epsom, UK

Rebecca Wallis
Business Development
Copywriter
UK & Ireland - Marketing
Communications, Aerospace,
Defence, Security and
Technology
Bristol, UK

Abstract

Ninety-nine per cent of the world's urban population live in areas that exceed air quality guidelines and, in the UK, between 29,000 and 43,000 deaths every year are linked to the effects of air pollution. Pollution contributes to cardiovascular and respiratory diseases and can cause and worsen health conditions.

To tackle this, UK Government has mandated several local authorities across the UK to introduce clean air zones in their towns and cities – designated areas which high-emitting vehicles pay a charge to enter, accelerating air quality improvements. Their goal is to encourage sustainable, non-polluting travel behaviours, including a shift to public transport, walking and cycling.

AtkinsRéalis experts have been working with several councils, helping them to implement their clean air zones by delivering support across the entire project lifecycle. From supporting them to overcome the complexities of integrating technology to monitor vehicle registrations; to developing business cases; to liaising with multiple stakeholder communities and partners to gain buy-in.

This paper outlines key considerations for implementing clean air zones, featuring a project example that demonstrates how our work is adding social value and engineering a better future for the planet and its people.

KEYWORDS
Pollution; Health; Technology; Social Value

1. Introduction

1.1 THE HUMAN IMPACT OF POOR AIR QUALITY

Public Health England has described poor air quality as "the largest environmental risk to public health in the UK" (Smith and Bolton, 2024). Figures from the Committee on the Medical Effects of Air Pollution report that air pollution is estimated to cause 29,000 to 43,000 deaths a year in the UK (Defra, Public Health), with long-term exposure reducing life expectancy by causing lung cancer, cardiovascular and respiratory diseases. Economically, the impact of air pollution in the UK was estimated at £157 million in 2017, with Public Health England suggesting inaction could see costs rising to as much as £18.6 billion by 2035 (Defra, Public Health, ibid).

The vehicles on our roads are a major contributor to air pollutants, and thus to poor air quality. Thirty per cent of nitrogen oxide (NOx) emissions came from road transport in 2022 (Defra, 2024). The correlation between high levels of nitrogen dioxide (NO_2) emissions and numbers of polluting vehicles has caused concern in many cities and urban areas throughout England. Exposure to NO_2 has adverse effects on health, impacting lung function and the prevalence of asthma, cancer, and neonatal difficulties.

As part of the UK Government's Department for Environment, Food and Rural Affairs' (Defra's) Clean Air Strategy (Defra, 2019), published in 2019, local authorities with areas of poor air quality have been asked to create 'Clean Air Zones' – targeted areas where action is taken to reduce NOx concentrations. Cities across England, including Bradford, Sheffield, Newcastle and Gateshead in the North; Birmingham in the Midlands; and Portsmouth, Bath and Bristol in the South West, have introduced these zones, while a future clean air zone in Greater Manchester is under review (Defra, Guidance).

Clean air zones designate areas, within the cities, which high-emitting vehicles must pay a charge to drive into/through. Automatic number plate recognition (ANPR) cameras scan vehicles' number plates, and enforcement letters are issued to those who do not pay the levy. This aims to deter higher polluting vehicles from entering the zone, reducing emissions in these areas to accelerate improvements in air quality. The zones are customised to reflect the location in which they operate: their ultimate goal is to encourage behavioural change in people's travel choices, with a shift to public transport, walking and cycling.

As part of our commitment to engineering a better future for our planet and its people, AtkinsRéalis' project teams have been working with several local authorities to help them set up and implement their clean air zones, with the aim of improving air quality for their residents. This paper describes some of the complex and interrelated activities delivered by our teams, to support these authorities to achieve their goal.

1.2 CLEAN AIR ZONES: COMPLEXITY FROM CONCEPT TO IMPLEMENTATION

To assist in the planning for clean air zones' implementation, and gain buy in from stakeholders, a strong business case is needed. There can be resistance to change from cities' populations, who may resent being charged to drive within their cities. In Portsmouth, for example, city centre traders were concerned that the zone would deter shoppers; while other stakeholders blamed the NO_2 and other, for example particulate, emissions on the ferries sailing to and from the city's port. Birmingham's large central train station was also considered a factor in the city's emissions.

These complex stakeholder landscapes mean that, to achieve success, the development of the business case, business processes, and systems architecture, together with the systems' testing and launch, must integrate seamlessly. In supporting local authorities across their entire project, from concept to implementation, we have helped them to ensure the successful launch of their clean air zones to deadline and budget. Working side-by-side with in-house teams, we enabled them to evaluate potential options, consider the behavioural changes needed, and develop tailored solutions that met their specific needs.

2. Case study: Our work with Newcastle City Council, Gateshead Council and North Tyneside Council on the Tyneside clean air zone

2.1 MAKING THE BUSINESS CASE

For the Tyneside clean air zone project, our cross-functional AtkinsRéalis project team developed the business processes and systems architecture, undertook systems integration and testing, and helped ensure a seamless launch.

As part of our work in Tyneside, we developed a service design document. This document drew upon learning from our previous work on clean air zones and acted as a 'one-stop' manual for staff members. It covered the cameras and associated systems, the processes, how the systems integrate, guidance on handling special cases (for example, taxis), enforcement, payments, failed payments and chargebacks, reconciliations and reporting. It also covered interfaces to allied organisations, such as the UK Government's Joint Air Quality Unit (JAQU) and the UK's Driver & Vehicle Licensing Agency (DVLA).

To enhance this guidance, we arranged a visit for key stakeholders to another local authority, where we had previously supported a successful clean air zone project. Representatives from each division presented to the Tyneside team, enabling significant learning from experience.

2.2 UNDERSTANDING THE INTERFACES AND INTERDEPENDENCIES

Our team then worked with the Tyneside team to produce a systems' interface diagram. This enabled everyone involved to know exactly what each system in the complex environment did and where the key interfaces were, including those with the supply chain. Systems included the clean air zone infrastructure, including cameras, image storage and review facilities, exemption lists (e.g., for public service vehicles such as ambulances), payment systems, and the central government clean air zone system. Further links were made between the DVLA systems, to check vehicles' compliance, and the council's penalty charge notice (PCN) processing system. Translated into a tool, this diagram provided an opportunity for stakeholders to understand how the new scheme would work and where and how their roles aligned to it.

In any clean air zone project, there are multiple complex interfaces and relationships which need to be defined and understood. These range from understanding how processes with colleagues in DVLA will work, to deciding how different scenarios would be handled, including potential customer queries and issue escalation. For Tyneside, we led this work on behalf of the council, briefing the helpdesk team due to receive queries, so they could engage productively with the public. To help non-technical stakeholders understand the risks, benefits, and advantages of different interface options, we produced papers that mapped out different scenarios. By translating the problem statement into a solution, we simplified a range of complex processes, driving efficiencies.

Other deliverables included a critical milestones' map to support project delivery, and integrated, joint end-to-end test plans for live payment/refund testing. Test plans, scripts, and user stories were created, and live payment testing was carried out successfully.

2.3 ENGAGING WITH STAKEHOLDERS

A key part of clean air zone projects is stakeholder engagement, not only to help those with non-compliant vehicles understand their options, but also to manage the challenging and complex internal and external stakeholder community, plus the partners responsible for specific products such as ANPR. In Tyneside, the internal project stakeholder landscape was complex, with enforcement, engagement, and communication teams; image, review, and processing teams; and the legal and financial reporting team all needing to play their part. It was essential that we navigate challenging stakeholder interactions without impact upon the quality of outcomes. These interactions had the potential to become complicated, particularly engagement with JAQU. In this work, our previous experience was of paramount importance in helping us cut through complexity and speed up processes; for example, when external legal advisers (who had no experience of how a clean air zone worked) had become entangled in legal definitions during the negotiations around data privacy and sharing arrangements.

We undertook extensive user engagement, liaising with the councils' internal teams to understand their ways of working, and to consider and discuss how the new clean air zone responsibilities (including testing) could fit into their workload. Having already built a strong working relationship with JAQU and DVLA from previous work on clean air zones, we had created trust that AtkinsRéalis could deliver on time. By applying the human side of consultancy, and by being empathetic to everyone's concerns, we ensured an open and collaborative approach.

For external stakeholders in the Tyneside area, significant engagement was undertaken at both local and national level. Early and proactive engagement with the community allowed the benefits of the clean air zone to be demonstrated, and vehicle owners to be encouraged to comply. Beneficial engagement was undertaken with many affected groups, including communities that didn't have English as a first language. This included highlighting the opportunities available for grant funding, and countering perceptions of the zone as a 'council money-making scheme'.

2.4   COMMUNICATING THE CLEAN AIR ZONE BENEFITS

Continuous communication created great working relationships and a psychologically safe environment where all perspectives were welcomed. A key need in Tyneside was for a centralised information resource, which could be used by multiple teams to answer queries – media requests from the press, or questions from councillors for example – and to inform essential reporting to JAQU. We ran workshops to understand each team's requirements, then created dashboards using Power BI which they could use to meet these information needs, and answer Freedom of Information or ad-hoc enquiries. The system also needed to validate that the correct data had been received, highlighting and error reporting, for example, if duplicate data was sent.

FIGURE 1

Example of reporting dashboard including test data
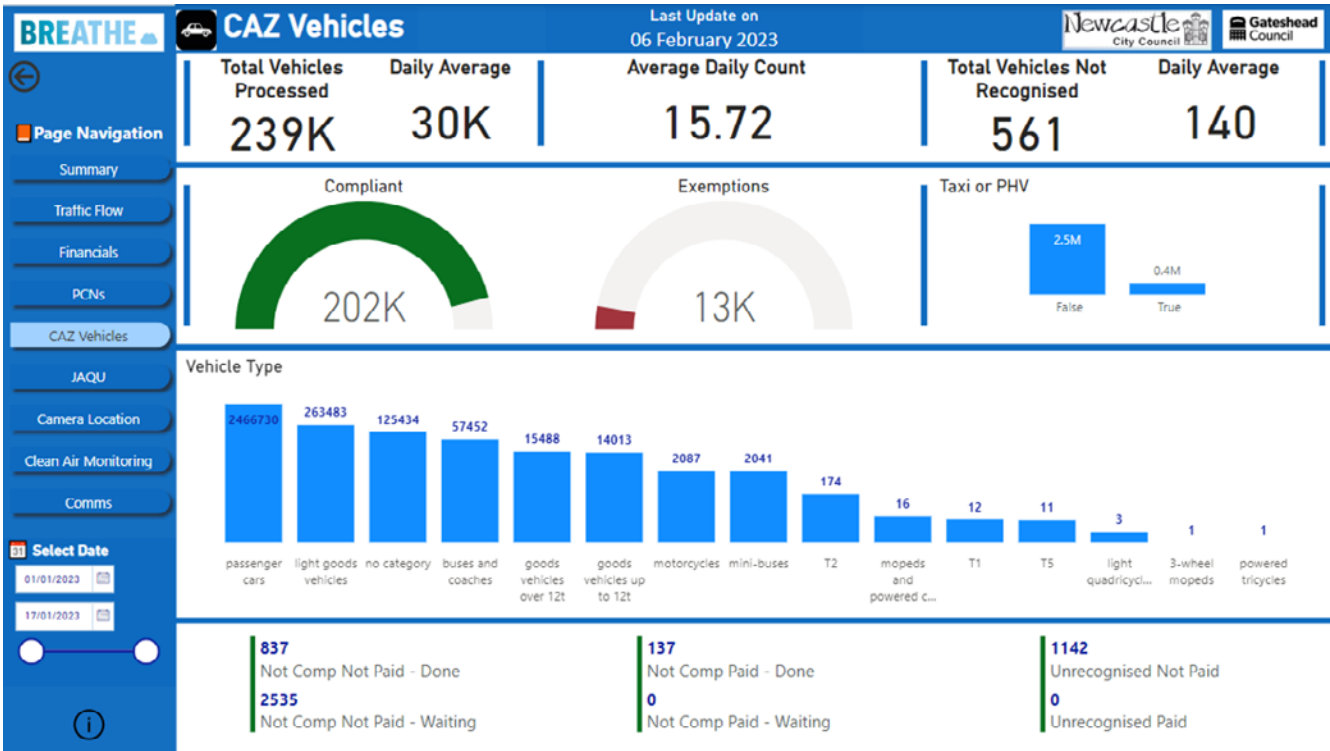
We supported Tyneside to undertake a risk review, and implement robust governance, through proactively anticipating issues and identifying options to address them, this helped to manage and mitigate risks and blockers. One risk was that the cameras which captured data on vehicles in the clean air zone might be sited incorrectly. To mitigate this, we walked around the city centre as a team – getting to know all the cameras by name, checking the angles and that the correct image was being captured.

Our work translated a series of connected, disparate systems, into a working scheme. Through Agile project management based on strong administrative foundations, extensive stakeholder engagement and the creation of a close relationships with the client, suppliers and government, the clean air zone was successfully launched on time, to budget and to the required standard.

FIGURE 2

AtkinsRéalis and Tyneside colleagues on a tour of the Tyneside cameras

3.   Results

3.1   WORK IN PROGRESS: CURRENT CLEAN AIR ZONE METRICS

Councils monitor air pollution through a range of measures, including diffusion tubes, which sample the concentration of gases in the area. This data is then reported to JAQU, which allocates the authority into one of four different states:

- **State 1** – on track to achieve success
- **State 2** – has achieved success
- **State 3** – demonstrated to be maintaining success with measures
- **State 4** – likely to continue maintaining success in the absence of measures

The latest Clean Air Zone Service Annual Report, published in April 2024, only covers the period from 15 March 2021 to 15 March 2022, so does not report on all the zones now in place. However, while local authorities are, in many cases, still assessing data to understand the impact of their clean air zone, many of those which have been in place for some time have reported successful reductions in air pollution, including Bristol, Bath and London.

3.1.1   Bath

Introduced in 2021 by Bath and North East Somerset Council, Bath's air quality improvements have been sustained for two consecutive years. In March 2024, it was classified at 'State 3', with no exceedances of the annual mean NO_2 limit value across all locations considered by the assessment. There was an average reduction of 27% in annual mean NO_2 concentration across all 125 measurement sites, with no increases in concentration at any site.

3.1.2   Bradford

While the effects of Bradford's clean air zone are still being assessed, one year after its launch in 2022, researchers had found improvements in both respiratory and cardiovascular health. The research, funded by the National Institute for Health and Care Research, recorded, on average each month, 598no. fewer GP visits for respiratory health and 134no. fewer for cardiovascular health.

3.1.3   Birmingham

Birmingham City Council launched its Clean Air Zone in June 2021. It reported in 2022 that the levels of NO_2 had reduced by an average of 17% against 2019 figures, and 37% against 2016 measurements. Light Goods Vehicles' (LGVs') compliance has improved, with 85.7% compliant in 2021, compared to 68.6% in June 2023; and Heavy Goods Vehicles' (HGVs') compliance increasing from 92.2% to 97.8% across the same period.

3.1.4   Bristol

With its clean air zone introduced by Bristol City Council in November 2022, data from Bristol in late 2023 indicated that air quality in the city would not exceed the Government's annual legal limit for the year, with 82% of cars compliant with the zone requirements. In January 2024, a report from the city found that NO_2 pollution was down by nearly 10% across Bristol, and almost 13% lower in the clean air zone. JAQU confirmed that Bristol's zone had passed its 'State 1' assessment in November 2023, and it is now working towards achieving 'State 2'.

3.1.5   London

In London, around 4,000 premature deaths are attributed to toxic air each year. Introduced in 2019, and expanded to cover a wider area in 2023, the London Ultra-Low Emissions Zone (ULEZ) is the world's largest clean air zone, covering all of London's boroughs. As with other areas' clean air zones, charges are only levied if vehicles do not meet emissions standards, and different charges apply to smaller and larger vehicles. Central London also has a Congestion Charge zone during peak hours.

A report issued in July 2024 identified that, in the outer London ULEZ area, NOx emissions from cars and vans are estimated to be 13% and 7% lower than without the expansion, equivalent to removing 200,000 cars from the road for one year. PM2.5 exhaust emissions from cars in outer London are estimated to be 22% lower than without the expansion. In Central London, roadside NO_2 concentrations are estimated as 53% lower; in Inner London as 24% lower, and in Outer London as 24% lower. A further report is expected in 2025.

3.1.6   Tyneside

The Tyneside clean air zone, a partnership between Newcastle City Council and Gateshead Council, went into operation in January 2023. The councils are currently working with JAQU to establish the effectiveness of the zone, but figures released in July 2024 suggested there had been a drop in the average level of NO_2 at all but one of the 70no. monitoring stations in Newcastle.

3.1.7   Portsmouth

A Class B charging clean air zone (CAZ) was launched in Portsmouth in November 2021. The CAZ has seen 94% of monitored areas comply with air quality standards. However, JAQU assessments reveal a critical need for it to be continued, as data reveals persistent challenges in specific locations – three of which continue to have pollution levels above the government's limits, and a further nine that also continue to be at risk of exceeding.

3.1.8   Sheffield

Sheffield's clean air zone was introduced in February 2023. Its initial findings from monitoring data have shown that air quality is improving, with an overall NO_2 reduction of 16% in the zone. All monitoring locations within the zone have shown a reduction in NO_2 and, in May 2024, 91% of journeys in the clean air zone were by compliant vehicles.

3.2   NO MAGIC BULLET SOLUTION

It must be highlighted, however, that clean air zones are just one element of improving air quality – they aren't a magic bullet solution to pollution issues. As a Commons Library Research Briefing of 11 August 2023 (Tyers and Smith, 2023) stated: "It can be difficult to assess the effectiveness of just one action alone on air quality. This is because many different factors, such as weather patterns, can affect air quality levels at any time." While Bath has demonstrated ongoing success, for example, JAQU's *Air Quality Monitoring State 2 2021 Summary* report (JAQU, 2021) cautioned that the risk of emissions' exceedance in future years was high, with increases in national traffic and fleets that are less clean than predicted in 2022.

Clean air zones can encourage drivers to upgrade to less polluting vehicles, and promote people's use of greener means of travel, including walking, cycling and public transport. However, they must be put in place alongside other sustainable travel options. London, for example, has put over 1000no. zero-emission buses on its roads (Transport for London, 2023); while Portsmouth has introduced additional greener methods of transport, including electric scooters, as well as more electric vehicle charging points (Portsmouth City Council).

Several councils have used the money from non-compliant vehicles entering their clean air zones to invest in active travel support. For example, Bristol has invested in repairs and improvements to roads and footpaths, and offers free cycling trials, eScooter and car club credit, and bus and train 'taster' tickets. Bradford has funded a greener vehicle fleet for the council and an electric vehicle charging network; and Bath has provided secure storage for bikes by building bike hangars. Local authorities are also keeping money in reserve to decommission the clean air zones, once emissions are consistently low and they are no longer needed (BBC News, 2024).

4   Conclusion

4.1   PROJECT MANAGEMENT, PROCESSES, BUT MOST OF ALL, PEOPLE

Our AtkinsRéalis team brought its extensive experience in project management and technological and business process understanding to deliver confidence to our clean air zone clients. We were able to draw upon experience of training civil service apprentices in project management techniques, and of mentoring their portfolio preparation; as well as skills in managing multifaceted test requirements' processes, and extensive expertise in software testing within an Agile environment. The clean air zone projects also offered a great opportunity for our junior project management consultants to develop their skills, with several seconded to the various projects at different points.

Throughout the projects, we ensured that a mutually supportive environment was created – while complex programmes require many core project management skills, from stakeholder management, to ensuring the integration of technologies to tight deadlines, at their heart they are about people. Experts deliver the project, stakeholders influence it, and the public benefit from it. Building relationships with all stakeholders requires a people-centric approach, using the 'softer' project management skills to develop a cohesive team – one that is based on friendliness, trust, and an open, supportive, psychologically safe culture. Stakeholder management is critical to the successful delivery of clean air zones: people at all levels, from government, to suppliers, to drivers need to understand their roles in improving air quality.

Buy-in from local authority leadership is key – the authority needs to have the resource capacity in place to deliver the zone. We help authorities to identify which resources they already have in place – an existing system to monitor bus lanes perhaps – and to consider whether people to manage the system can be sourced internally or need to be recruited. The resource requirements and business process flows are multi-layered and complex: clean air zone projects must translate a series of connected systems and infrastructure into a working scheme, so that people can understand when they need to pay, and how they do so. With expertise and experience in integrating technology, together with an in-depth understanding of the challenges facing local authorities, we have helped authorities manage the creation of relationships between the multiple suppliers and owners of their systems, ensuring integration runs smoothly and that target outcomes are successfully delivered.

Within such a multi-stakeholder environment, a key challenge was building trust between participants, including upwardly-influencing government. Recognising that all participants were on a learning journey, we took ownership of problems, acting to resolve them – ensuring a culture where there was trust between JAQU, the teams, and all stakeholders, to enable effective, cohesive and smart working.

For any clean air zone project, excellent communication with stakeholders is essential. This should include as many of the groups affected as possible: from taxi drivers and transport company representatives; to people who run recovery vehicles and the local ambulance service. To combat potential protests, it's important that authorities are transparent about the scope of the scheme: for example, the reasoning behind both the area covered by the zone and any vehicle exemptions. Communication can also share information on the support available to stakeholders, such as incentive schemes for those who choose to replace their vehicles for ones with lower emissions. Early engagement can produce great results: in one authority, we saw 95% compliance with the clean air zone by local taxis.

Discussions with diverse stakeholders can also help everyone understand that these zones are not put in place as 'money-making' schemes, they are aimed at protecting the health of residents. This message is reinforced if the revenue generated is used to invest in environmentally-beneficial measures, such as cycleways, to subsidise electric- or hydrogen-powered buses, or to redesign infrastructure to encourage walking. In providing evidence of responsible investment by the local authority, clean air zones can also demonstrate to central government that the authority is a 'safe pair of hands' for additional investment opportunities.

4.2   A BEST PRACTICE EXAMPLE

Our AtkinsRéalis team's work has been used by JAQU as a best practice exemplar, and a template for other clean air zones. To ensure continuous learning from each project with which we were involved, we held a lessons-learned workshop to capture key points and the rationale behind these, creating recommendations to take forward in future launches. For example, we gained understanding about implementation timescales and their key associated risks, which could be carried forward into other projects to inform realistic timeframe expectations.

4.3   SUSTAINABLE SOLUTIONS FOR A BETTER FUTURE

Our work on clean air zones is one example of the sustainable solutions we create, to connect people, data and technology.

Throughout our clean air zone projects, it became apparent that they are about so much more than just technical solutions. They are aiming to make a difference to people whose lives are affected by poor air quality, helping city residents of all ages. Incredibly, 99% of the world's urban population live in areas that exceed air quality guidelines (World Health Organisation, 2022) . As a consultancy, we have the ability to help make the world a better place, and with AtkinsRéalis' commitment to engineering a better future, clean air zones are a demonstration of the impact people can have on their city when consultants, councils, and the public work together.

The story doesn't end here, of course. There's so much more that can be done to combat climate change and make our cities safer to live in, and our teams will continue to deliver successful projects that engineer a better future for our planet and its people.

References

BBC News. *Clean air zones: What is the money raised spent on?* https://www.bbc.co.uk/news/articles/c1ej7knvd7vo. Published 16 June 2024.

Cleaner Air Portsmouth. *What are we doing to lower air pollution.* https://cleanerairportsmouth.co.uk/what-are-we-doing/. Not dated.

Department for Environment, Food and Rural Affairs. *Accredited official statistics: Emissions of air pollutants in the UK – Nitrogen oxides (NOx).* https://www.gov.uk/government/statistics/emissions-of-air-pollutants/emissions-of-air-pollutants-in-the-uk-nitrogen-oxides-nox. Updated 19 February 2024.

Department for Environment, Food and Rural Affairs. Guidance: *Clean air zones.* https://www.gov.uk/guidance/driving-in-a-clean-air-zone#cities-with-clean-air-zones. Not dated.

Department for Environment, Food and Rural Affairs. *Policy paper: Clean Air Strategy 2019.* https://www.gov.uk/government/publications/clean-air-strategy-2019

Department for Environment, Food and Rural Affairs. *Public Health.* https://laqm.defra.gov.uk/air-quality/guidance/public-health/. Not dated.

Joint Air Quality Unit. *Bath and North East Somerset: Air Quality Monitoring State 2 2021 Summary.* https://www.bathnes.gov.uk/sites/default/files/2021%20BaNES%20State%202.pdf.

Smith, Louise; Bolton, Paul. *Air quality: policies, proposals and concerns.* House of Commons Library Research Briefing, https://commonslibrary.parliament.uk/research-briefings/cbp-9600. Published Monday, 19 February, 2024

Transport for London. Press Release: *London reaches major milestone with more than 1,000 zero emission buses.* https://tfl.gov.uk/info-for/media/press-releases/2023/august/london-reaches-major-milestone-with-more-than-1-000-zero-emission-buses. Published 18 August 2023.

Tyers, Dr Roger; Smith, Louise. *Clean Air Zones, Low Emission Zones and the London ULEZ.* House of Commons Library Research Briefing. Published 11 August 2023. https://researchbriefings.files.parliament.uk/documents/CBP-9816/CBP-9816.pdf

World Health Organization. News story: *Billions of people still breathe unhealthy air: new WHO data.* https://www.who.int/news/item/04-04-2022-billions-of-people-still-breathe-unhealthy-air-new-who-data. Published 4 April 2022.

08: Controlling the Error in the Interpretation of Non-Homogeneous Smoke Visibility Data

Significance Statement

Clear visibility during fire evacuation is crucial to ensure safe and swift escape. Our work provides an efficient, reproducible and accurate method to interpret fire smoke visibility data and properly manage the associated risks. The analysis provided is centered around a data-driven approach, based on smoke visibility data obtained from numerical simulations or from other means. Our method goes beyond what is described in fire safety regulations to ensure that the services we provide are aligned with AtkinsRéalis' values of safety, integrity, collaboration, innovation and excellence.

Énoncé d'importance

Une bonne visibilité pendant l'évacuation en cas d'incendie est essentielle pour assurer une sortie sécuritaire et rapide. Notre travail fournit une méthode efficace, reproductible et précise pour interpréter les données de visibilité de la fumée d'incendie et gérer correctement les risques connexes. L'analyse est centrée sur une approche fondée sur des données, elle-même basée sur les données de visibilité de la fumée obtenues à partir de simulations numériques ou d'autres moyens. Notre méthode va au-delà de ce qui est décrit dans les règlements de sécurité incendie pour assurer que nos services sont conformes aux valeurs de sécurité, d'intégrité, de collaboration, d'innovation et d'excellence d'AtkinsRéalis.
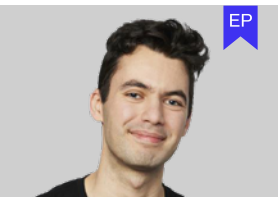
Daniel Lévesque

Appl. Math, Numerical Simulation Professional

Canadian Capabilities - Rail, Transit & Mobility TPO

Montreal, QC, Canada

Olivier Rouch

Appl. Math, Numerical Simulation Expert

Canadian Capabilities - Rail, Transit & Mobility TPO

Montreal, QC, Canada

Bowen Xu

Digital Simulation Professional

Canadian Capabilities - Rail, Transit & Mobility TPO

Montreal, QC, Canada

Loan Grimm

Numerical Modeling Professional

Canadian Capabilities - Rail, Transit & Mobility TPO

Montreal, QC, Canada

Abstract

The interpretation of smoke visibility data is an important task that is not trivial. Engineering teams must carry out these interpretations when designing a building's fire smoke extraction system and emergency egress paths. The fire protection standards (NFPA-130, SFPE and ASHRAE) provide guidelines on how to define and interpret visibility through fire smoke, but they do not provide the knowledge needed to control the numerical errors that arise from highly non-homogeneous smoke conditions. This is an issue when managing the risks associated with a building design. Our previous work presents a method that enables effective communication of smoke visibility data. Here, we present an analysis which highlights and quantifies in what way we can control this interpretation error. This analysis shows how to quickly extract as much value from the smoke visibility data as possible, empowering all project actors who need to understand the fire safety issues at hand.

1.   Introduction

Engineering teams need to make sure that the buildings they design follow fire safety regulations, which include guidelines for the safe egress of occupants in case of a fire incident (NFPA-130, SFPE and ASHRAE). The fire smoke extraction systems must provide clear visibility for the occupants to safely evacuate along the designated paths. Correctly interpreting smoke visibility data will assure a balance between safety and sustainable development practices.

This is where AtkinsRéalis' Simulation and Modeling Team steps in. This team provides detailed smoke visibility data that is specific to the engineering design. It also provides a clear and reliable interpretation of the data that goes beyond what is specified in fire protection standards. In this section, the definition of visibility through fire smoke is reviewed. Next, the limitations of the numerical interpretation of smoke visibility are detailed. Finally, the methods used to address this problem in the past are presented.

1.1.   VISIBILITY THROUGH FIRE SMOKE

Smoke visibility is defined through the concept of light obscuration with the formula

$$V = \frac{K}{\alpha} \qquad (1)$$

where α is the light extinction coefficient and K is a proportionality constant which depends on whether the target is illuminated *(K=8)* or not *(K=3)*. In the case of fire smoke, the extinction coefficient is a function of soot yield of the fuel (ASHRAE). This means that once the numerical simulation has produced the smoke visibility data, the visibility can be defined as a scalar field at every point in space. An example of this type of visibility data, taken from the authors' previous work (Lévesque and Rouch, 2025), is shown in Figure 1.1.

FIGURE 1.1

Smoke visibility data
(2 m above ground) from a
train station fire simulation
(Lévesque and Rouch, 2025)
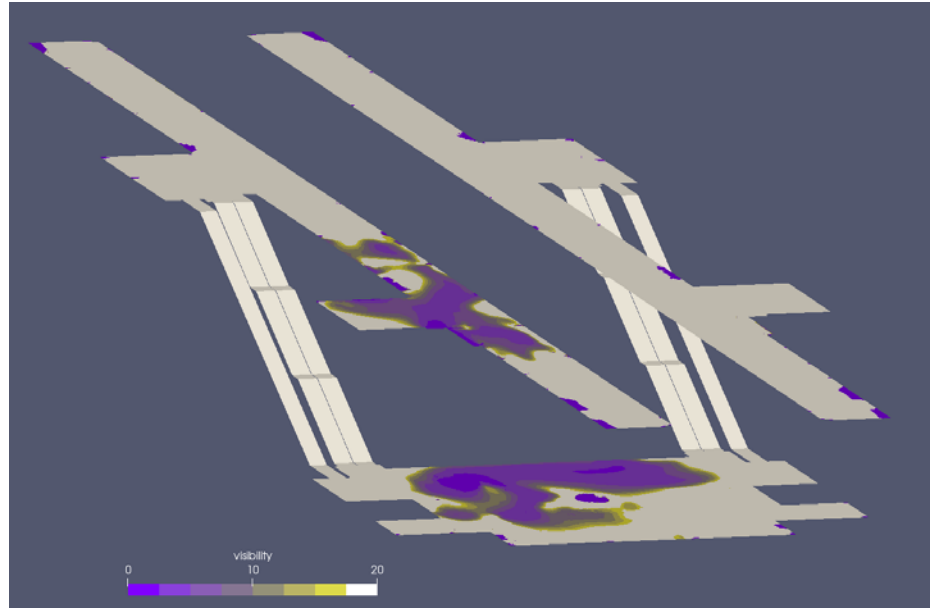
The prescribed way to determine if an observer can see an object located at a distance L is to compute the average visibility along the line that connects the observer to the object:

$$\langle V \rangle = \frac{1}{L} \int_0^L V\,dx \qquad (2)$$

Now take another look at Figure 1.1 and determine if people inside the station can clearly see any emergency signs that would be placed on the walls nearby. Keep in mind that you need to compute the line integral given in Eq. 2, for any observer and in all directions. As previously mentioned, this task is not trivial.

1.2 LIMITATIONS OF THE NUMERICAL INTERPRETATION OF SMOKE VISIBILITY

The main source of numerical error comes from large visibility values that can lead to the wrong interpretation of the data. Large visibility values happen in the absence of smoke obscuration ($\alpha \approx 0$) which creates unbounded values of visibility ($V \rightarrow \infty$, see Eq. 1). It is clear from Eq. 2 that when V becomes large, it's average value also becomes large, even if this only happens on short distances. This typically happens when the smoke visibility data is non-homogeneous, as is illustrated in Figure 1.2.

FIGURE 1.2

Example of non-homogeneous smoke visibility for which the calculated average visibility is greater than the actual visibility
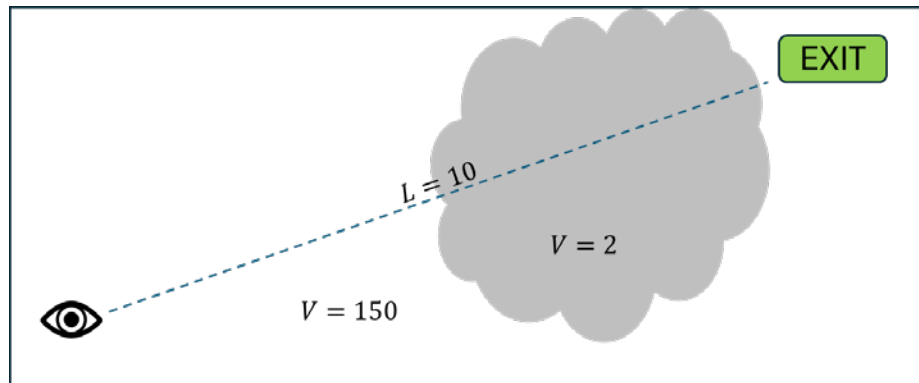
Let us consider the following visibility field:

$$V(x) = \begin{cases} 150 \text{ m}, & x < L/2 \\ 2 \text{ m}, & x \geq L/2 \end{cases}$$

where L=10m is the distance between the target and the observer. Since V=2m on more than 2m, this means that there is complete smoke obscuration on half of the distance near the target and the observer shouldn't be able to see it. Equation 2 tells us that the mean visibility across the sightline is:

$$\langle V \rangle = \frac{1}{L} \int_0^L V dx = \frac{1}{L} \int_0^{L/2} 150 dx + \frac{1}{L} \int_{L/2}^L 2 dx = 76 \text{ m}$$

It can be concluded that the target is visible since $\langle V \rangle$=76m > 10m. This conclusion would be wrong since V=2m means that we can only see through two meters of distance in this smoke density, not 76m.

The problem comes from the fact that V=150m on half of the sightline. Remember that visibility is an unbounded variable. It can have much larger values in regions where smoke density is practically zero. On a clear day, the atmospheric visibility is measured in kilometers. A non-homogeneous smoke visibility field is likely to be produced by an effective smoke extraction system, because it is designed to prevent smoke from mixing with clean air. The average smoke visibility calculation, on the other hand, is usually considered for a well-mixed environment, where smoke and hot air have time to create semi-homogeneous visibility conditions. This is a good enough approximation as long as smoke is well mixed and fills the space almost evenly.

To obtain an accurate interpretation of the smoke visibility data in non-homogeneous conditions, it is necessary to eliminate large values of visibility from the calculations. Many questions need to be answered if we are to modify the data. Which value should be used for calculations? What will be the impact of this choice on the mean visibility estimate along a sightline? How do we control the error associated with our interpretation? The analysis presented in this paper provides an answer to these questions.

## 1.3. ADDING SIGHTLINES AS AN EFFECTIVE COMMUNICATION TOOL

After a few years of providing many interpretations, these authors have developed and published a method that assures an effective communication of smoke visibility data (Lévesque and Rouch, 2025). This team has generated thousands of smoke visibility datasets to assist in the design of more than 20 train stations and other buildings. During this work, an algorithm was created that generates sightlines that can be added directly on top of the smoke visibility data to remove any interpretation issues, as can be seen in Figure 1.3. This approach enables a repeatable, precise and consistent interpretation of smoke visibility data. These sightlines are constructed by creating a vector field based on the visibility field and by modifying an existing numerical integration method. The sightlines can then be seen as the streamlines associated with the visibility-based vector field.

The error associated with these sightlines can be obtained from an error analysis associated with the numerical integration method that was employed. This can be a difficult task because of the way the numerical integration method is modified. Moreover, a quicker approach might be needed to provide answers to a particular problem. To resolve these difficulties, and to promote an error-control oriented approach, an equivalent approach can be formulated that might be better suited in situations where only a small number of sightlines need to be studied.

Other approaches have been developed to provide a more immersive interpretation of smoke visibility data (Kang, Macdonald 2005; Forney 2011; Cha, Han, Lee and Choy 2012; Xu, Lu, Guan, Chen and Ren 2014; Wahlqvist and van Hees 2018; Wahlqvist and Rubini 2023). These approaches give an interesting perspective on smoke visibility data, but their format makes it difficult for them to be generated in batches and they can be resource-intensive to produce.

FIGURE 1.3

Sightlines added to the smoke visibility data to remove any interpretation issues (Lévesque and Rouch, 2025)
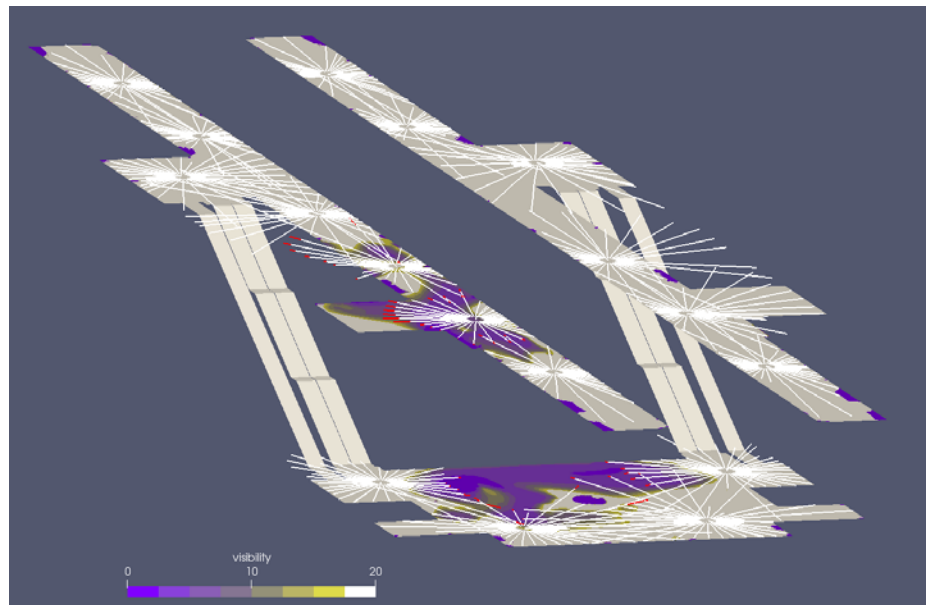
2.   Method

The analysis presented in this section provides the tools needed to control the error associated with the numerical interpretation of smoke visibility data. The process starts by choosing a maximum error value. This value corresponds to the overall error associated with the numerical interpretation of the smoke visibility data. Then, choose a numerical integration method that respects the maximum error value. Finally, the numerical integration method is demonstrated to generate the correct average visibility value and avoid a wrong interpretation.

2.1   CHOOSING A MAXIMUM ERROR VALUE

Let ϵ_{max} denote the chosen maximum error value. This requires the following inequality to hold:

$$\langle V \rangle - \langle V \rangle_{approx} < \epsilon_{max} \qquad (3)$$

where $\langle V \rangle_{approx}$ is the numerical approximation of $\langle V \rangle$, the actual average visibility value. The ϵ_{max} value could be imposed by special regulations, by the uncertainty associated with the visibility data itself, or by client needs and requirements.

2.2   CHOOSING A NUMERICAL INTEGRATION METHOD

There are a few numerical integration methods that can be used with a predefined maximum error value (Hamming, 2012). This is where the current approach differs from the one used to generate the sightlines shown in Figure 1.3. The objective followed here is to leverage the error associated with the numerical integration method to control the overall error associated with the average visibility result. To simplify the presentation, the composed trapezoidal rule was used to integrate along the sightline on a set of (N+1) uniformly distributed points:

$$\int_0^L V dx \approx \frac{L}{2N}\left[V(0) + 2\sum_{i=1}^{N-1} V\left(\frac{iL}{N}\right) + V(L)\right] \qquad (4)$$

From Eq. 4, the error associated with this integration formula satisfies

$$\left| \frac{1}{L} \int_0^L V\, dx - \frac{1}{2N}\left[V(0) + 2\sum_{i=1}^{N-1} V\left(\frac{iL}{N}\right) + V(L) \right] \right| \leq C\left(\frac{L}{N}\right)^2$$

where C is a determinable constant. This provides a formula and its associated error for the approximated average visibility:

$$\langle V \rangle_{approx} = \frac{1}{2N}\left[V(0) + 2\sum_{i=1}^{N-1} V\left(\frac{iL}{N}\right) + V(L) \right] \qquad (5)$$

Eq. 3, Eq. 4 and Eq. 5 yield

$$\langle V \rangle - \langle V \rangle_{approx} \leq C\left(\frac{L}{N}\right)^2 < \epsilon_{max} \qquad (6)$$

This inequality can then be used to obtain a value of N since L is known:

$$N > L\sqrt{\frac{C}{\epsilon_{max}}} \qquad (7)$$

The exact value of the constant C cannot be found without having some information relative to the second derivative of V as a function of distance. It would be possible to approximate the value of C by using a sequential process, but this is out of scope. We will arbitrarily use C=1 for the purpose of this paper, since this choice will not affect the presented methodology. For example, if L=10 and ϵ_{max}=0.1, then Eq. 7 tells us to use N>32.

2.3 GENERATING THE AVERAGE VISIBILITY VALUE

The discussion presented in Section 1.2 concludes that the large visibility values must be dealt with to avoid overestimating the average visibility. The first question that arose was about which values should be used for the practical calculation. To answer this question, it is essential to remember that the average visibility is computed to determine if an observer can see an object located at a distance L. If the computation reveals that $\langle V \rangle < L$, it can be confidently concluded that the observer cannot see the object.

Consider the average visibility on a subinterval of the sightline, where the visibility values are small. The result indicates that the observer cannot see the object if this average visibility value is smaller than the length of the subinterval on which it is calculated. This should demonstrate that the object will remain unseen no matter how large the visibility values are everywhere else along the rest of the sightline. An incorrect interpretation arises only if the larger visibility values are added into the calculations, as shown in Section 1.2.

The solution to this problem can be addressed in two steps. First, the total length L_{low} of the sightline for which $V \leq L$ must be determined. Then, the average value of the modified visibility is computed where the values for which $V > L$ have been replaced by $V = 0$. This is done by creating an indicator function:

$$X = \begin{cases} 1, & V \leq L \\ 0, & V > L \end{cases} \qquad (8)$$

This results in:

$$\langle V \rangle_{low} = \frac{1}{L_{low}} \int_0^L X V\, dx \approx \frac{L}{2NL_{low}} \left[X(0)V(0) + 2 \sum_{i=1}^{N-1} X\left(\frac{iL}{N}\right) V\left(\frac{iL}{N}\right) + X(L)V(L) \right] \qquad (9)$$

where

$$L_{low} = \int_0^L X\, dx \approx \frac{L}{2N} \left[X(0) + 2 \sum_{i=1}^{N-1} X\left(\frac{iL}{N}\right) + X(L) \right] \qquad (10)$$

If $\langle V \rangle_{low} < L_{low}$, then confidence that the observer cannot see the object can be assured. If $\langle V \rangle_{low} \geq L_{low}$ then reliance can be placed on $\langle V \rangle$. It should be noted that if $L_{low} = L$, then the observer cannot see the object. Conversely, if $L_{low} = 0$, then the observer can see the object.

3. Results and Discussion

The approach described in Section 2.3 will be demonstrated by first applying it to the problematic example given in Section 1.2, and then by applying it to a visibility dataset of a similar situation.

3.1 ANALYTICAL CASE

The method described in Section 2.3 is applied to the problematic example given in Section 1.2, where L=10m and

$$V(x) = \begin{cases} 150 \text{ m}, & x < 5 \\ 2 \text{ m}, & x \geq 5 \end{cases}$$

The corresponding indicator function is

$$X = \begin{cases} 1, & x < 5 \\ 0, & x \geq 5 \end{cases}$$

The portion of the sightline for which $V \leq L$ is given by

$$L_{low} = \int_0^{10} X dx = \int_5^{10} dx = 5 \text{ m}$$

and the modified average visibility value is evaluated at

$$\langle V \rangle_{low} = \frac{1}{L_{low}} \int_0^L X V dx = \frac{1}{5} \int_5^{10} 2 dx = 2 \text{ m}$$

Since $\langle V \rangle_{low}$=2m<L_{low}=5m it can safely be concluded that the observer would not be able to see the object located 10m away. This contrasts with the average visibility value initially obtained for this scenario in Section 1.2, which was $\langle V \rangle$=76m>L=10m. The reader is invited to modify $V(x)$ and repeat the exercise for different values.

3.2 NUMERICAL CASE

The method described in Section 2.3 is applied to smoke visibility data that describes a problematic situation similar to the analytical case described in Section 3.1. The data consists of 7200 values of visibility, ranging between 1 and 150 meters, uniformly distributed on a rectangular grid. This data has been generated numerically, by using a normal distribution with added noise, and it represents the typical situations that the authors have learned to overcome.

In this case, the observer is located in the lower left corner of the diagram and the object is in the top right corner as can be seen in Figure 3.1. The sightline connecting the observer and the object has a length of L=13.4m.

FIGURE 3.1
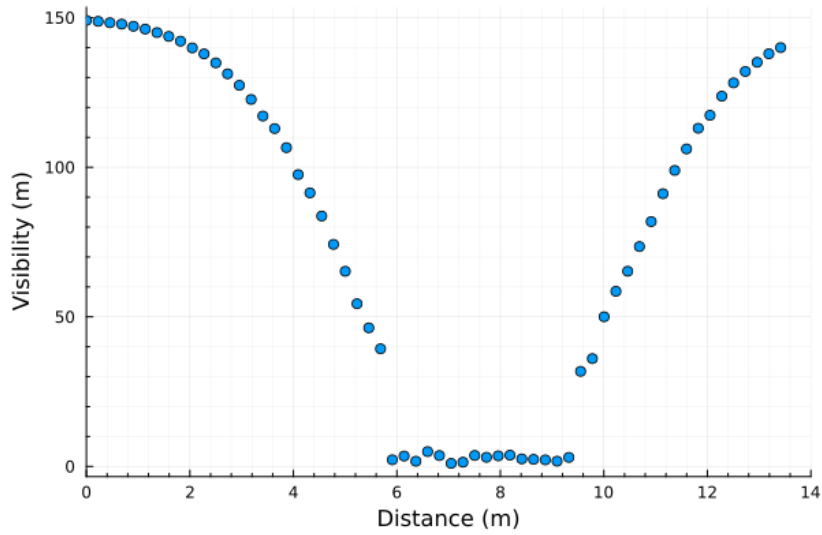
Non-homogeneous smoke visibility data
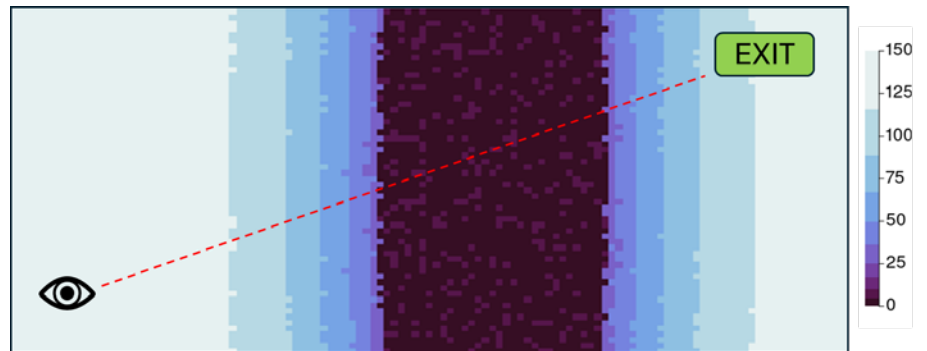
Let ϵ_{max}=0.05m, which means that the overall numerical error should be no greater than 5cm. According to Eq. 7, at least N=60 should be used. The smoke visibility function, evaluated at these points, is shown in Figure 3.2.

FIGURE 3.2

Smoke visibility data
evaluated at N=60 points
along the L=13.4 m sightline

The average visibility along the sightline is

$$\langle V \rangle_{approx} = \frac{1}{2N}\left[V(0) + 2\sum_{i=1}^{N-1} V\left(\frac{iL}{N}\right) + V(L)\right] = 79.3 \text{ m}$$

Since L=13.4 m, then $\langle V \rangle_{approx}$>$L$ and an incorrect conclusion could be drawn that the observer can see the exit sign. A quick look at Figure 3.1, or Figure 3.2, will cast serious doubt on that conclusion. By applying the method described in Section 3.2, we find that

$$L_{low} = \frac{L}{2N}\left[X(0) + 2\sum_{i=1}^{N-1} X\left(\frac{iL}{N}\right) + X(L)\right] = 3.6 \text{ m}$$

and that

$$\langle V \rangle_{low} = \frac{L}{2NL_{low}}\left[X(0)V(0) + 2\sum_{i=1}^{N-1} X\left(\frac{iL}{N}\right)V\left(\frac{iL}{N}\right) + X(L)V(L)\right] = 2.8 \text{ m}$$

Since $\langle V \rangle_{low}$<L_{low} this indicates that the observer cannot see the exit sign. Note that the distance L_{low} on which the visibility is critically low is rather narrow. Choosing fewer points than N=60 would yield ϵ_{max}>0.05 m (for C=1) and this could lead to misinterpretation. This underscores the necessity of determining ϵ_{max} at the start by either complying with an imposed value or by inspecting the smoke visibility data for any inherent uncertainties.

4. Conclusion

This analysis provides a quick and error-centered approach to interpreting smoke visibility data. The approach presented in this paper can be used to complement a method that was developed in a previous paper to promote effective communication of smoke visibility data (Lévesque and Rouch, 2025). Together, these two methods provide a toolkit than enables engineering teams to properly manage the risk associated with the interpretation of smoke visibility data. As virtual reality technologies are becoming increasingly accessible, more work can be done in creating cutting edge tools that will give us a wider range of methods for the interpretation of smoke visibility data. This will allow engineers and stakeholders to better understand the risks associated with fire safety designs.

References

Hamming, R. W. 2012: Numerical methods for scientists and engineers. Courier Corporation, New York.

Jin, T. 2008: Visibility and Human Behavior in Fire Smoke. In: The SFPE Handbook of Fire Protection Engineering, fourth ed., pp. 2-54–2-66. National Fire Protection Assoc., Quincy, MA.

Klote, J.H., Milke, J.A., Turnbull, P.G., Kashef, A., Ferreira, M.J. 2012: Handbook of Smoke Control Engineering, ASHRAE, Atlanta.

Lévesque, D., and Rouch, O. 2025: Effective communication of smoke visibility data. Proceedings of the Canadian Society of Civil Engineering Annual Conference 2024, Niagara Falls, Ontario, Canada. [Not yet published]

National Fire Protection Association: NFPA 130 - Standard for Fixed Guideway Transit and Passenger Rail Systems, 2017 Edition.

Cha, M., Han, S., Lee, J., & Choi, B. 2012. A virtual reality based fire training simulator integrated with fire dynamics data. Fire safety journal,50: 12-24.

Forney, G. 2011. A note on visualizing smoke and fire. Fire and Evacuation Technical Conference, Baltimore, Maryland, USA.

Kang, K., and Macdonald, H. 2005. Modeling smoke visibility in CFD. Proceedings of the 8th Intl Symp for Fire Safety Science, Beijing, China: 1265-1276.

Wahlqvist, J., & Rubini, P. 2023. Real-time visualization of smoke for fire safety engineering applications. Fire safety journal, 140, 103878:1-9.

Wahlqvist, J., & van Hees, P. 2018. Visualization of fires in virtual reality. Division of Fire Safety Engineering, Lund University, SE-221 00 Lund, Sweden, Tech. Rep. ISRN: LUTVDG/TVBB-3222-SE.

Xu, Z., Lu, X. Z., Guan, H., Chen, C., & Ren, A. Z. 2014. A virtual reality based fire training simulator with smoke hazard assessment capacity. Advances in engineering software, 68:1-8.

AtkinsRéalis

Contact Information

Dorothy Gartner
Sr Librarian
Office of the COO, Group Quality
& Knowledge Management
dorothy.gartner@atkinsrealis.com

atkinsrealis.com